POSSIBLE BASEMENT INFLUENCE ON CRETACEOUS CARDIUM SANDBODY ORIENTATIONS IN THE GARRINGTON AREA, ALBERTA BASIN

POSSIBLE BASEMENT INFLUENCE ON CRETACEOUS CARDIUM SAND BODY ORIENTATIONS IN THE GARRINGTON AREA, ALBERTA BASIN

By

Victoria Hunter

A thesis

in Partial Fulfilment of the Requirements

for the Degree

Bachelor of Science

McMaster University

1996

Bachelor of Science (1996)
(Geology)

McMaster University
Hamilton, Ontario

TITLE: Possible Basement Influence on Cretaceous Cardium Sand Body Orientations in the Garrington Area, Alberta Basin

AUTHOR: Victoria Hunter

SUPERVISOR: Dr. R. G. Walker

NUMBER OF PAGES: xi, 94

ABSTRACT

The Upper Cretaceous Cardium Formation contains extremely long, linear sandstone and conglomerate bodies. Four of the most linear are; Caroline, Garrington, Crossfield and Lochend; they trend northwest-southeast. The factors controlling the linearity of these sandbodies, which are presently interpreted to be incised shorefaces, have been questioned. Jones (1980) proposed that the orientation of these sandbodies is dictated by vertical faults in the basement that have effectively controlled the position of the Cardium oil fields. Hart and Plint (1993) suggested that remobilized basement structures during Cardium times affected the orientation of these sandbodies.

Fourteen continuous stratigraphic intervals from the top of the Mannville to the base of the Belly River were studied in the Garrington area by correlation of 797 resistivity well logs. Regional and residual trends were observed in isopach, quadratic trend surface, and residual maps. Residual trends occur at oblique angles to regional trends, which would indicate differing factors affecting local and regional sedimentation. Regional thinning trends were observed from SW - NE in Layers 4-2, 6-4, 12-11, 13-12, and 15-14; SE - NW in Layers 7-6, and 9-8; W - E in Layers 8-7, 11-10, and 14-13; NW - SE in Layer 10-9; and NE - SW in Layer 16-15. No trends were found to penetrate through the stratigraphic layers, suggesting that underlying basement control was not important. Basement movements would have to propagate through 2.2 to 3.5 km of Phanerozoic sediment in order to influence the orientation of the Cardium

sandbodies in the study area. Thus, the present sedimentological interpretation of these sandbodies, namely incised shorefaces deposited during a lowstand and then abandoned on the shelf during the following transgression, appears adequate.

ACKNOWLEDGEMENTS

Dr. Roger Walker is an exceptional supervisor. I would like to thank him for the knowledge that he passed on to me; the enthusiasm with which he motivated me; and the time and dedication he so generously gave to me. I also acknowledge support from the Lithoprobe grant awarded to Dr. Bergman and Dr. Walker, and thank them for sharing their research funding so that I could do a thesis.

I am grateful to Imperial Oil Resources Ltd. for their support of this project. In particular, I thank Lawrence West (now with AEC) and Dr. Charle Gamba (now with Canadian Occidental) for setting me up at Imperial and answering my numerous questions. My summer in Calgary was truly a summer to remember, I thank those who welcomed me and kept me entertained.

My family and friends are my life-line. I thank them for their love, support and encouragement; without them I would not have been able to achieve all that I have during my university career.

I thank everyone in the department of geology; my friends, professors, lab mates (who are also my friends and fellow sed heads), and the ladies in the office (who took great care of me). I particularly need to thank Nicoleta Badescu who contributed many hours to assist me with the data entry. A special thank-you goes out to those that helped me to produce the final copy; Dr. Hillary Stuart-Williams, Jack Whorwood, and Evan Edinger for their photography; Branimir Gojsic for his support and printing services; Chris Boerboom for being

my buddy and mental saviour; and Danielle Parker, a dear friend that also helped keep me sane.

"There is no feeling in the world like climbing to the top of a mountain - I will cherish this memory forever. From the bottom of my heart I thank everyone that helped me get to the top of this thesis mountain."

Victoria Hunter

DEDICATION

My motivation for challenging myself and reaching success stems from watching others strive, succeed, and obtain happiness. I would like to dedicate this thesis to the two women who have been the hardest working women I have been blessed with knowing.

The first woman, is my Great Aunt Sally Glickman. No woman worked so hard in life and expected so much out of her loved ones. I want her to know that I loved her for pushing me. I know that she would have been so very proud of the accomplishments that I have made, but of course would not let me know this and would continue to demand more.

My Mum is the most important person in the world to me. I dedicate this to her for guiding me along my path of life. The goals set and attained in my life are as much hers as they are mine. This accomplishment is for her, her hard work, and her dedication to her family.

TABLE OF CONTENTS

LIST OF FIGURES

CHAPTER 1: INTRODUCTION

1.1 Objectives

Many Cretaceous Formations in the Western Interior Seaway, such as the Shannon, Frontier, Ferron, Gallup, Viking, and Cardium, are characterized by a series of linear sandstone and conglomerate bodies. There is an ongoing debate regarding the sedimentological and tectonic controls that influence the formation of linear sandbodies. There are three possibilities: 1) the orientation of the sandbodies is the result of purely sedimentological control; 2) orientation is due to tectonic control as a result of basement movements; or 3) a combination of tectonic control by recurring movements in the basement making topographic irregularities on the seafloor that influence the sedimentology. There is also an ongoing argument concerning the formation of the linear sandbodies. The arguments regarding the possibility that the Cardium linear sandbodies are offshore bars versus lowstand or transgressive incised shore faces are summarized in detail by Bergman and Walker (1987, 1988). In the present study area, Cardium sandbodies exist at Caroline, Garrington, Crossfield, and Lochend. In the Viking Formation, extremely linear sandbodies extend from Gilby through Joffre, Mikwan, Fenn and Chain, from Central Alberta toward Saskatchewan. Downing and Walker (1988) interpreted Joffre as a transgressive incised shoreface. Some of the Viking fields were interpreted by Hein et al. (1986) and Leckie (1986) as offshore bars.

The objective of this thesis is explore the possibility that the basement

has influenced the orientation of the Cretaceous Cardium sandbodies in the Garrington Area, Alberta Basin. These basement trends have been described by Ross et al. (1995) in the Alberta Basin. The hypotheses proposed by Jones (1980) and Hart and Plint (1993), that there have been basement controls on the orientation of the Cardium sandbodies, will be discussed and tested. Isopach maps, quadratic trend surface maps, and residual maps of 14 stratigraphic intervals from Lea Park to the top of the Viking will be presented and the resulting trends interpreted. In order to establish the influence of basement trends on these layers the regional trends in each layer, as well as localized residual trends, will be examined. To further explore possible basement tectonic influence potential trends between layers will be compared.

1.2 Scientific Problem

The sandbodies of the Cardium Alloformation (Burnstick Allomember) occur in four long, straight and narrow marine sand bodies. These sandbodies form the Caroline, Garrington, Crossfield, and Lochend oil fields. Crossfield and Garrington are among the longest, straightest and narrowest sandbodies ever described. Crossfield is approximately 70 x 4 km, and Garrington is estimated to be 100 x 3 km. These Cardium sandbodies are very important economically because the sandstones and conglomerates in the Cardium as a whole contain at least 3.18×10^8 m^3 (2 billion barrels) of recoverable oil (Wadsworth and Walker, 1991). Thus, determining the controls influencing the formation of these

long, linear sandbodies can assist in the exploration for oil and the development of existing reservoirs.

These long, straight sandbodies were originally interpreted as "offshore bars" (Berven, 1966) but have been reinterpreted by Pattison and Walker (1991) as "incised shoreface deposits formed on a transgressive, sequence-bounding ravinement surface". Pattison and Walker (1991) determined the depositional and erosional history of the Burnstick Allomember. Cardium erosion surface 4 (E4) was shown to control the morphology of these three long, narrow and parallel steps, each steeper on the northeast-facing side and flattening basinward. These steps have been interpreted as incised shorefaces, parallel to the regional strike, and cut during stillstands within a period of an overall rise of the relative sea level.

No clear consensus exists to explain why the Viking fields such as Joarcam, Joffre, and Gilby are long and narrow and are oriented roughly NW - SE as shown in Figure 1. The Joffre sandbody is encased in mudstones and is 38 km long by 3-4 km wide. Some of the Viking sandbodies were originally interpreted by Hein et al., (1986) and Leckie (1986) as offshore bars. Downing and Walker (1988) reinterpreted Joffre as an incised shoreface cut during a sea level lowstand. These sands were supplied to the shoreface during the lowstand and then covered with marine muds during the subsequent transgression.

Davies and Walker (1993) studied the Viking Formation (Lower Cretaceous) in the area of the Caroline and Garrington reservoirs. These fields

occur in sandstone and conglomerate, and are relatively small. Davies and Walker (1993) established a two-part stratigraphy for the Viking in this area. The lower part consists of a northeast-prograding coastal succession of offshore and shoreface storm deposits, capped in places by nonmarine facies. This succession is dissected by a regionally-extensive transgressive surface of erosion (TSE) that rises stratigraphically in the southwest. The upper stratigraphic unit consists of marine shales, with five tongues of coarse sandstone and conglomerate that were interpreted to onlap the underlying transgressive lag toward the southwest. These were interpreted as extensions of the lower shoreface that formed during minor regressions interspersed with the main transgression. Thus, the coarse-grained reservoir rocks appear to have been deposited as a result of forced regressions, which are in turn controlled by high-frequency fluctuations of relative sea level.

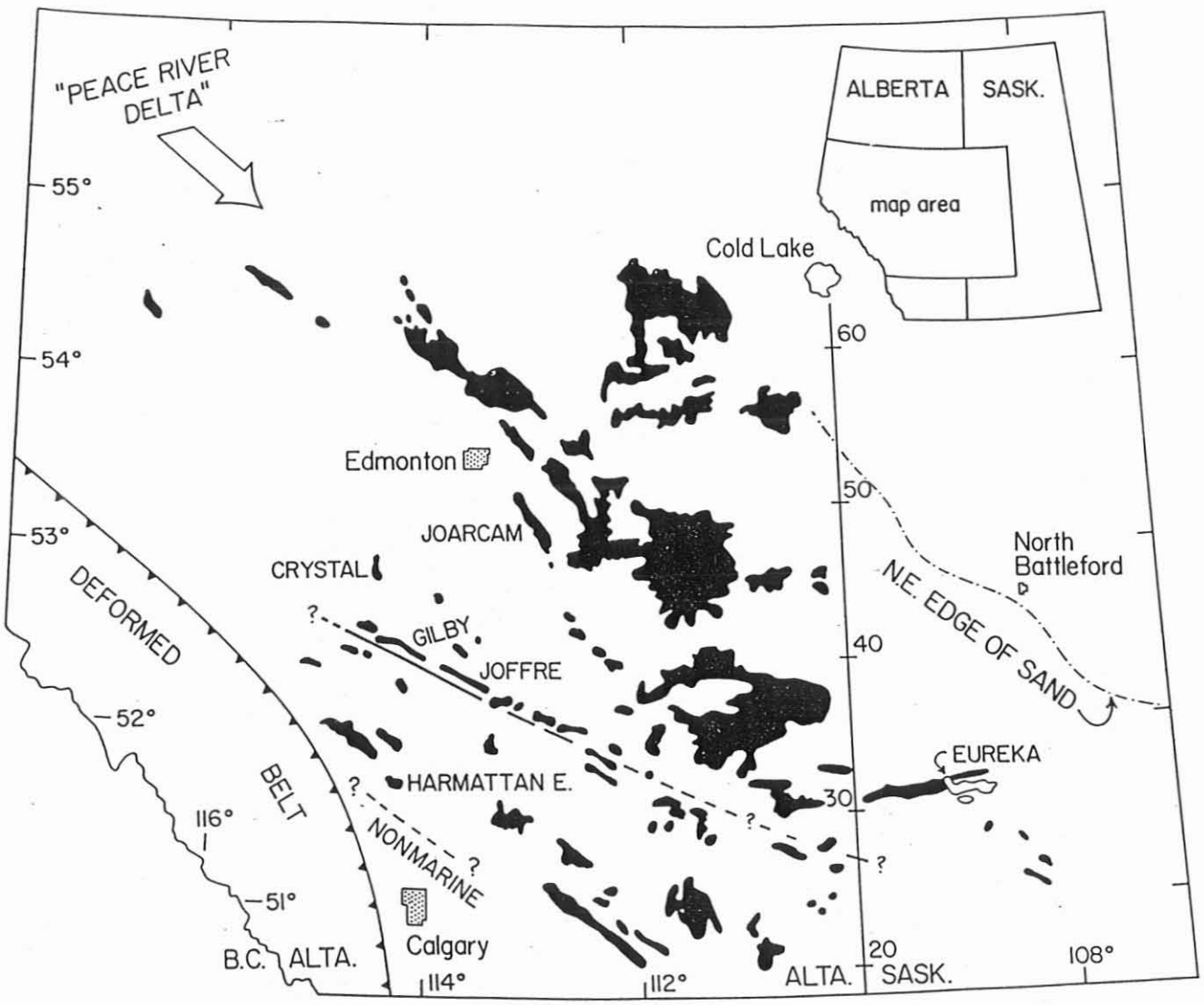

Figure 1. Location of major oil and gas fields in the Viking Formation, Alberta and Saskatchewan. (From Downing and Walker, 1988)

Jones (1980) presented a series of structural cross sections through the Western Canadian Sedimentary Basin, in which he presented evidence for the existence of widespread vertical faults. Some of these faults appear to have influenced the boundaries defining Cardium Formation production fields such as Pembina and Garrington, as shown in Figure 2. He suggested that these fault planes have existed since the Precambrian, and that possibly most of them had originated soon after a thin lithosphere crust first formed. Jones stated that the porous sand lens forming the Viking and Cardium fields generally follows closely along the strike of the isostatic adjustment faults. He suggested that the fault displacements he observed are the result of late Tertiary isostatic adjustment.

Jones also examined a portion of the Garrington, Cardium oil fields (Figure 3), in which two separate bodies of productive Cardium sand were deposited in somewhat different areas. Jones concluded that the upper Cardium"A" sand was deposited both downdip and well updip from the main North 44° West "strike" fault, as shown in Figure 3. The lower Cardium "B" sand was concluded to terminate updip right at the fault line. This is illustrated in the cross section L-L' constructed by Jones shown in Figure 3. Cross section M-M' (in Figure 3) shows the presence of a crossover "dip" fault running North 47° East which Jones suggested may have influenced the area of "A" sand deposition. Jones also suggests that this "dip" fault may have changed the direction of the main "strike" fault from North 44° West, north of the fault, to North 37° West on the south. Jones recognised that the sands at Garrington

and in numerous Viking and Cardium linear fields appear to have developed in a shallow, wave-winnowed environment. The stratigraphically equivalent shales and silty shales that surround them were deposited in somewhat deeper water. The model Jones used to account for such a pattern of deposition would be a long narrow roll or fold following very closely along the strike of an isostatic adjustment fault. Jones postulated that the crest of such a fold would be fairly close to contemporaneous sea level. He noted that the main NW - SE faults appear to be located at approximately 16 km intervals. He proposed that the magnitude of throw of isostatic adjustment faults, within the undisturbed Western Canadian Basin, ranges from 75 m in several large faults in the Peace River Arch to barely recognizable throws of 1.5 m. Jones states that these would appear to represent a gradient of isostatic restoration across the basin.

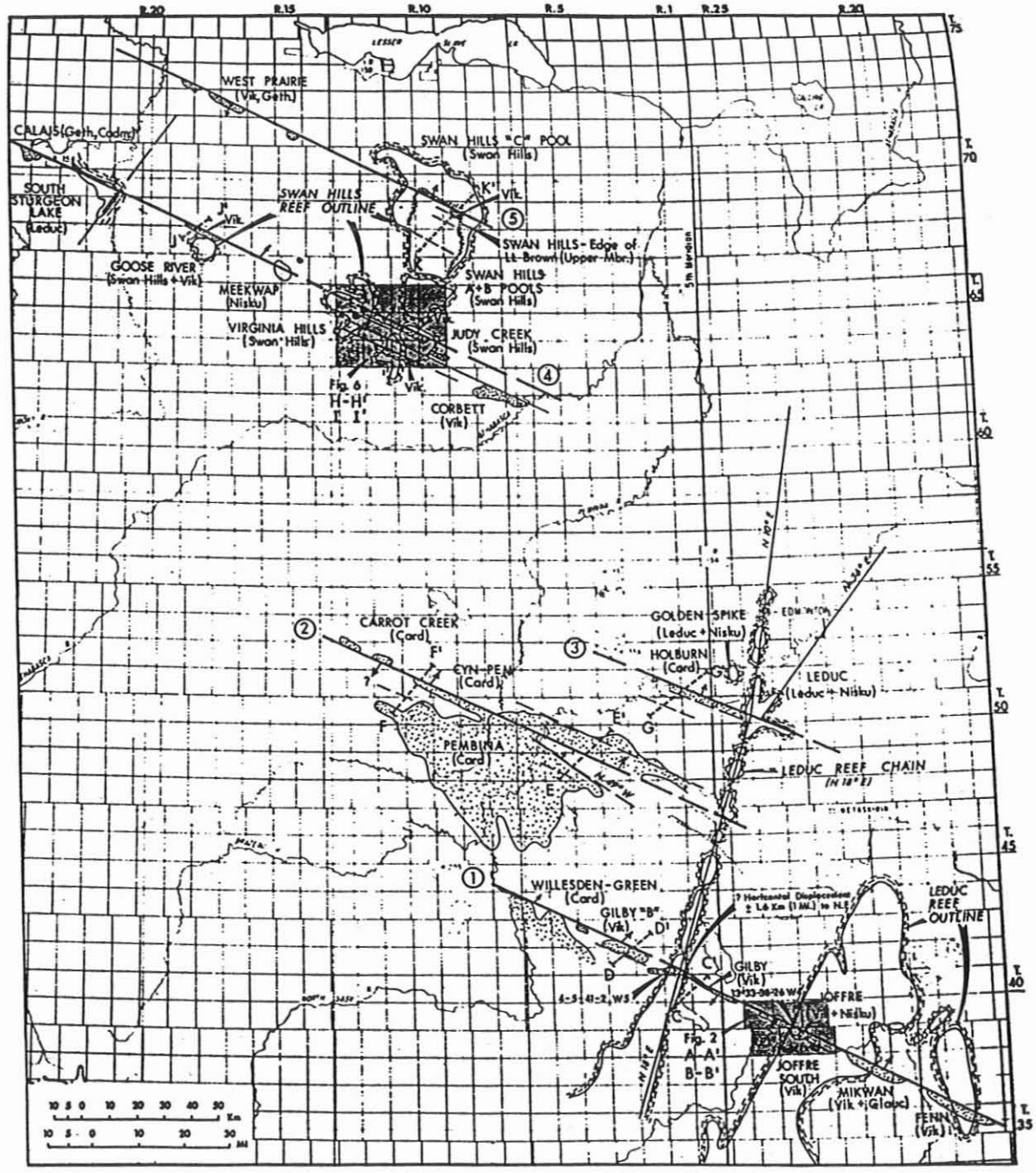

Figure 2. Central Alberta hydrocarbon trends with a common North 65° West strike from Jones (1980).

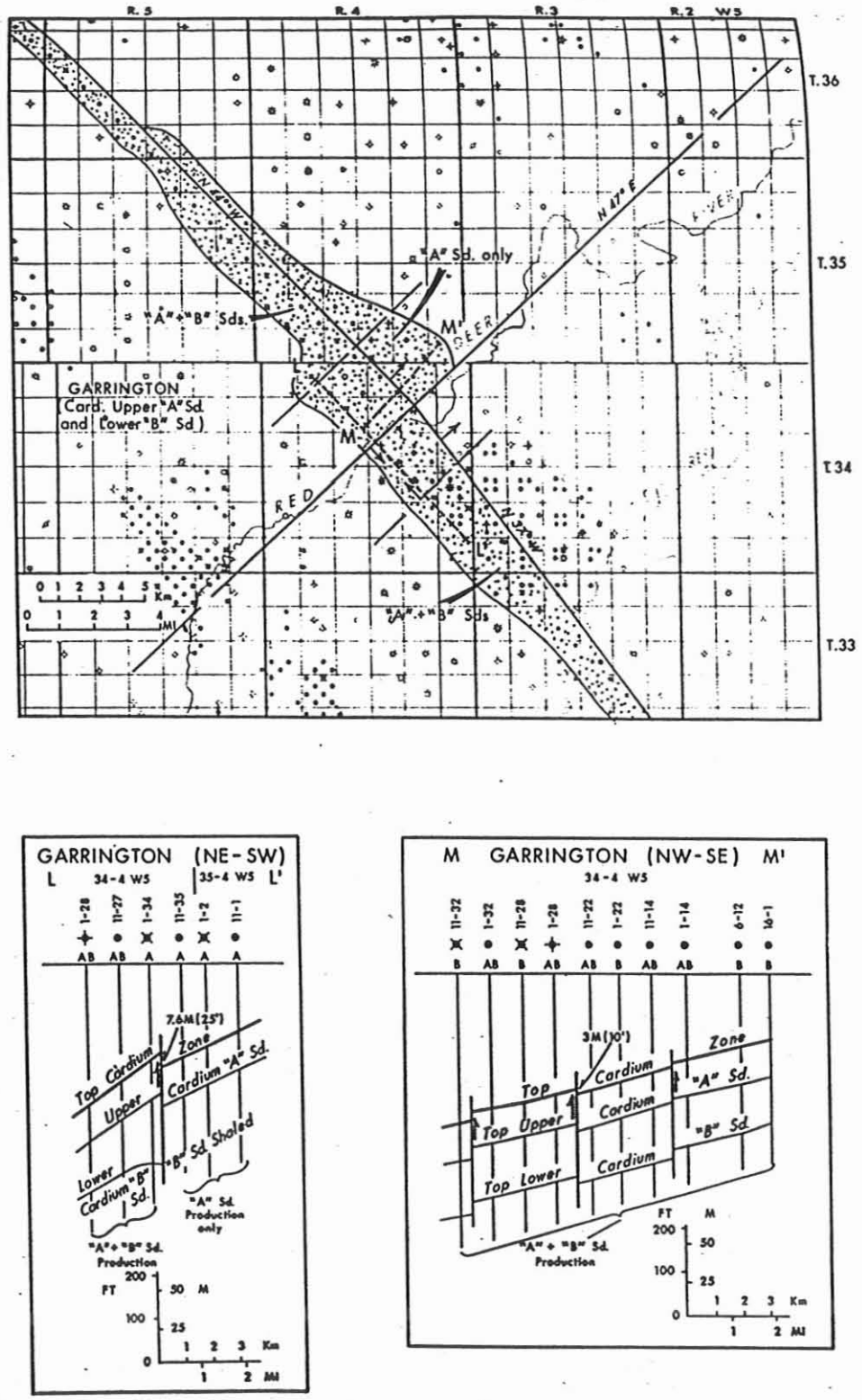

Figure 3. Map of Garrington area showing isostatic adjustment faulting, and cross sections L-L' and M-M', from Jones (1980).

Hart and Plint (1993) examined the tectonic influence on deposition and erosion in the Upper Cretaceous Cardium Formation. Hart and Plint (1990) presented an isopach map of the entire Cardium Formation (E1-E7) that they modified in 1993, shown in Figure 4. The main thinning trend is to the northwest. (Isopach strike of about 55° - 235°). They observed, superimposed on this regional trend, a succession of NW - SE trending (about 320° - 140°) thickness variations. Hart and Plint highlighted a number of known or inferred basement structural elements that are parallel to the NW - SE trending lineaments and features shown in Figure 4. These include a series of inferred faults mapped by Cant (1988) under the northern area of Hart and Plint's study area. There may also be a possible shear zone in the Proterozoic basement, termed the "Chinchaga low" (Ross and Stephenson, 1989 fide Hart and Plint, 1993) They suggested that a genetic link may exist between the orientation of these basement trends and the trends observed in the Cardium. Closer to the area examined in this thesis, Hart and Plint observed superimposition of Cardium E4 and E7 and other overlying formations, as shown in Figure 5. They suggested that basement structures were being remobilized during the deposition of the Cardium, possibly in response to thrusting in the orogenic belt. Hart and Plint (1993, p. 2092) concluded; "In places, trends of isopaches, facies transitions, erosional bevels on transgressive erosion surfaces, synsedimentary faults, and modern production trends can be directly superimposed and closely correspond to basement structural trends".

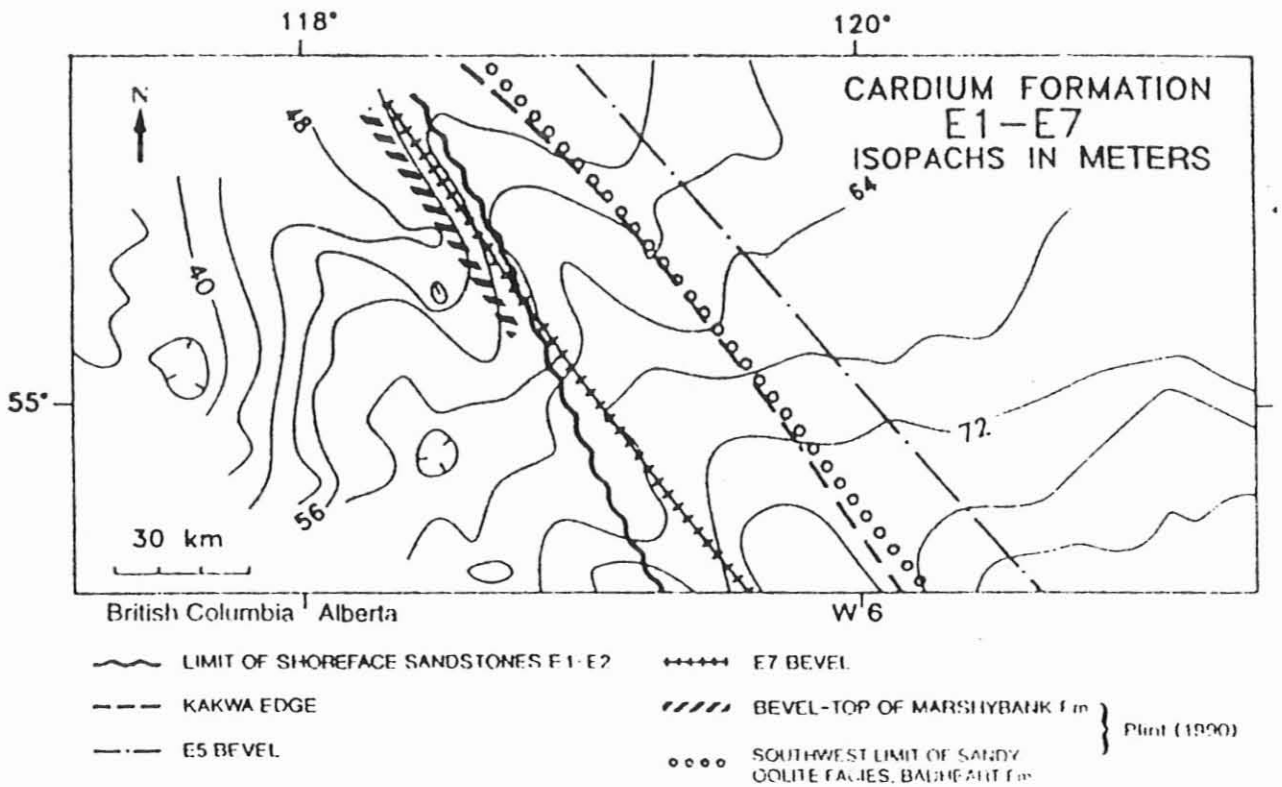

Figure 4. Isopach map of Cardium Formation (E1-E7), showing facies and structural trends of Cardium and overlying Formations. From Hart and Plint (1993)

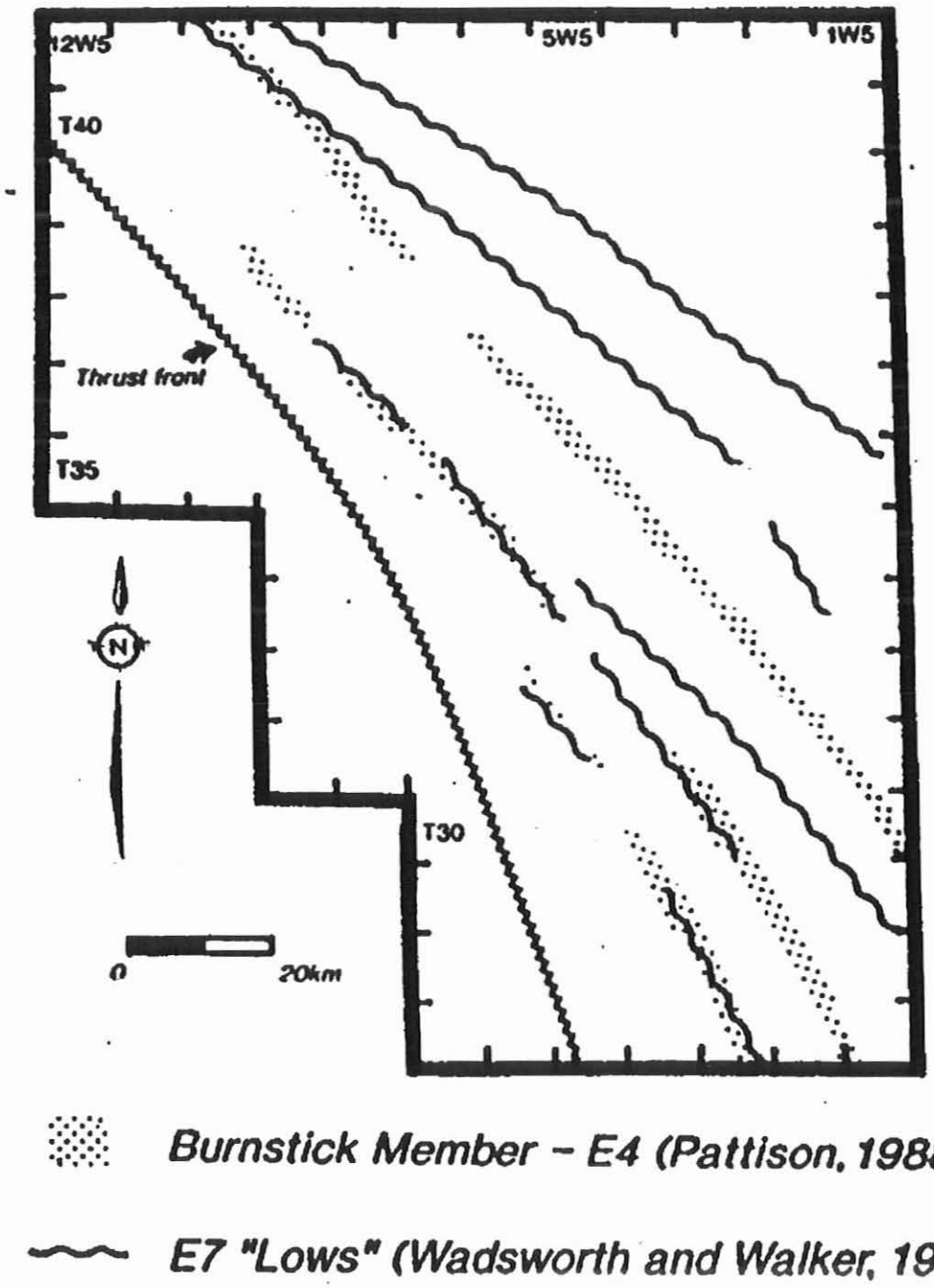

Figure 5. Evidence for structural control of erosional topography in the Caroline-Garrington area. Trends in the distribution of lowstand shoreface deposits of Burnstick allomember (associated with E4 horizon) are matched by trends in topographic "lows" on E4 surface. From Hart and Plint (1993).

Others have observed the effects of remobilization of Precambrian basement structures on deposition during the Cretaceous in the Western Interior seaway. Cant (1988) suggested that localized remobilization of the Peace River arch structures affected deposition of the Albian Spirit River Formation. Barclay et al. (1990, fide Hart and Plint 1993) describe a graben complex in Carboniferous and Permian strata, in a study area that overlaps Hart and Plint's area, and found faults that are parallel to the Cardium trends described by Hart and Plint (1993). The seismic data they presented represent reactivated basement structures. O'Connell (1988 fide Hart and Plint, 1993) also studied an area that overlaps Hart and Plint's, and inferred basement control of subsidence patterns during the Early Cretaceous.

This thesis is testing the idea of **basement control** on the orientation of Cretaceous Cardium linear sandbodies proposed by Jones (1980) and Hart and Plint (1993). The idea of tectonic control in the basin is not being disputed. There is doubt that movements of the basement floor are occurring, and indeed there may also be small Cretaceous events producing faults.

1.3 Basement Trends

The crystalline Precambrian basement of the Prairie Provinces underlies about 3.5 to 2.2 km of Phanerozoic sedimentary strata in the study area, within the Western Canadian Sedimentary Basin. Ross et al. (1995) have subdivided the basement beneath Alberta and eastern British Columbia into distinct crustal

domains based on their interpretation of the aeromagnetic signatures shown in Figure 6 and U-Pb geochronology of drill cores. By extrapolation of areas exposed in the Canadian Shield, the mosaic of crustal domains in the subsurface shown in Figure 7 is inferred by Ross et al. (1991) to have formed during arc accretionary events and continental collision that began in the Archean and continued until 1.78 to 2.0 Ga. The basement is typified by north-northeast trending domains as shown by Ross et al. (1991, 1995) in Figures 6 and 7.

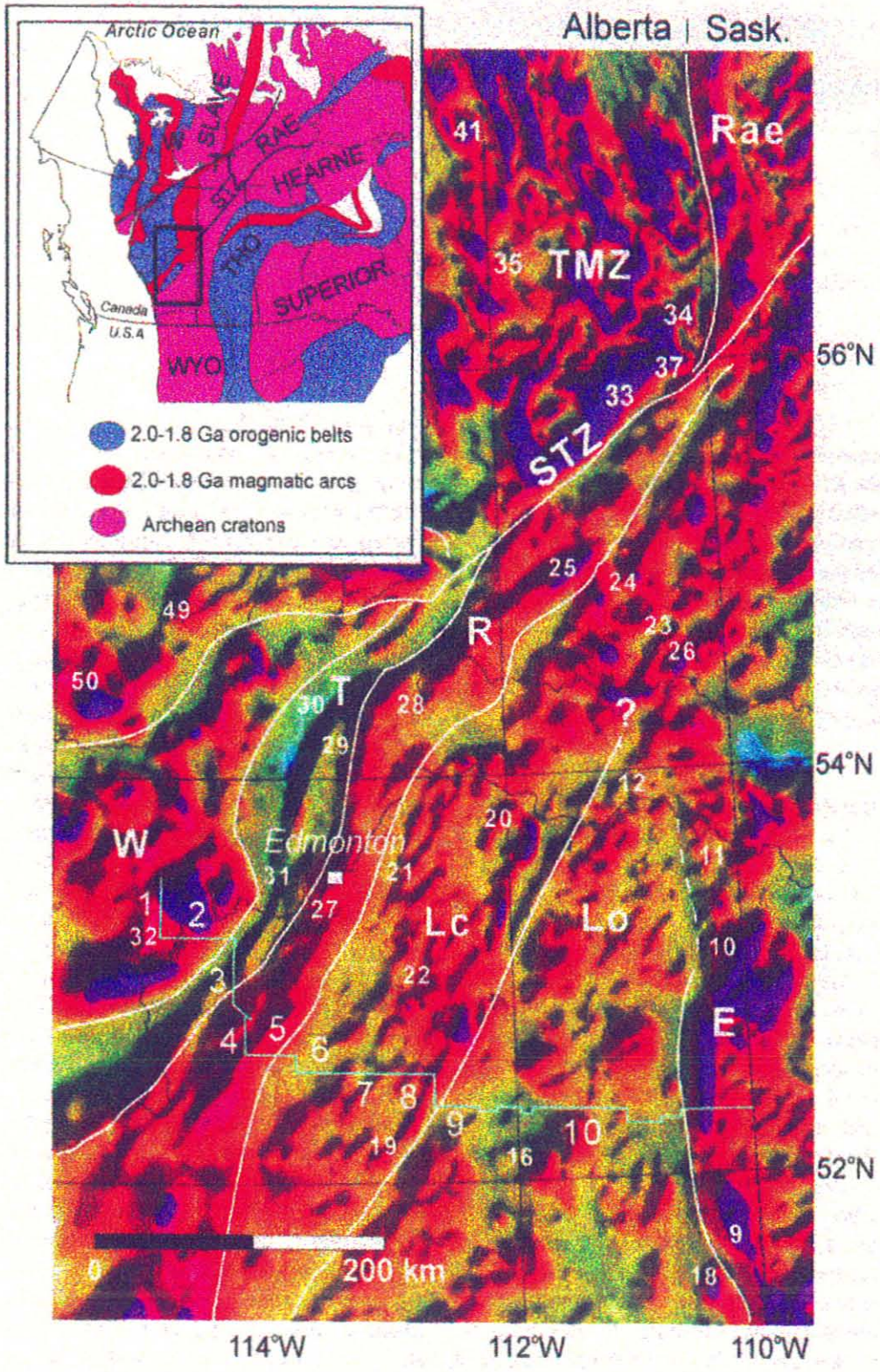
Alberta | Sask.
Arctic Ocean
SLAVE
RAE
HEARNE
TNO
SUPERIOR
WYO
Canada
U.S.A
2.0-1.8 Ga orogenic belts
2.0-1.8 Ga magmatic arcs
Archean cratons
Rae
TMZ
STZ
R
T
?
W
Edmonton
Lc
Lo
E
41
35
34
37
33
25
24
23
26
49
50
30
28
29
12
20
11
31
21
27
1
2
32
3
22
10
4
5
6
7
8
9
10
19
16
18
0
200 km
56°N
54°N
52°N
114°W
112°W
110°W

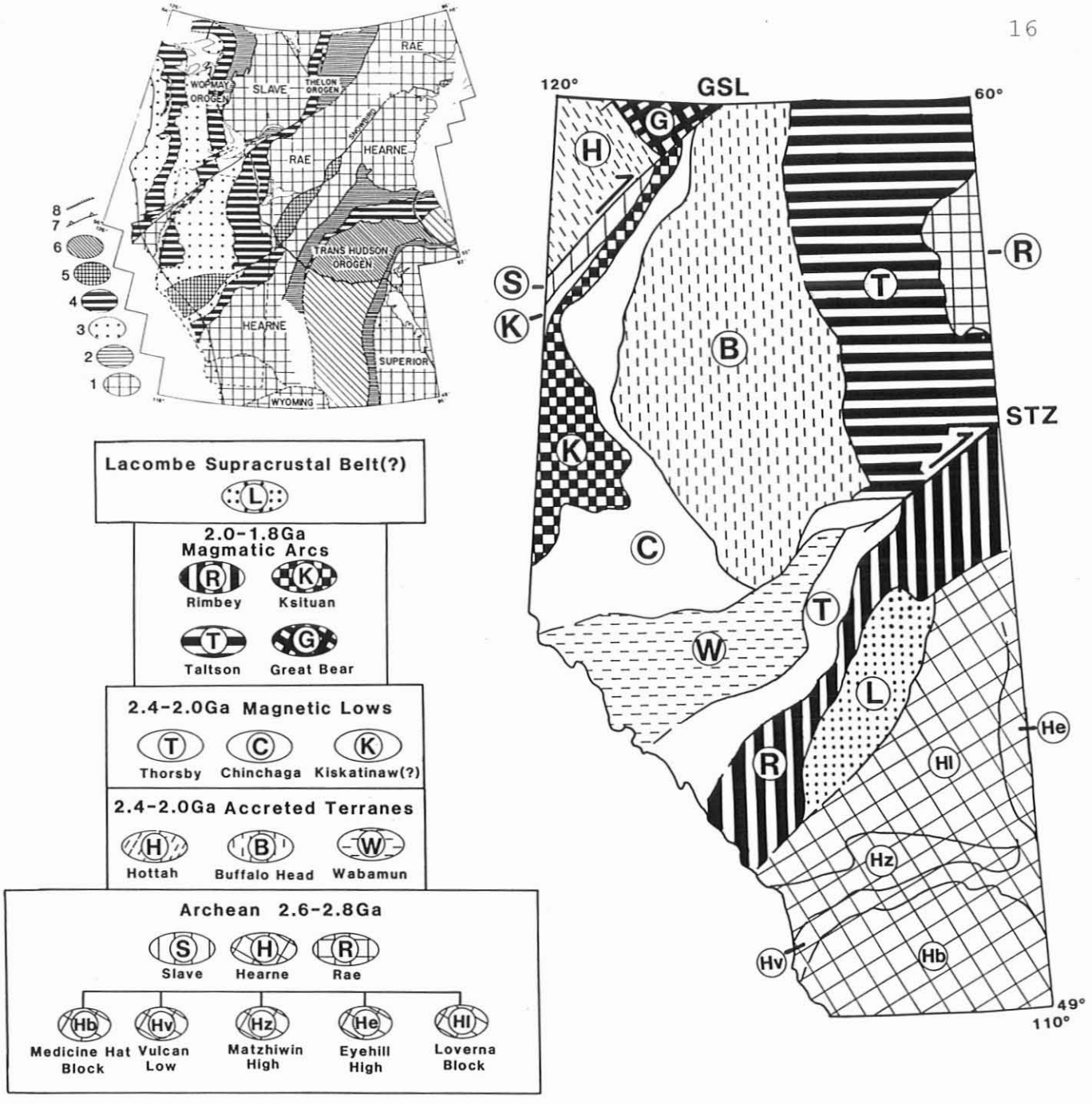

Figure 7. Map of tectonic domains postulated in the basement of Alberta. Key for inset: 1. Archean (.2.6 Ga); 2. Reactivated Archean crust; 3. Early Proterozoic (2.4-2.1 Ga) crust' 4. 1.97-1.81 Ga magmatic arcs; 5. Crustal blocks of uncertain age along Snowbird tectonic zone; 6. Juvenile Proterozoic (1.91-1.85 Ga); 7. Edge of Cordilleran deformation; 8. Edge of Phanerozoic cover. From Ross et al. 1991.

CHAPTER 2: STUDY AREA

2.1 Site

The study area is located in south central Alberta in the Western Canadian Sedimentary Basin as shown in Figure 8. In total 1764 resistivity and gamma ray well logs were collected in the 'database area' shown on Figure 8. The area studied for this thesis is square in shape and includes 25 townships (2 500 km^3). The detailed area studied for this thesis is centred on Garrington, covering Townships 33-37, and Ranges 2-6 west of the fifth Meridian. Caroline extends into the southwest corner of the area. Caroline and Garrington are elongated Cardium sandbodies that trend NW - SE.

This area was selected because the rocks are flat-lying and are not known to be tectonically active. The decision to select this area was also based on the observation that Cardium sandbodies overlie Viking. As stated above, it has been proposed that the orientation of long, linear, sandbodies was influenced by basement tectonics. This thesis focuses on some of the longest, and most linear sandbodies presently known.

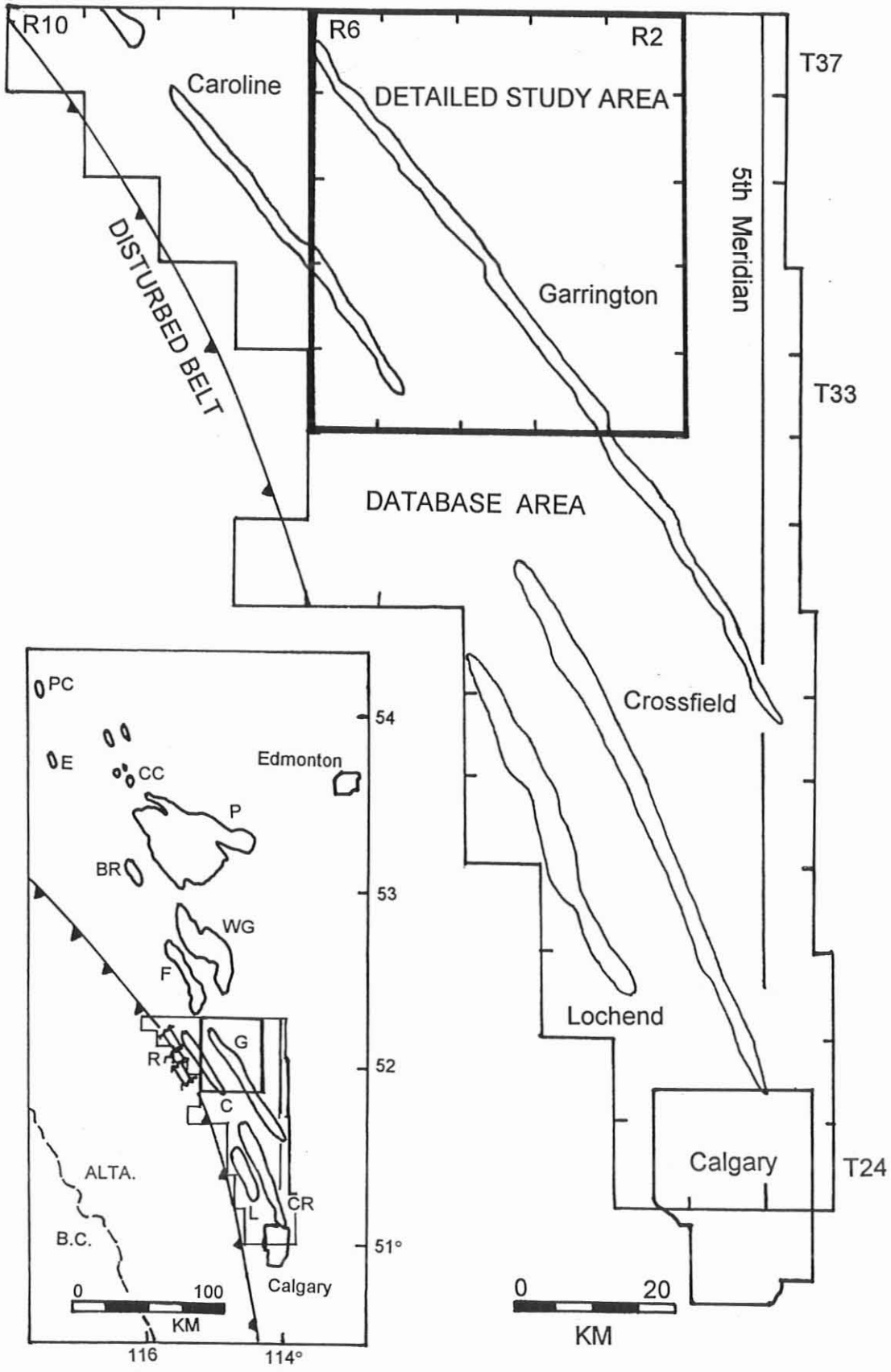
R10
R6
R2
T37
Caroline
DETAILED STUDY AREA
5th Meridian
DISTURBED BELT
Garrington
T33
DATABASE AREA
Crossfield
PC
54
E
CC
Edmonton
P
BR
53
WG
F
Lochend
G
R
52
C
Calgary
T24
ALTA.
CR
L
B.C.
51°
0
100
KM
Calgary
0
20
KM
116
114°

2.2 General Stratigraphy

The stratigraphy of the foreland basin is shown in Figure 9. All of the sediments in the Western Canadian Sedimentary Basin were derived from the active Canadian Cordillera to the west. They are presently flat-lying, tectonically undeformed and unfaulted in the study area. The units studied in this thesis range from the top of the Mannville Group to the base of the Belly River Formation. The Dunvegan Formation does not appear in the study area. The major stratigraphic packages composing the Zuni Sequence include : 1) the Upper Jurassic clastic wedge, 2) the Lower Cretaceous clastic wedge, 3) the Upper Cretaceous clastic wedge (shale-dominated), and 4) the Tertiary clastic wedge. The sub-Cretaceous unconformity represents a period of tectonic reorganization as the Cretaceous sediments extend much further to the east than those of Jurassic age, suggesting that the locus of tectonic loading, subsidence, and the axis of the foreland basin had migrated cratonward. The shaly Colorado and Alberta groups studied here contain up to 800 m of shale, with several intercalated sandstones. This period of relative quiescence is believed to correspond to a period of generally rising sea level (as shown in Haq et al., 1988 - Figure 10), possibly due to the expansion of the Mid-Atlantic Ridge. Cant (*in* Ricketts, ed. 1989) explains the sediment distribution in terms of minor amounts of clastic detritus generated in the orogenic belt being trapped near the orogen, and thus starving the deeper parts of the basin. The sandstones are associated with brief hiatuses: the Upper Albian - Viking Formation was

observed by Hein et al. (1986) to have at least one central erosion surface between its lower sandy clastic wedge and upper conglomeratic unit. The Turonian Cardium Formation displays a basal upward-coarsening clastic wedge, followed by a number of unconformity-bounded sequences (Plint et al., 1986).

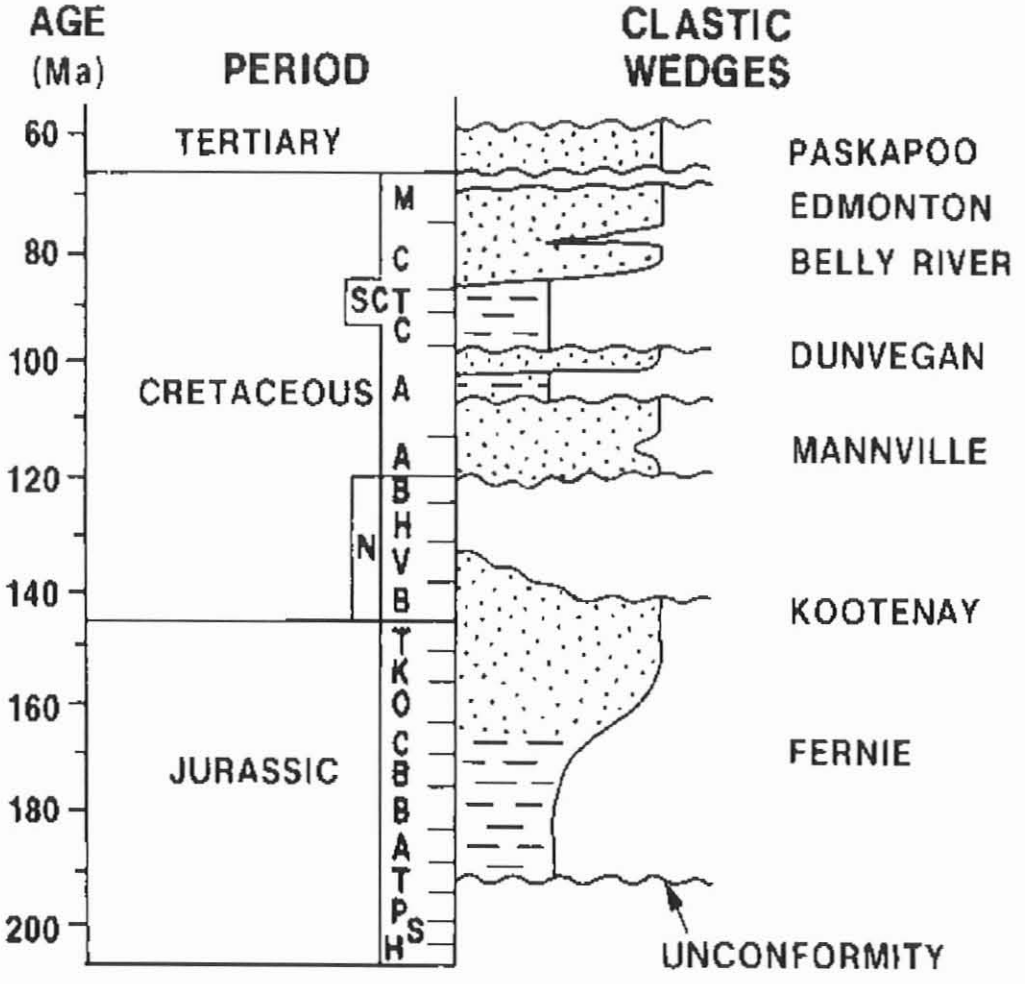

Figure 9. The stratigraphy of the foreland basin. From Cant *in* Ricketts ed., 1989.

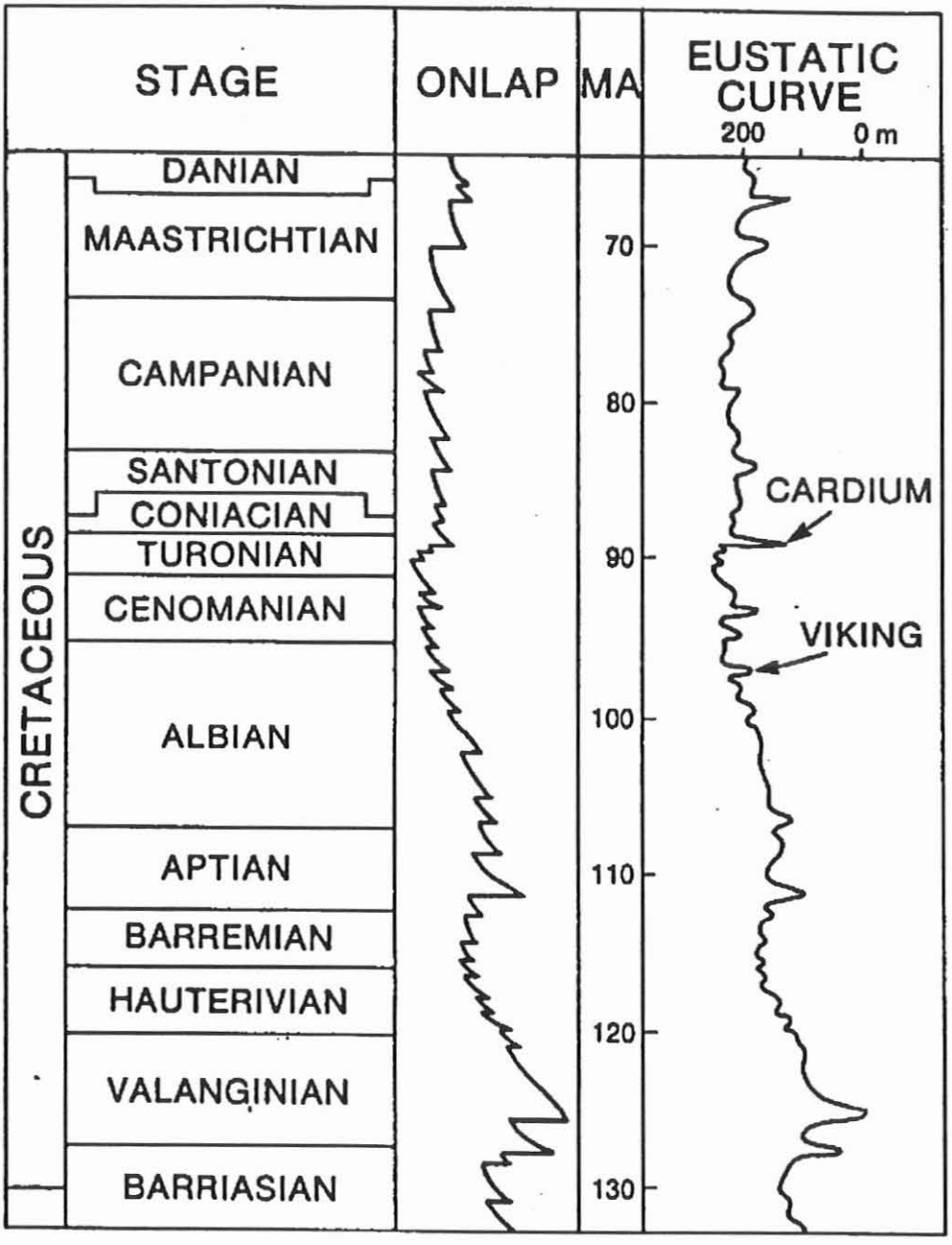

Figure 10. A detailed eustatic sea-level curve for the Cretaceous. The Viking sea-level drop corresponds to the Late Albian (98 Ma), and the Cardium in the Late Turonian (90 Ma). From Haq et al., 1987.

CHAPTER 3: METHODOLOGY

3.1 Database

This study was based on measurement of 797 resistivity and gamma ray well logs, giving an average of about 32 wells per township. The locations of these wells are indicated in Figure 11 and on an acetate in Appendix 1. By constructing many cross sections, it was found that fourteen markers could be consistently picked across the area. Each well log was traced and superimposed over the next. Thus individual log shapes as well as log deflections were used to ensure consistent recognition of the log picks. Slight variations in the log markers occur across the area, but the log picks are estimated to be accurate within 0.5 to 1 m.

For each well log examined; the latitude, the longitude, the well identification number, and the depth below kelly bushing for each pick, were entered into a computer database in Quattro Pro.

Thicknesses of each layer were then computed and edited to correct or remove incorrect entries. Isopach maps of the interval thicknesses between successive picks were then generated using Surfer 6.0 (Golden Software) software package. The maps generated were edited and any "bulls-eyes" or points dictating trends were double checked and changed if incorrect.

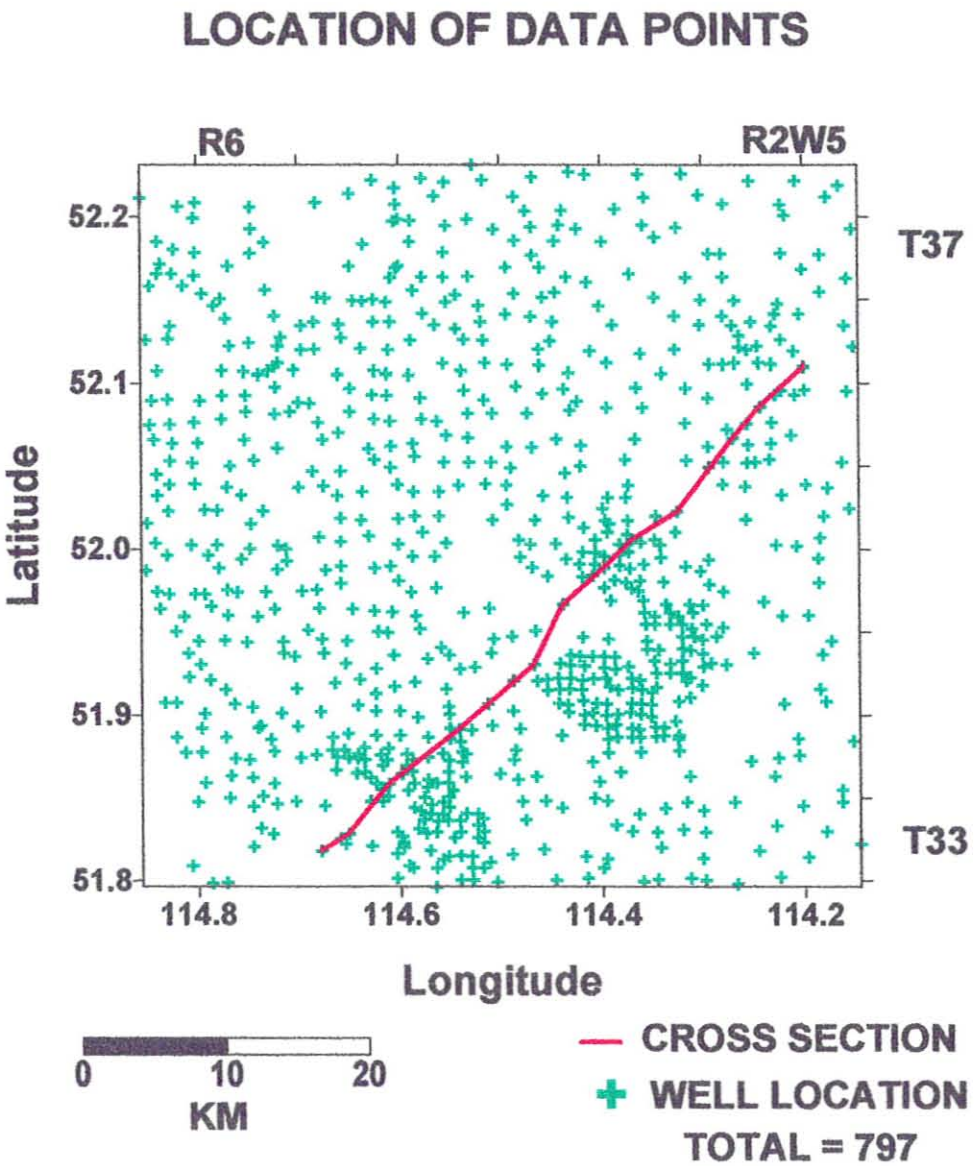

Figure 11. Location of 797 well from which the resistivity logs were collected.

3.2 Cross Section

Figure 12 is the cross section that trends SW - NE as shown in Figure 11.

In the cross sections, only resistivity logs were used as they were the only logs available for every well. The correlation and extent of the picks were studied by constructing a grid of cross sections.

The Base of the Fish Scales Sand was used as the datum as this horizon is considered to be a true structural horizon and is correlatable over a wide area; it probably represents a sea floor that was as smooth and flat as can reasonably be reconstructed.

Some of the picks were made at horizons with a stratigraphic name, e.g. pick 16 is the top of the Viking, whereas others were made at inflection points of no specific stratigraphic name e.g. pick 4.

CHAPTER 4: MAPPING

4.1 Gridding Method

Surfer 6.0 (Golden Software) was used to grid the data and contour the isopach maps, using the Kriging gridding method. Kriging is a geostatistical gridding method that produces visually appealing contour plots from irregularly spaced data. Kriging attempts to express trends that are suggested in the data, so that, for example, high points might be connected along a ridge rather than isolated by bull's-eyes type contours. The default parameters and a quadratic variogram model were used to grid the data.

In order to test that the trends created by Kriging are a result of the actual data, and not an artifact of the gridding method, the variogram anisotropy was used to bias specific directions to observe possible biases that were created by Kriging. Layer 4-2 ("read this as the thickness obtained from pick 4 minus pick 2") was used to observe possible biases created by Kriging. The results of biasing specific directions are shown in Figures 13, 14, 15, 16, and 17. Figure 13, is the default isopach map of Layer 4-2, in which trends in all directions were considered equally. Figure 14, is the isopach map in which N - S trends were biased. Figure 15, is the isopach map in which E - W trends were biased. Figure 16, is the isopach map in which NW - SE trends were biased. Figure 17, is the isopach map in which NE - SW trends were biased. It is very obvious that the trends calculated in each of these 5 maps are extremely similar. Comparison between these maps demonstrates that the trends created by Kriging are in fact real, and not an artifact of the gridding method.

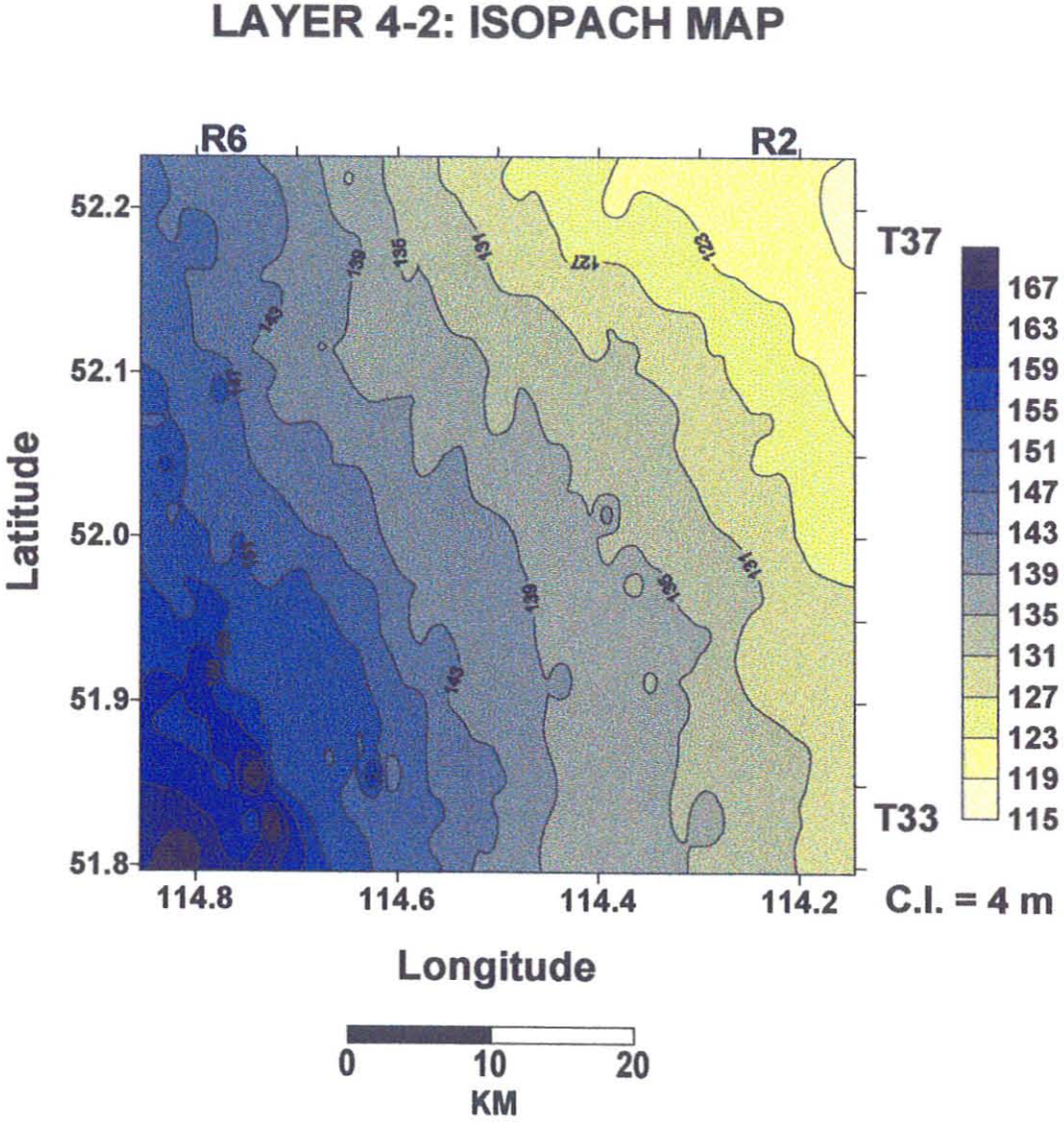
LAYER 4-2: ISOPACH MAP
R6
R2
T37
T33
52.2
52.1
52.0
51.9
51.8
Latitude
114.8
114.6
114.4
114.2
Longitude
C.I. = 4 m
167
163
159
155
151
147
143
139
135
131
127
123
119
115
0
10
20
KM

Figure 13.

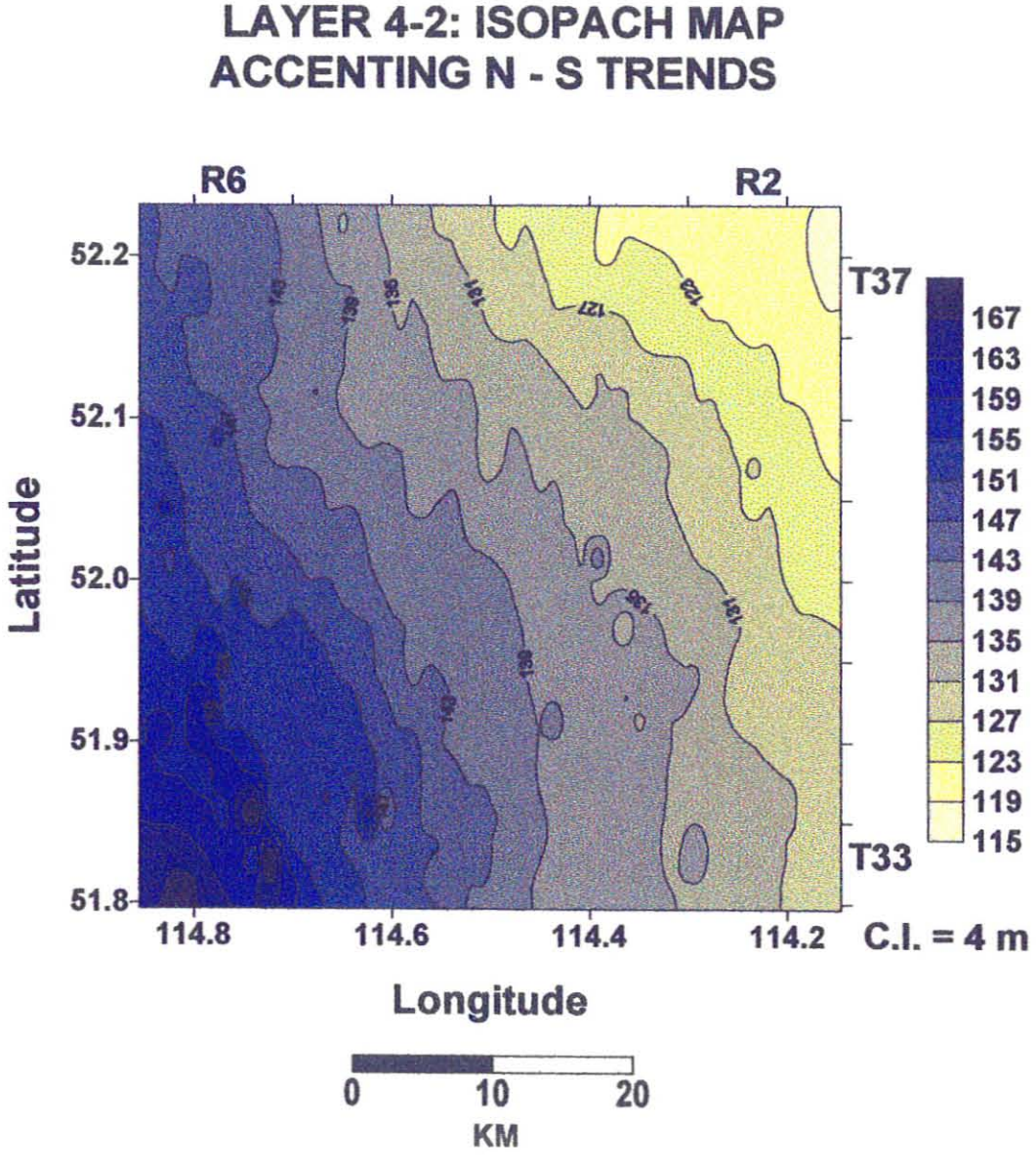
LAYER 4-2: ISOPACH MAP
ACCENTING N - S TRENDS
R6
R2
T37
T33
52.2
52.1
52.0
51.9
51.8
Latitude
114.8
114.6
114.4
114.2
Longitude
C.I. = 4 m
167
163
159
155
151
147
143
139
135
131
127
123
119
115
0
10
20
KM

Figure 14.

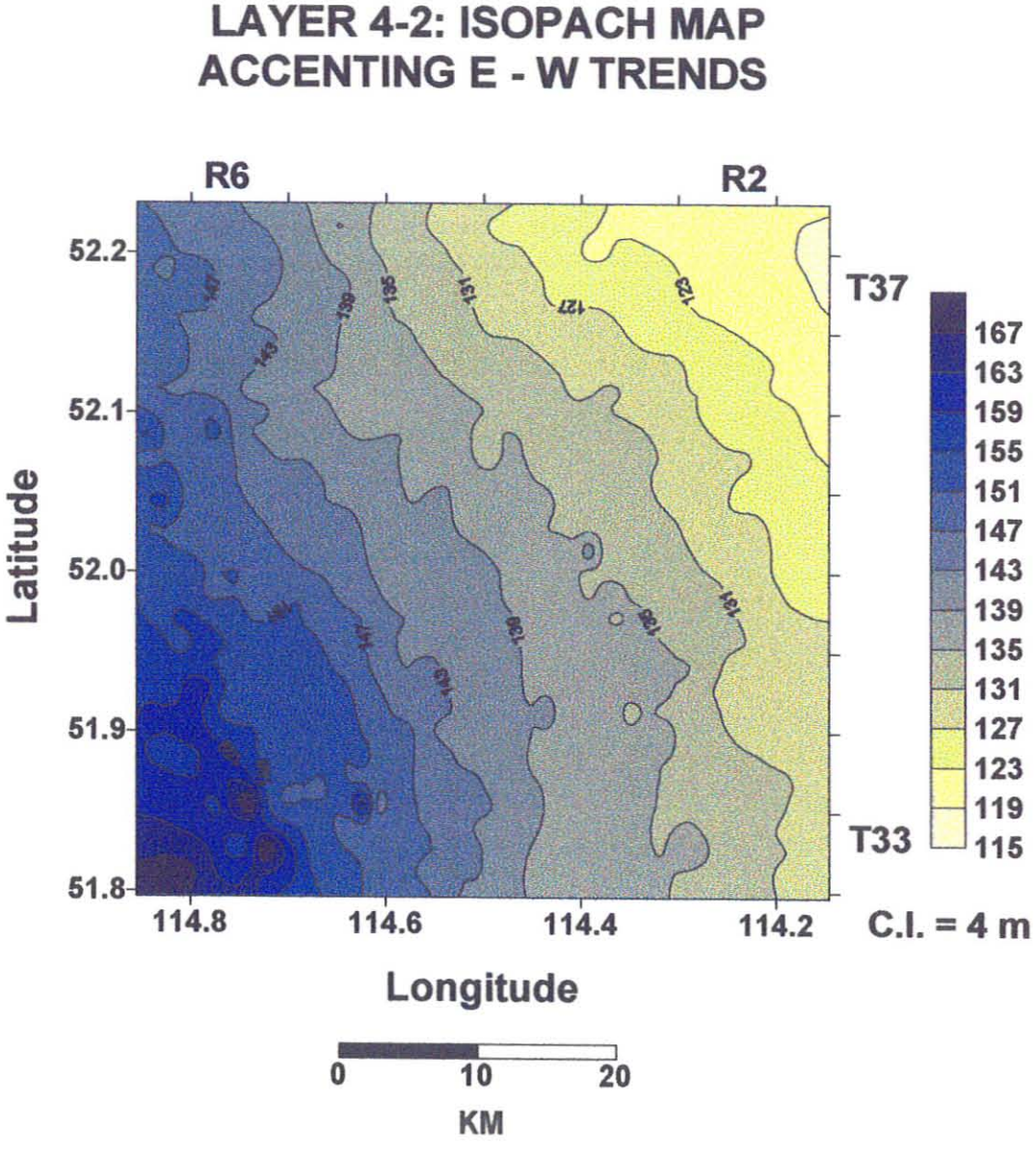
LAYER 4-2: ISOPACH MAP
ACCENTING E - W TRENDS
R6
R2
T37
T33
52.2
52.1
52.0
51.9
51.8
Latitude
114.8
114.6
114.4
114.2
Longitude
C.I. = 4 m
167
163
159
155
151
147
143
139
135
131
127
123
119
115
0
10
20
KM

Figure 15.

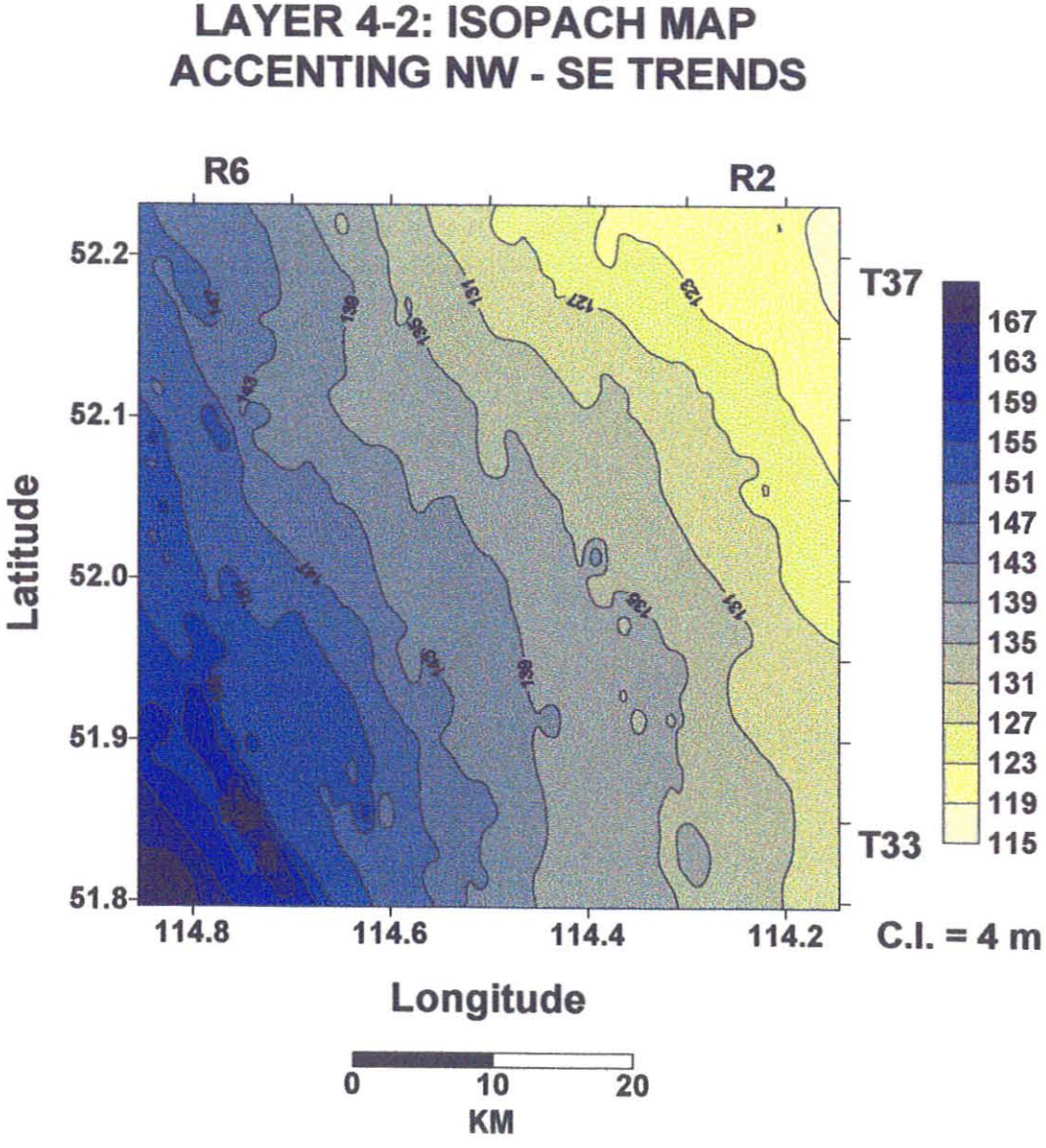
LAYER 4-2: ISOPACH MAP
ACCENTING NW - SE TRENDS
R6
R2
T37
T33
52.2
52.1
52.0
51.9
51.8
Latitude
114.8
114.6
114.4
114.2
Longitude
C.I. = 4 m
167
163
159
155
151
147
143
139
135
131
127
123
119
115
0
10
20
KM

Figure 16.

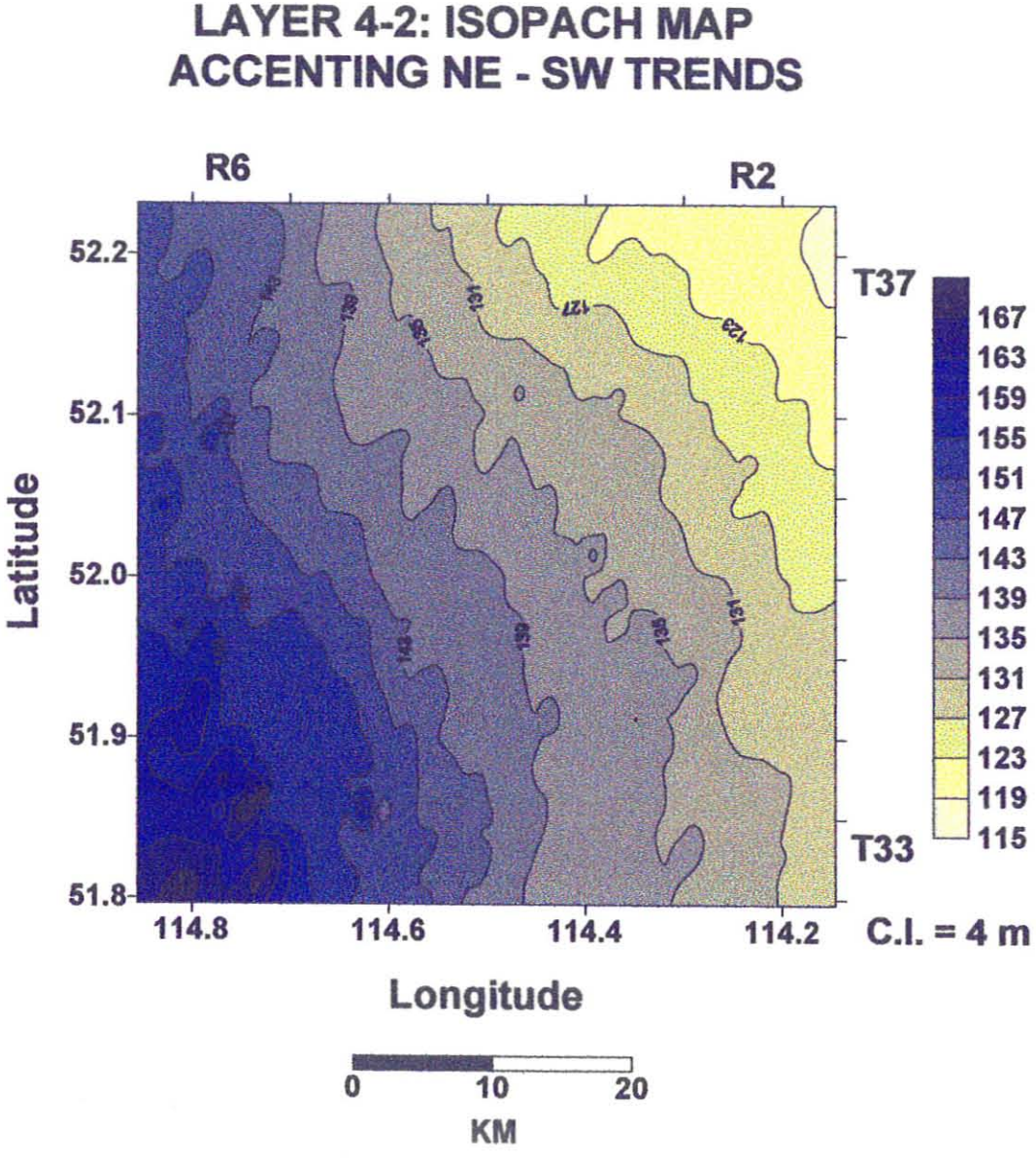
LAYER 4-2: ISOPACH MAP
ACCENTING NE - SW TRENDS
R6
R2
T37
T33
52.2
52.1
52.0
51.9
51.8
Latitude
114.8
114.6
114.4
114.2
Longitude
C.I. = 4 m
167
163
159
155
151
147
143
139
135
131
127
123
119
115
0
10
20
KM

Figure 17.

Polynomial Regression was used to define large scale trends and patterns in the isopach data. A quadratic trend surface polynomial was applied to each layer, and the resulting grid contoured.

Residual maps were also constructed for each layer in order to observe possible underlying, or smaller trends in the data. The Grid Math command in Surfer was used to compute the vertical difference between the Z value in the isopach data file and the interpolated Z value on the gridded quadratic trend surface.

CHAPTER 5: RESULTS

5.1 Presentation of Maps

For every layer indicated in the cross section (Figure 12) an isopach map, a quadratic trend surface map, and a residual map were produced. The contours are scaled in meters as indicated by the Contour Interval (C.I). On the isopach maps and quadratic trend surface maps the maximum thicknesses are indicated in deep navy blue and the minimum thicknesses in chalk yellow. The contours on the residual maps are colour scaled from deep navy blue to white to red. For the residual maps, the negative thickness values, shown in deep navy blue, represent points where the Z value interpolated by the kriging grid is less than the Z value interpolated by the polynomial regression quadratic trend grid. The positive values, shown in red, represent points where the Z value interpolated by the kriging grid is greater than the Z value interpolated by the polynomial regression quadratic trend grid. The points shown in white represent zero difference between the kriging grid and the polynomial trend surface maps. The colours on the residual maps appear to "bleed" in places as the colours produced on the map were created from an image map in Surfer and overlain on the contour map. The image map blends the colours to produce a smooth colour gradation over the map, which does not match perfectly with the grid contours displayed on the residual map.

5.1.1 Layer 2-1

Layer 2-1 ("read as pick 2 minus pick 1") is a shale interval in the Lea Park Formation. It extends from an inflection point (pick 2) to the top of a sandy kick (pick 1) on the well logs.

The maps produced from Layer 2-1 are shown in Figures 18, 19, and 20. The isopach thicknesses of this layer range from 24 to 36.9 m. The average thickness is 30.6 m with a standard deviation of 2.1 m. On the isopach map (Figure 18), the layer is thickest in the northeast and southwest corners. The thinnest regions trend NW - SE across the map. Most isopachs have a NW - SE orientation. The quadratic trend surface map (Figure 19) shows NW - SE contour trends in a trough shape with the thinnest area in the southeast. The thicknesses on the residual map (Figure 20) range from -2.4 to 4.3 m. The positive and negative contours also trend NW - SE. The negative contours occur in the SW and NE corners and through the interior of the map in a NW - SE direction. The overall trends in the residual map are very similar to those in the isopach map and quadratic trend surface map.

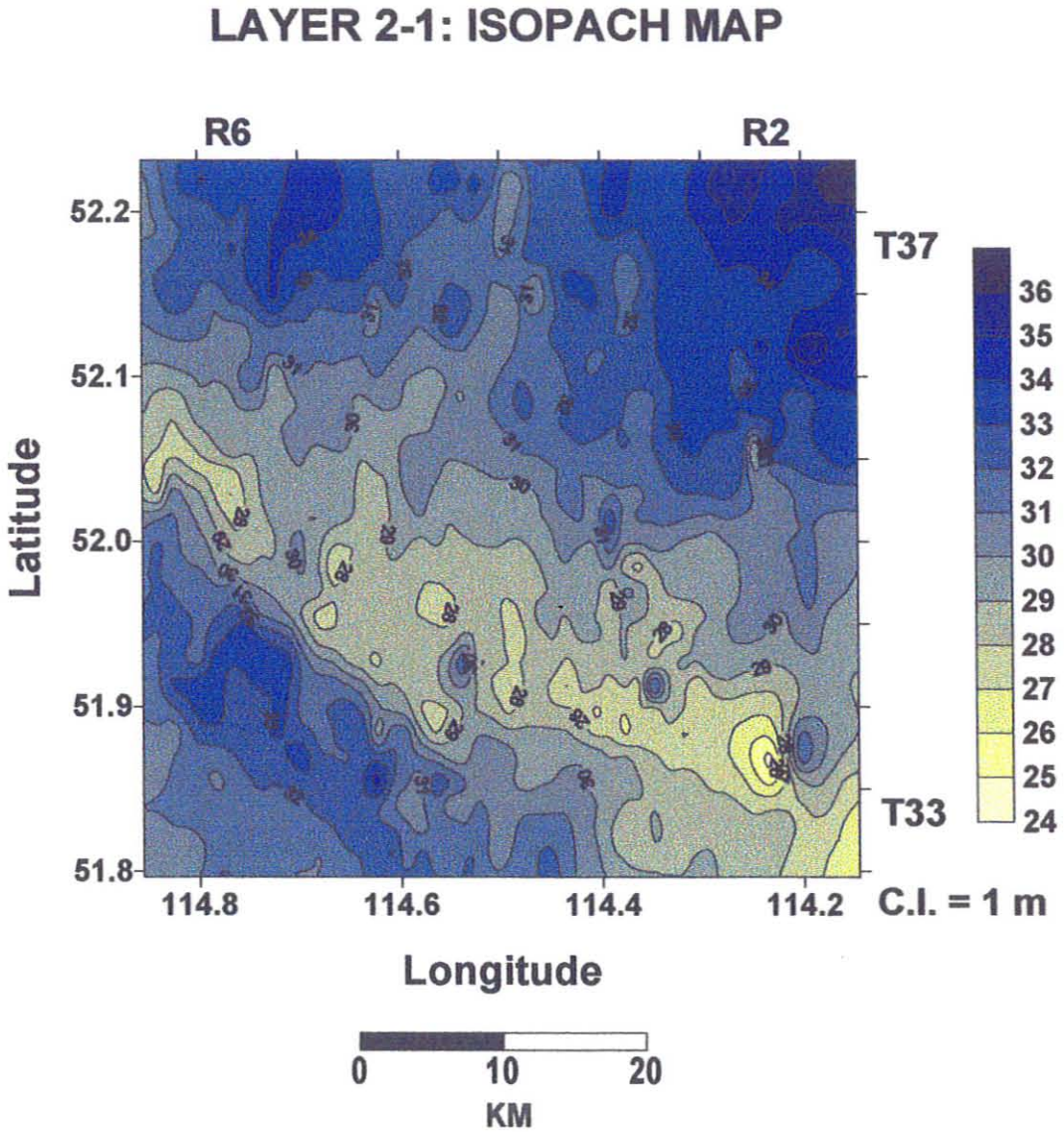
LAYER 2-1: ISOPACH MAP
R6
R2
T37
T33
52.2
52.1
52.0
51.9
51.8
Latitude
114.8
114.6
114.4
114.2
Longitude
C.I. = 1 m
36
35
34
33
32
31
30
29
28
27
26
25
24
0
10
20
KM

Figure 18.

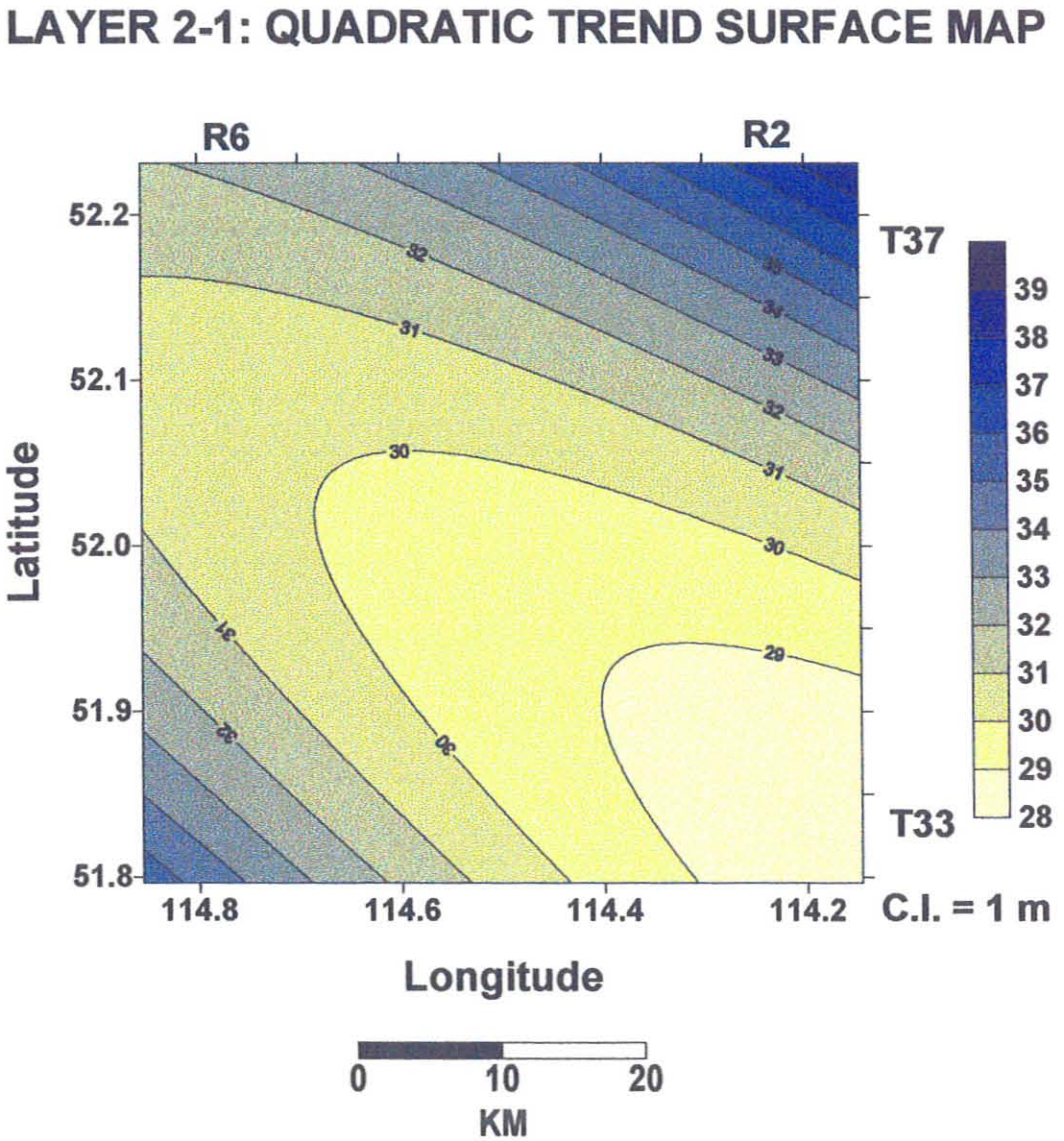
LAYER 2-1: QUADRATIC TREND SURFACE MAP
R6
R2
T37
T33
52.2
52.1
52.0
51.9
51.8
Latitude
114.8
114.6
114.4
114.2
Longitude
C.I. = 1 m
39
38
37
36
35
34
33
32
31
30
29
28
0
10
20
KM

Figure 19.

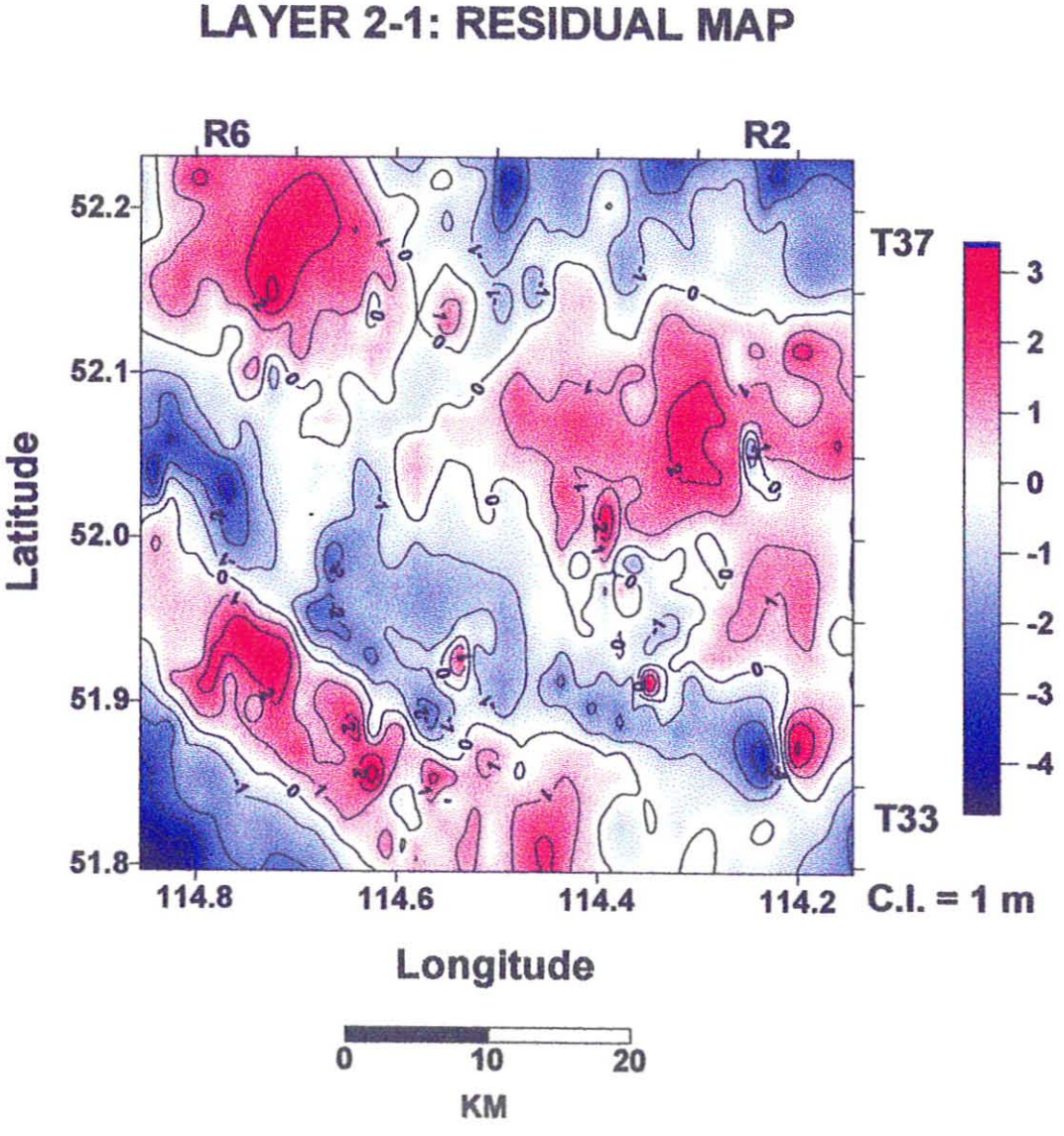
LAYER 2-1: RESIDUAL MAP
R6
R2
T37
T33
52.2
52.1
52.0
51.9
51.8
Latitude
114.8
114.6
114.4
114.2
Longitude
C.I. = 1 m
3
2
1
0
-1
-2
-3
-4
0
10
20
KM

Figure 20.

5.1.2 Layer 4-2

Layer 4-2 is dominantly shale and contains the First White Speckled Shale. This layer extends from the base of a "bump" in the resistivity log (pick 4) to the inflection point used to determine pick 2.

The maps of Layer 4-2 are shown in Figure 21, 22, and 23. The isopach thicknesses of this unit range from 118.3 to 173 m. The average thickness is 139.9 m with a standard deviation of 9.5 m. On the isopach map (Figure 21), the layer is thickest in the southwest corner and thinnest in the northeast corner. The isopachs have a generally NNW - SSE orientation. The quadratic trend surface map (Figure 22) for this layer also shows NNW - SSE and NW - SE trends. On the residual map (Figure 23) the thicknesses range from -4.5 to 14.0 m. The positive and negative values are bounded by N - S and E - W contours. In the northwest corner the positive contours trend E - W, as compared to the N - S contour in this area on the isopach map. The positive trend in the east is oriented N - S at an oblique angle to the regional (isopach and quadratic trend surface trends) NNW - SSE trends in this area. The negative values form trends that are oblique to the regional trend. The negative trend in the east trends N - S. At 114.6° longitude, the negative contours extend N - S. Overall, the residual contours trend N - S or E - W at oblique angles to the trends illustrated by the isopach map and the quadratic trend surface map.

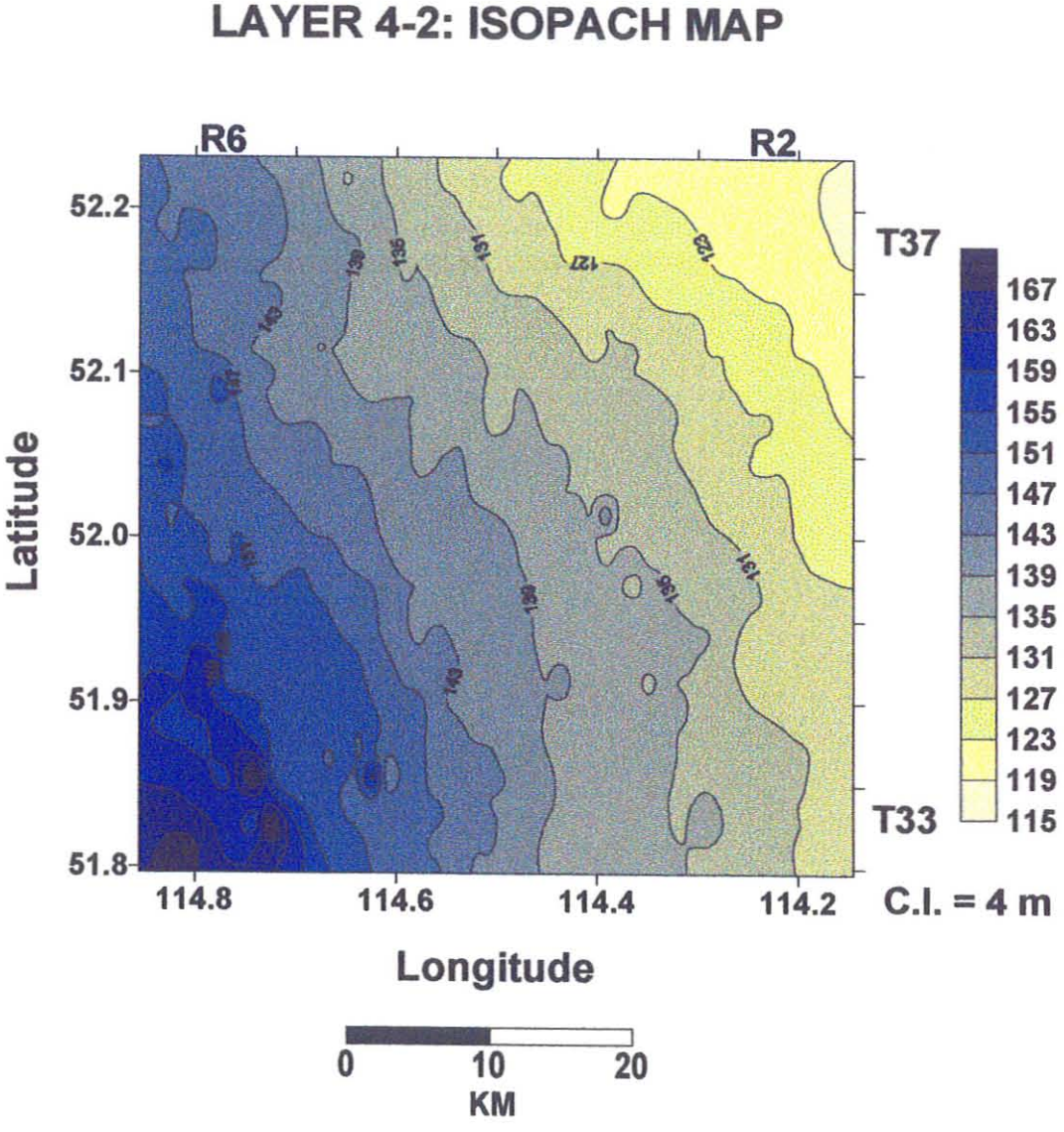
LAYER 4-2: ISOPACH MAP
R6
R2
T37
T33
52.2
52.1
52.0
51.9
51.8
Latitude
114.8
114.6
114.4
114.2
Longitude
C.I. = 4 m
167
163
159
155
151
147
143
139
135
131
127
123
119
115
0
10
20
KM

Figure 21.

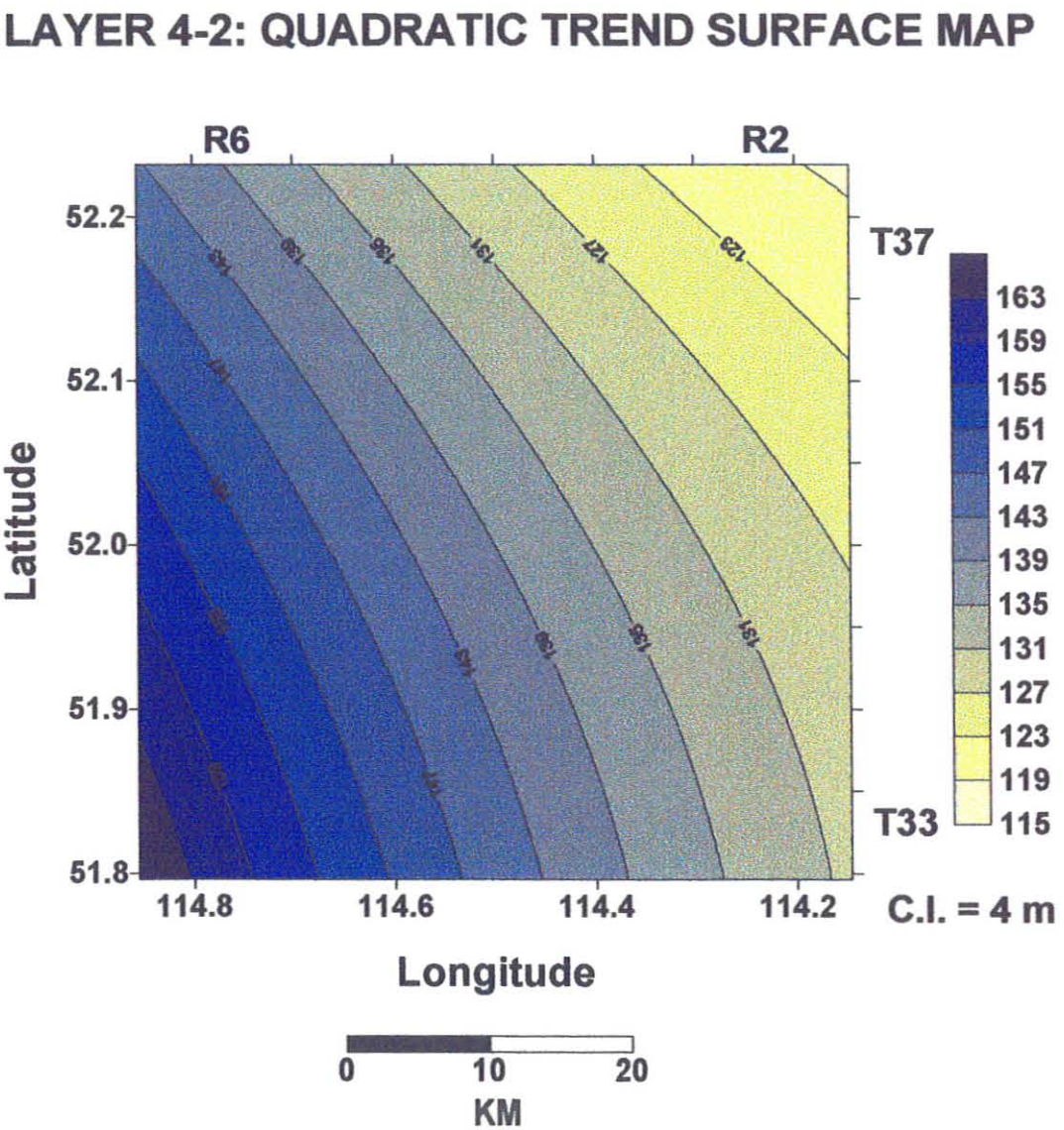
LAYER 4-2: QUADRATIC TREND SURFACE MAP
R6
R2
T37
T33
52.2
52.1
52.0
51.9
51.8
Latitude
114.8
114.6
114.4
114.2
Longitude
163
159
155
151
147
143
139
135
131
127
123
119
115
C.I. = 4 m
0
10
20
KM

Figure 22.

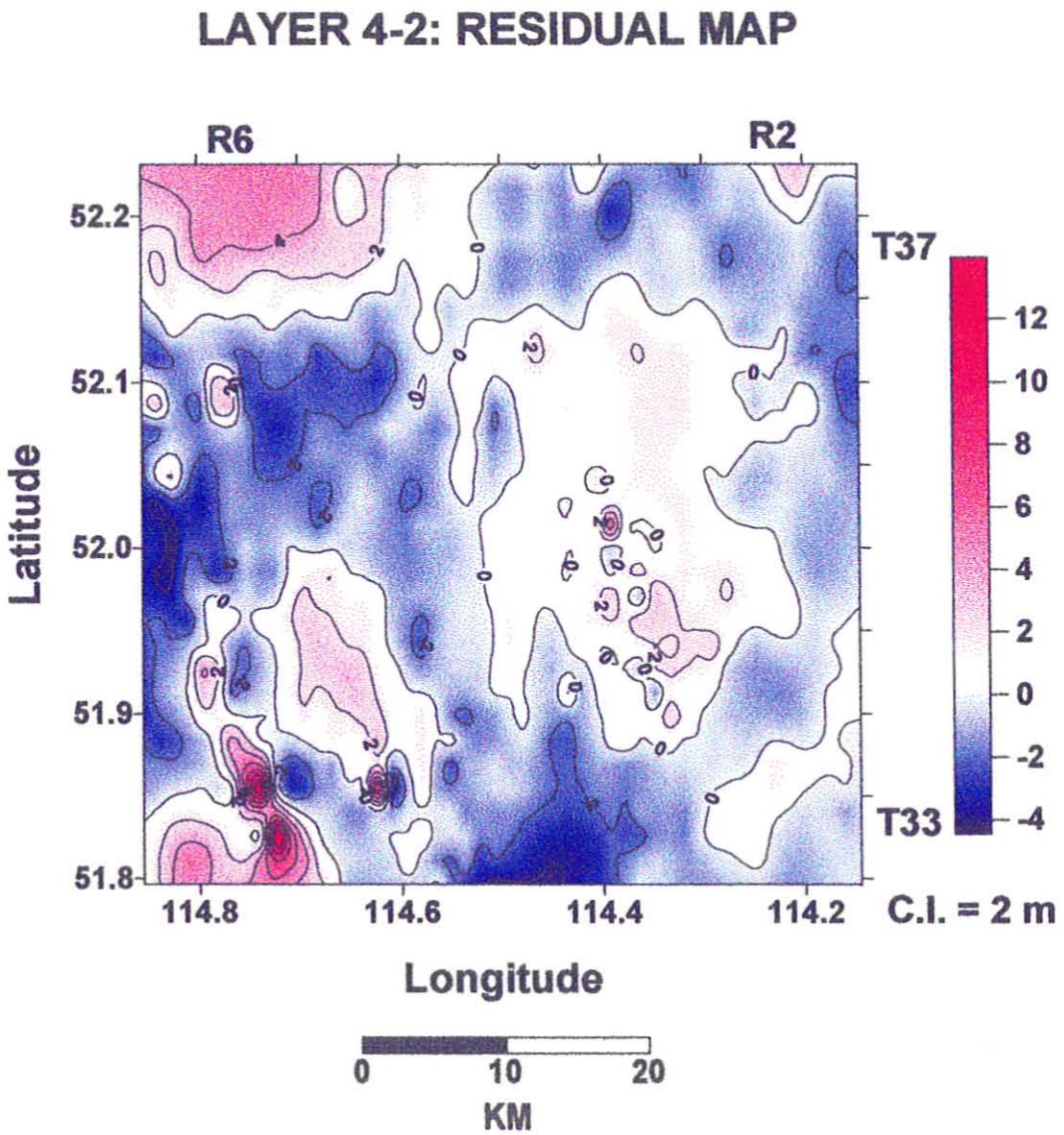
LAYER 4-2: RESIDUAL MAP
R6
R2
T37
T33
52.2
52.1
52.0
51.9
51.8
Latitude
114.8
114.6
114.4
114.2
Longitude
12
10
8
6
4
2
0
-2
-4
C.I. = 2 m
0
10
20
KM

Figure 23.

5.1.3 Layer 6-4

Layer 6-4 extends from pick 6, the inflection point defining a sandier upward succession, to the inflection point described as pick 4. The pattern of the well log in this layer shows a dominantly muddy interval.

The maps of Layer 6-4 are shown in Figure 24, 25, and 26. The isopach thicknesses of this layer range from 64.6 to 106 m. The average thickness is 74.6 m with a standard deviation of 6.0 m. The contours on the isopach map (Figure 24) are thickest in the southwest and thinnest in the east. The isopach trends thin from the west to the east. The overall contour trends have a NW - SE orientation in the southern area, swinging to a N - S trend in the northern part of the map. The contours on quadratic trend surface map (Figure 25) also show this change from NW - SE in the south, to N - S in the north. The trend surface map also shows the thickest area in the southwest and the thinnest in the north-northeast. The residual thicknesses computed for this layer range from -5.7 to 12.9 m as shown in Figure 26. No strong trends exist in the residual map.

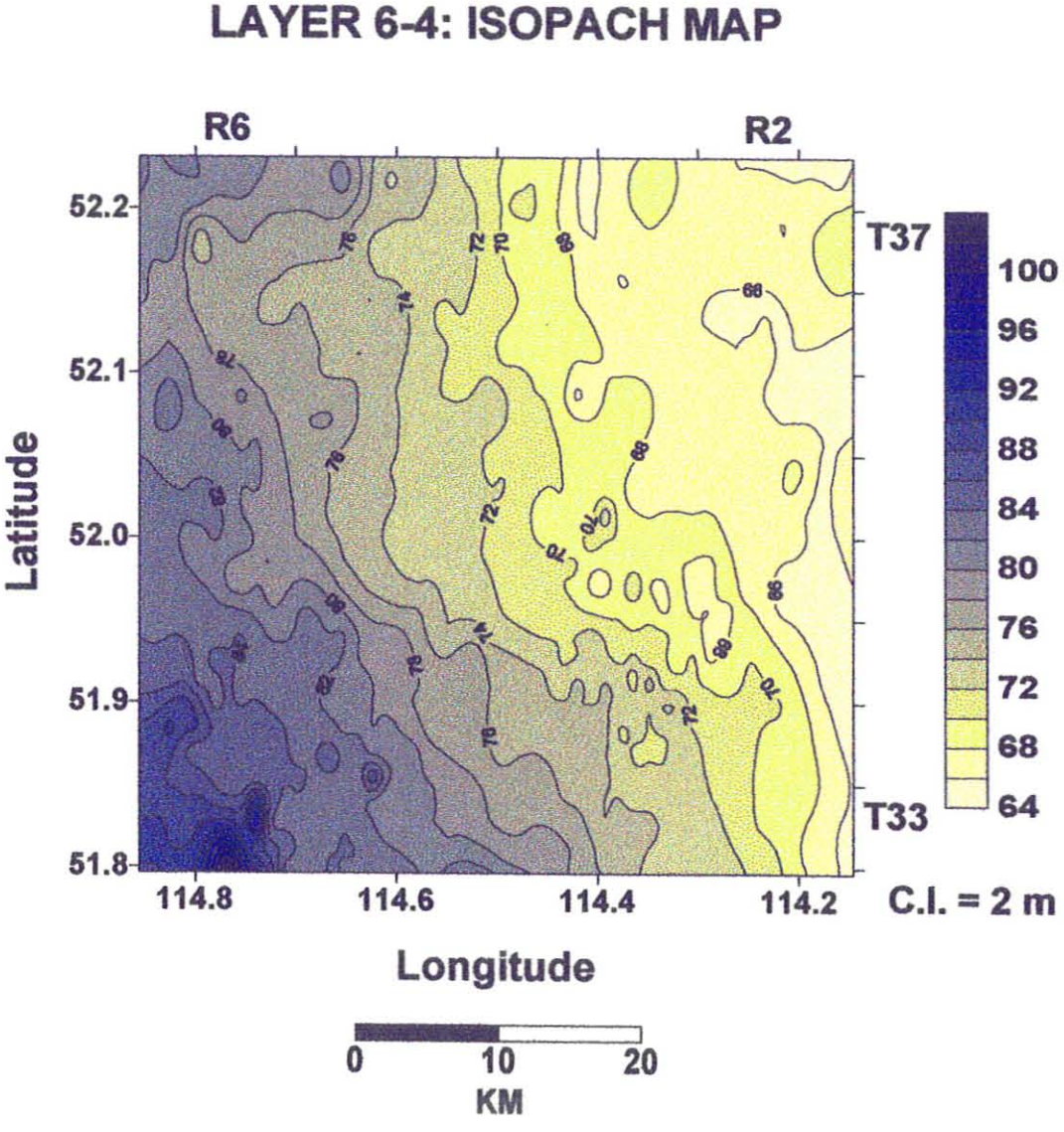
LAYER 6-4: ISOPACH MAP
R6
R2
T37
T33
52.2
52.1
52.0
51.9
51.8
Latitude
114.8
114.6
114.4
114.2
Longitude
C.I. = 2 m
100
96
92
88
84
80
76
72
68
64
0
10
20
KM

Figure 24.

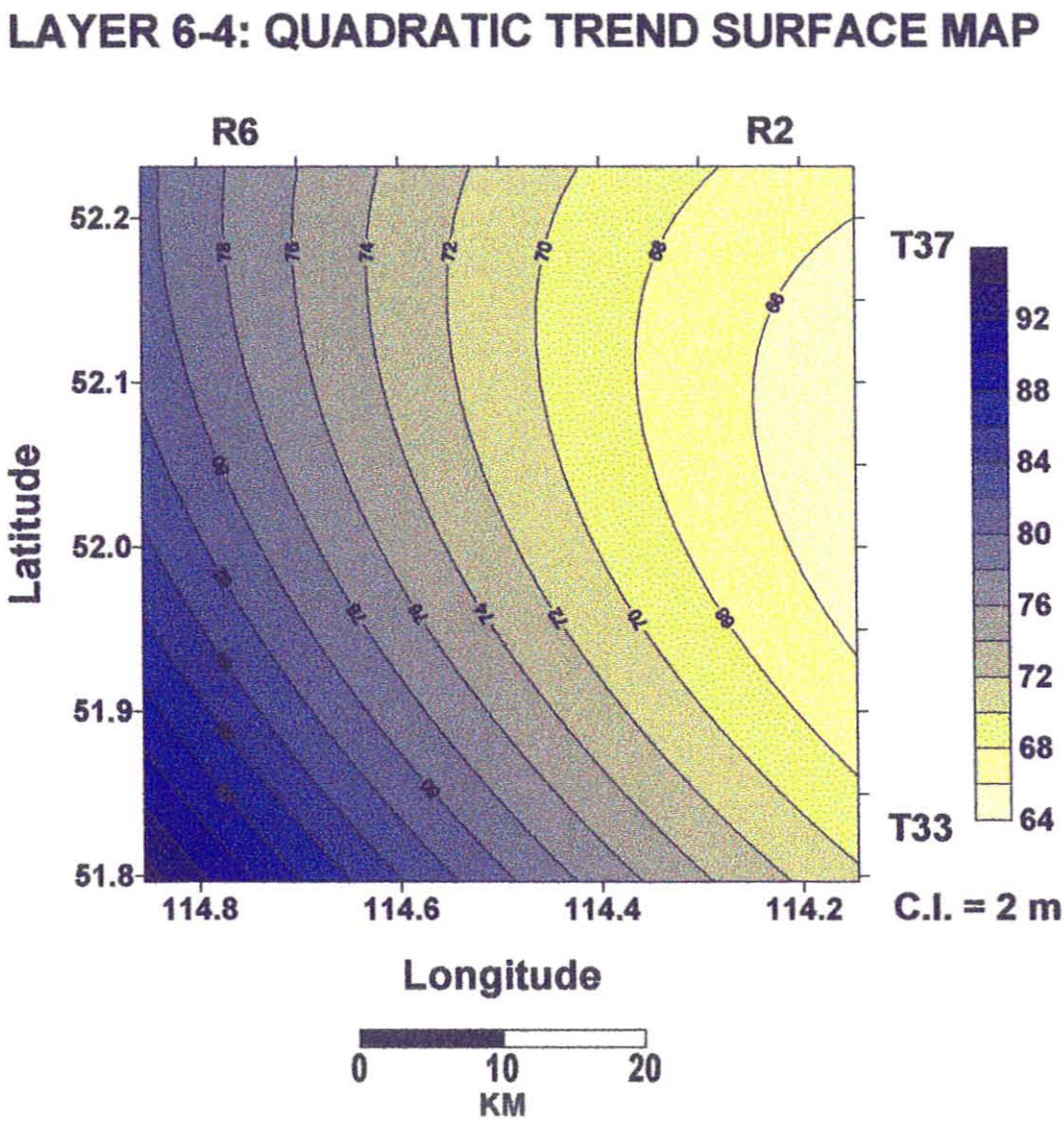
LAYER 6-4: QUADRATIC TREND SURFACE MAP
R6
R2
52.2
52.1
52.0
51.9
51.8
Latitude
114.8
114.6
114.4
114.2
Longitude
T37
T33
92
88
84
80
76
72
68
64
C.I. = 2 m
0
10
20
KM

Figure 25.

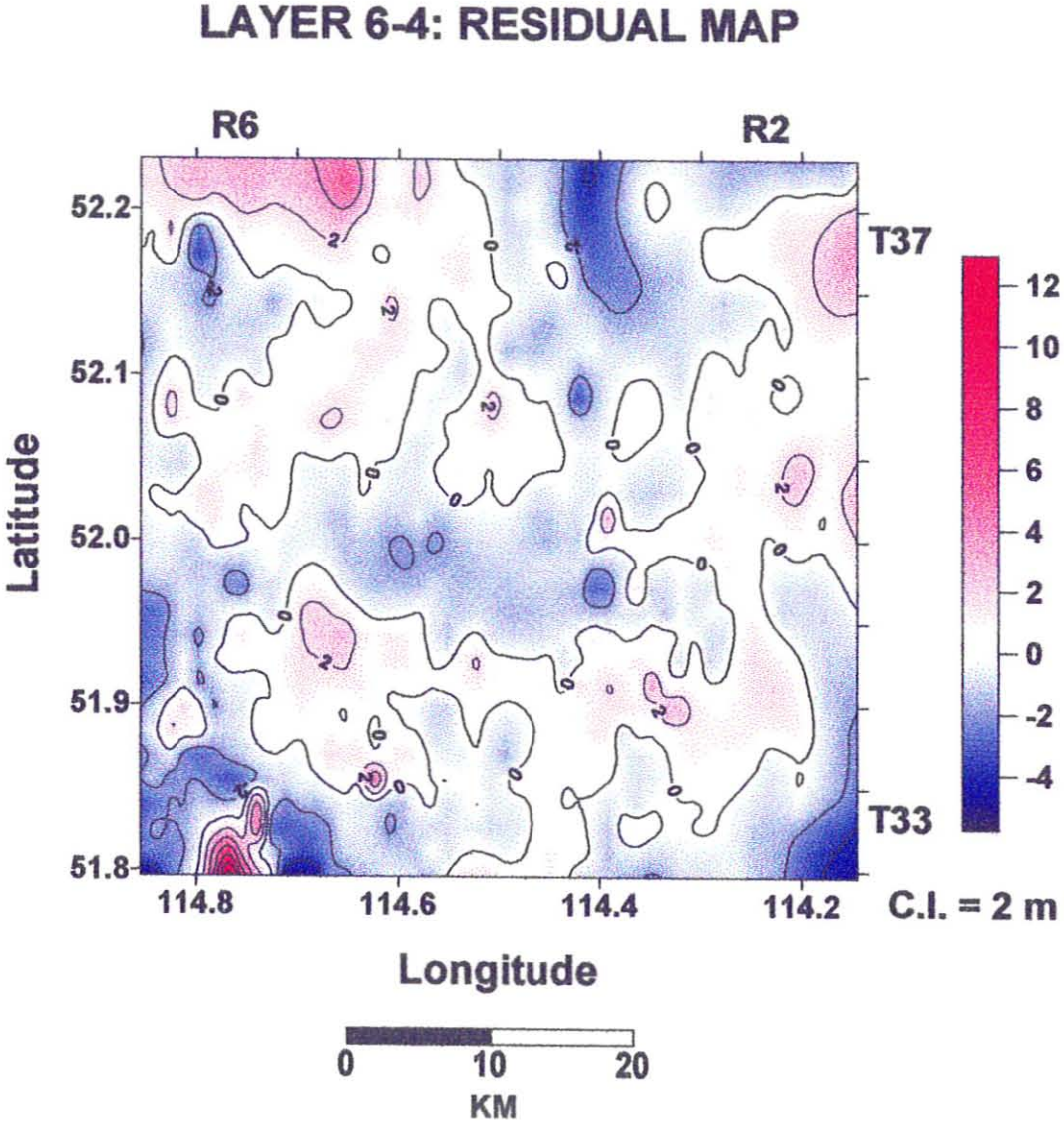
LAYER 6-4: RESIDUAL MAP
R6
R2
T37
T33
52.2
52.1
52.0
51.9
51.8
Latitude
114.8
114.6
114.4
114.2
Longitude
12
10
8
6
4
2
0
-2
-4
C.I. = 2 m
0
10
20
KM

Figure 26.

5.1.4 Layer 7-6

Layer 7-6 extends from the E5 flooding surface (pick 7) to an inflection point used to define pick 6. The log response in this layer is very quiet, indicating a shale interval.

The maps of Layer 7-6 are shown in Figures 27, 28, and 29. The isopach thicknesses of this layer range from 48 to 87 m. The average thickness is 57.7 m with a standard deviation of 4.7 m. On the isopach map (figure 27), the isopach lines trend NW - SE parallel to the deformed belt in the southwest corner, and NE - SW over the rest of the map. The area is thickest in the southwest corner that is bounded by the NW - SE contour trends. There is an overall thinning from the southeast to the northwest in this layer. The quadratic trend surface map (Figure 28) for this layer shows NE - SW contour trends in the thickest area that occurs in the southeast. The orientation of the contour lines change to an E -W in the north. On the residual map (Figure 29), the thicknesses range from -5.1 to 22.1 m. Most of the contour trends on the residual map trend NW - SE, which is perpendicular to the contour trends in the isopach and quadratic trend surface maps. There is a well defined high in the SW with NW - SE trending contours that are the same as the regional trends observed in this layer.

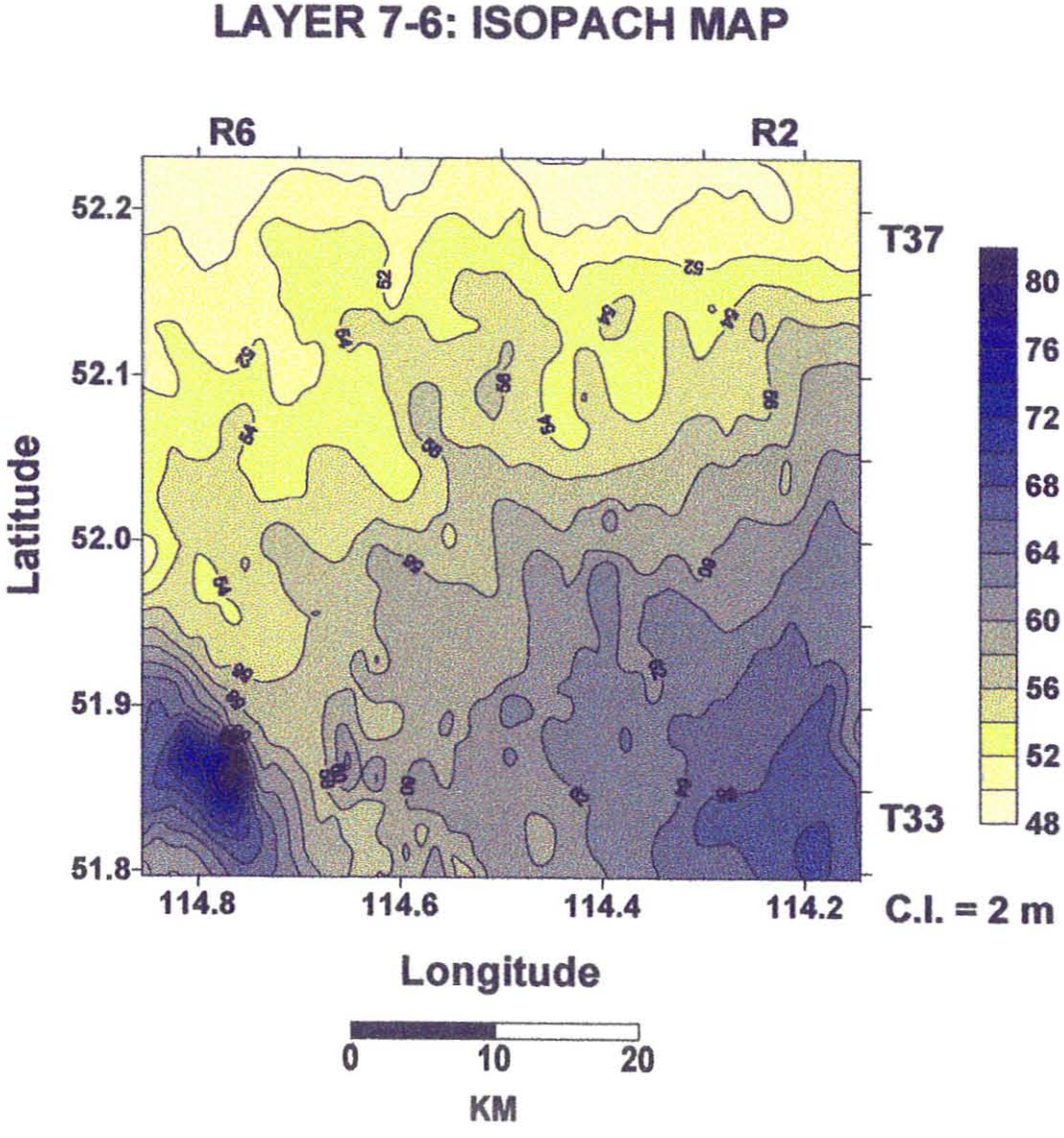
LAYER 7-6: ISOPACH MAP
R6
R2
T37
T33
52.2
52.1
52.0
51.9
51.8
Latitude
114.8
114.6
114.4
114.2
Longitude
C.I. = 2 m
80
76
72
68
64
60
56
52
48
0
10
20
KM

Figure 27.

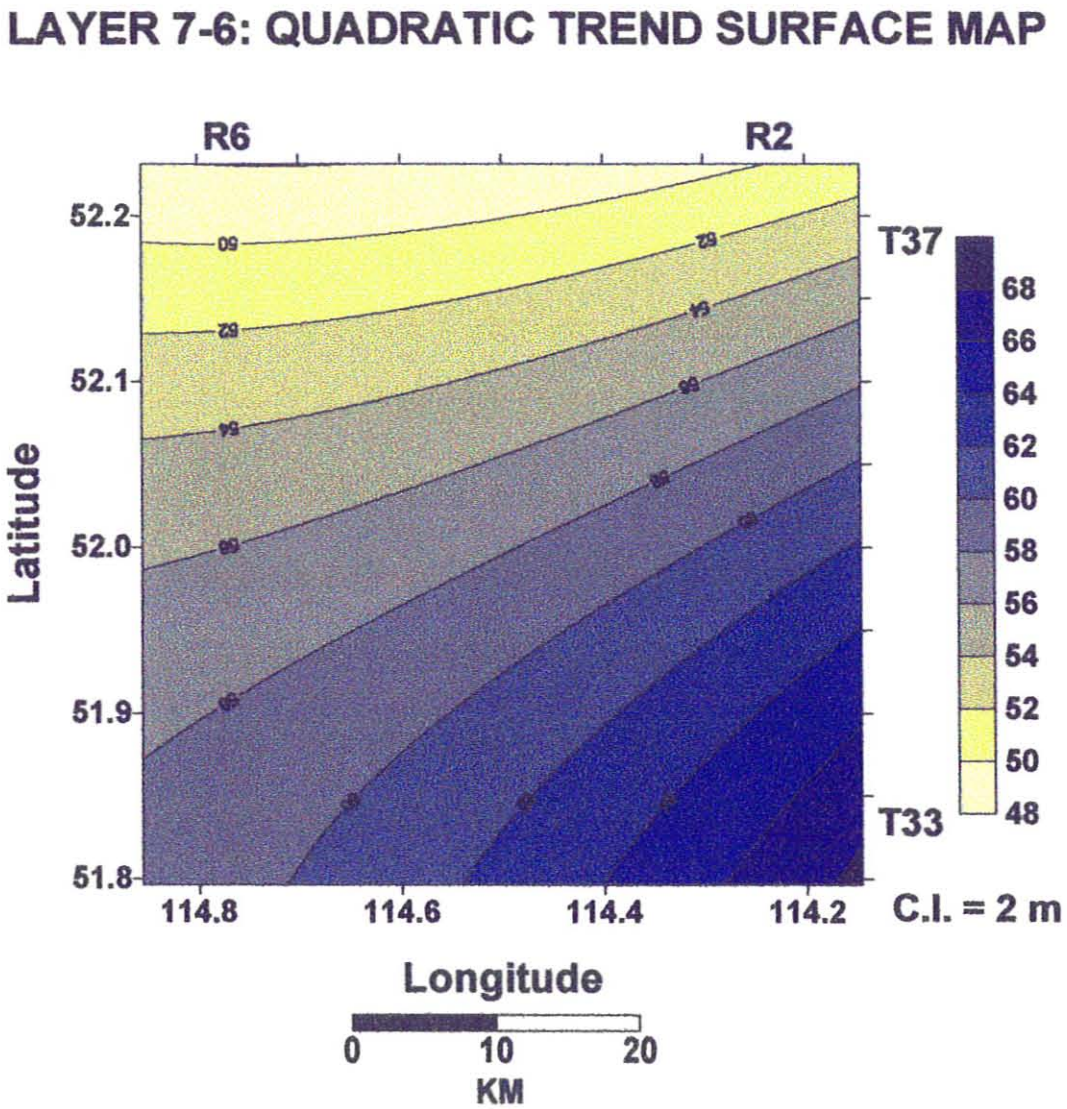
LAYER 7-6: QUADRATIC TREND SURFACE MAP
R6
R2
52.2
52.1
52.0
51.9
51.8
Latitude
T37
T33
68
66
64
62
60
58
56
54
52
50
48
114.8
114.6
114.4
114.2
C.I. = 2 m
Longitude
0
10
20
KM

Figure 28.

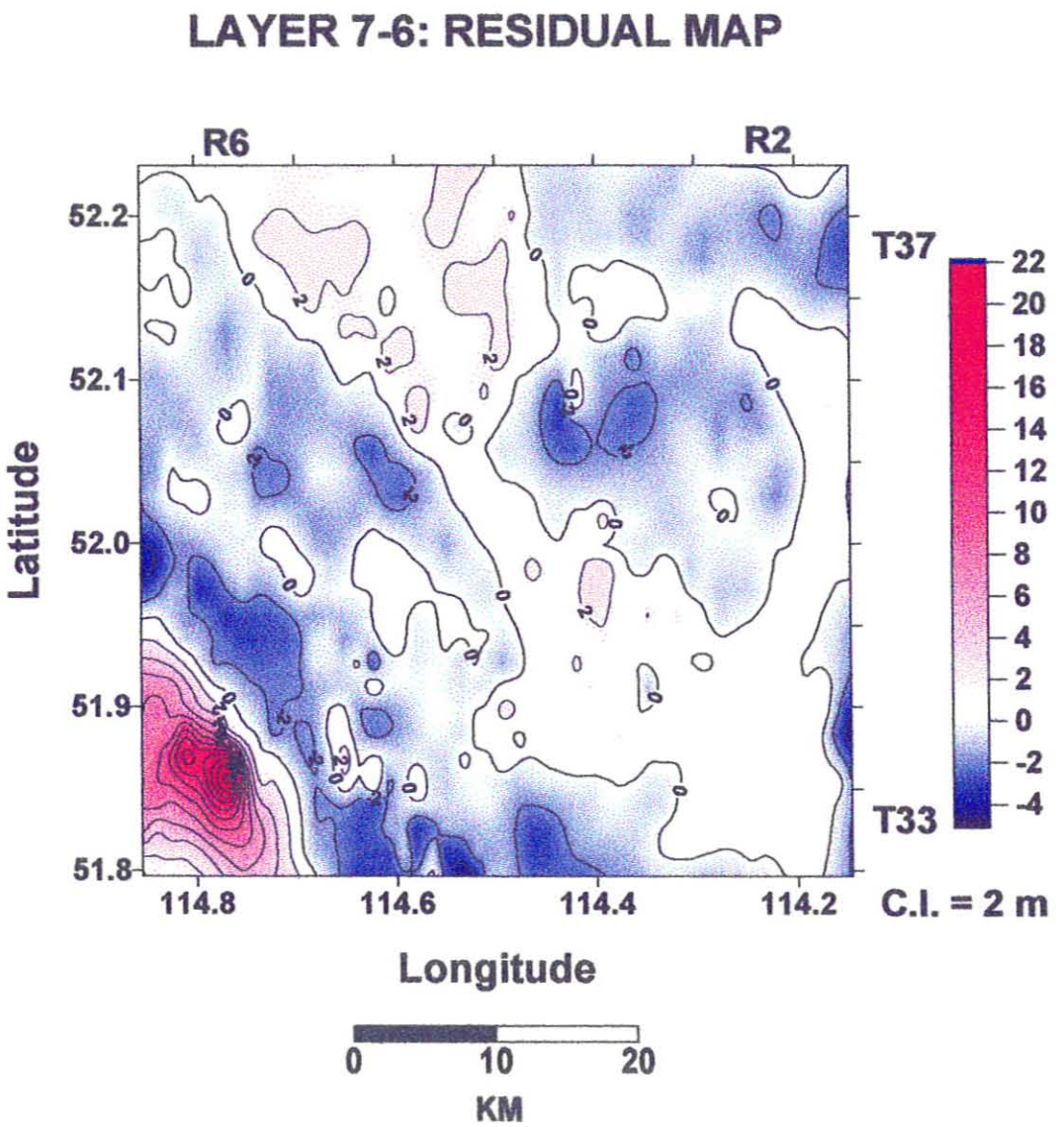
LAYER 7-6: RESIDUAL MAP
R6
R2
52.2
52.1
52.0
51.9
51.8
Latitude
114.8
114.6
114.4
114.2
Longitude
T37
T33
22
20
18
16
14
12
10
8
6
4
2
0
-2
-4
C.I. = 2 m
0
10
20
KM

Figure 29.

5.1.5 Layer 8-7

Layer 8-7 extends from the base of the Cardium (pick 8) to the E5 flooding surface (pick 7). This layer shows an overall coarsening upward facies succession.

The maps of Layer 8-7 are shown in Figures 30, 31, and 32. The isopach thicknesses of this unit range from 62 to 91.4 m. The average thickness is 77.5 m with a standard deviation of 5.7 m. On the isopach map (Figure 30), the contour lines are oriented NW - SE in the SW (which is the thickest area) but gradually veer to N - S in the east. There is an overall thinning in this layer from the west to the east. The quadratic trend surface map (Figure 31) shows NNW - SSE contour lines. On the residual map (Figure 32), the thicknesses range from -10.7 to 8.2 m. The positive and negative trends have the same orientation as the regional isopach trends. Note the extreme low in the southwest that has NW - SE oriented contours.

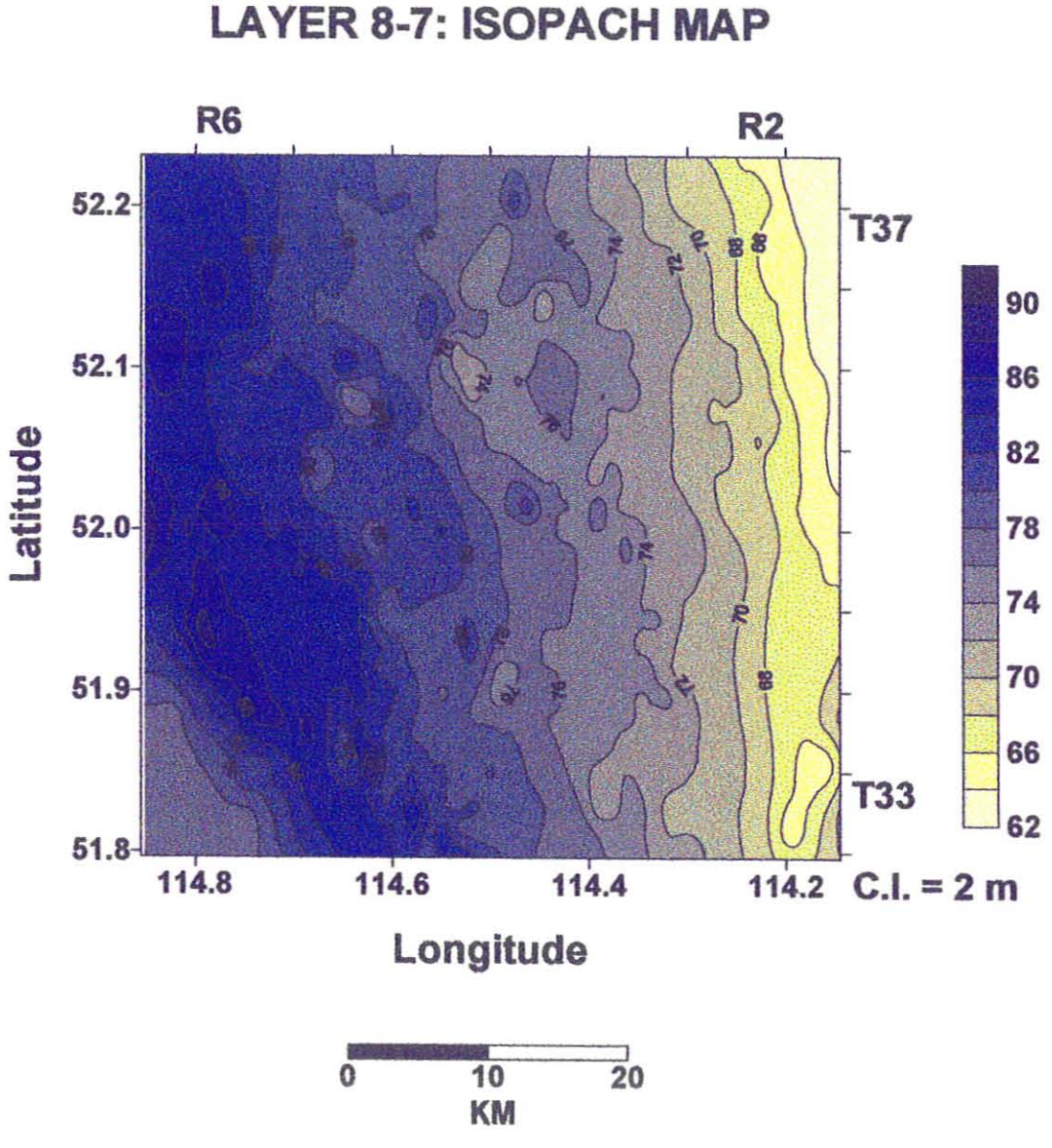
LAYER 8-7: ISOPACH MAP
R6
R2
T37
T33
52.2
52.1
52.0
51.9
51.8
Latitude
114.8
114.6
114.4
114.2
Longitude
C.I. = 2 m
90
86
82
78
74
70
66
62
0
10
20
KM

Figure 30.

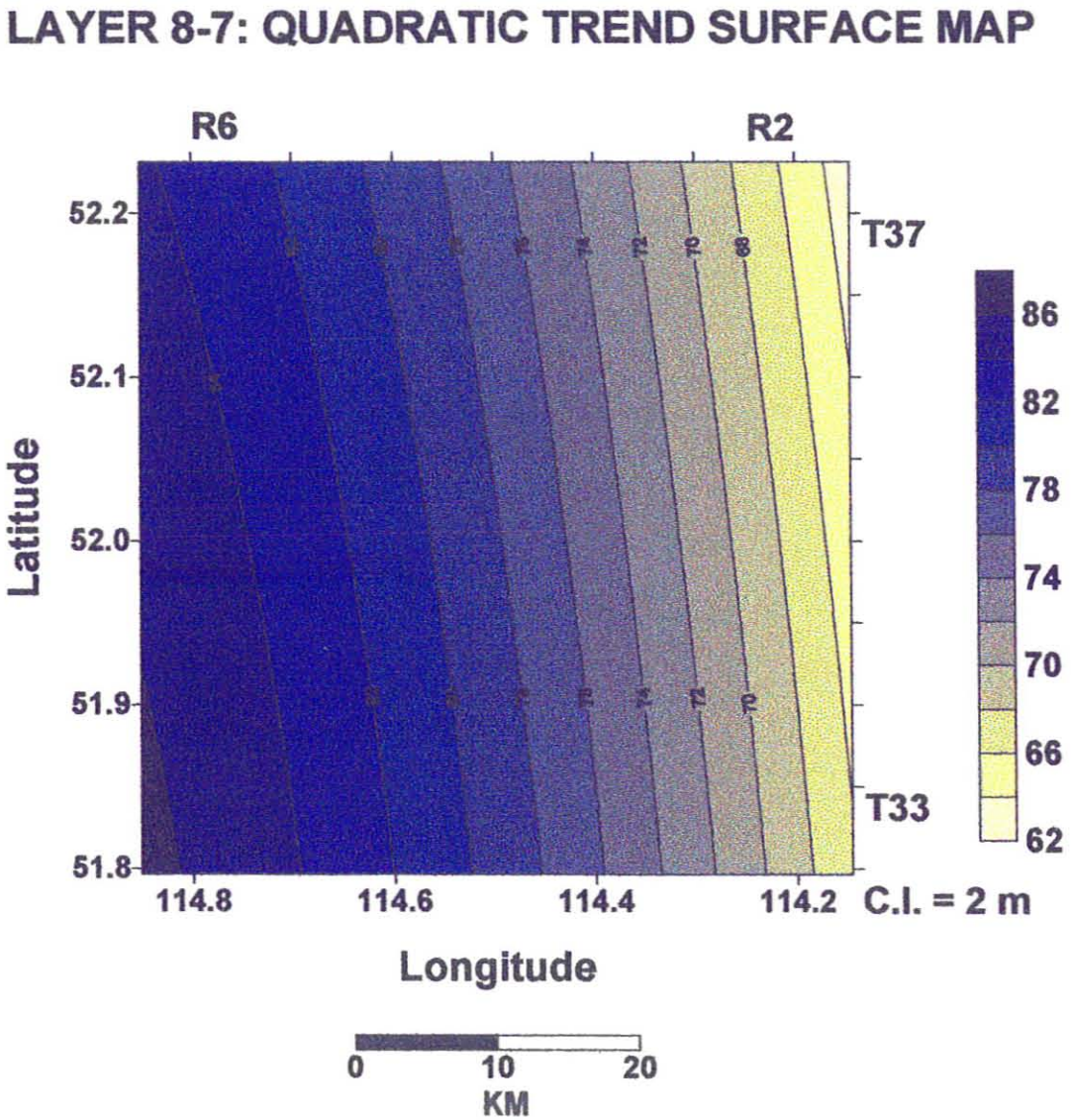
LAYER 8-7: QUADRATIC TREND SURFACE MAP
R6
R2
T37
T33
52.2
52.1
52.0
51.9
51.8
Latitude
114.8
114.6
114.4
114.2
Longitude
C.I. = 2 m
86
82
78
74
70
66
62
0
10
20
KM

Figure 31.

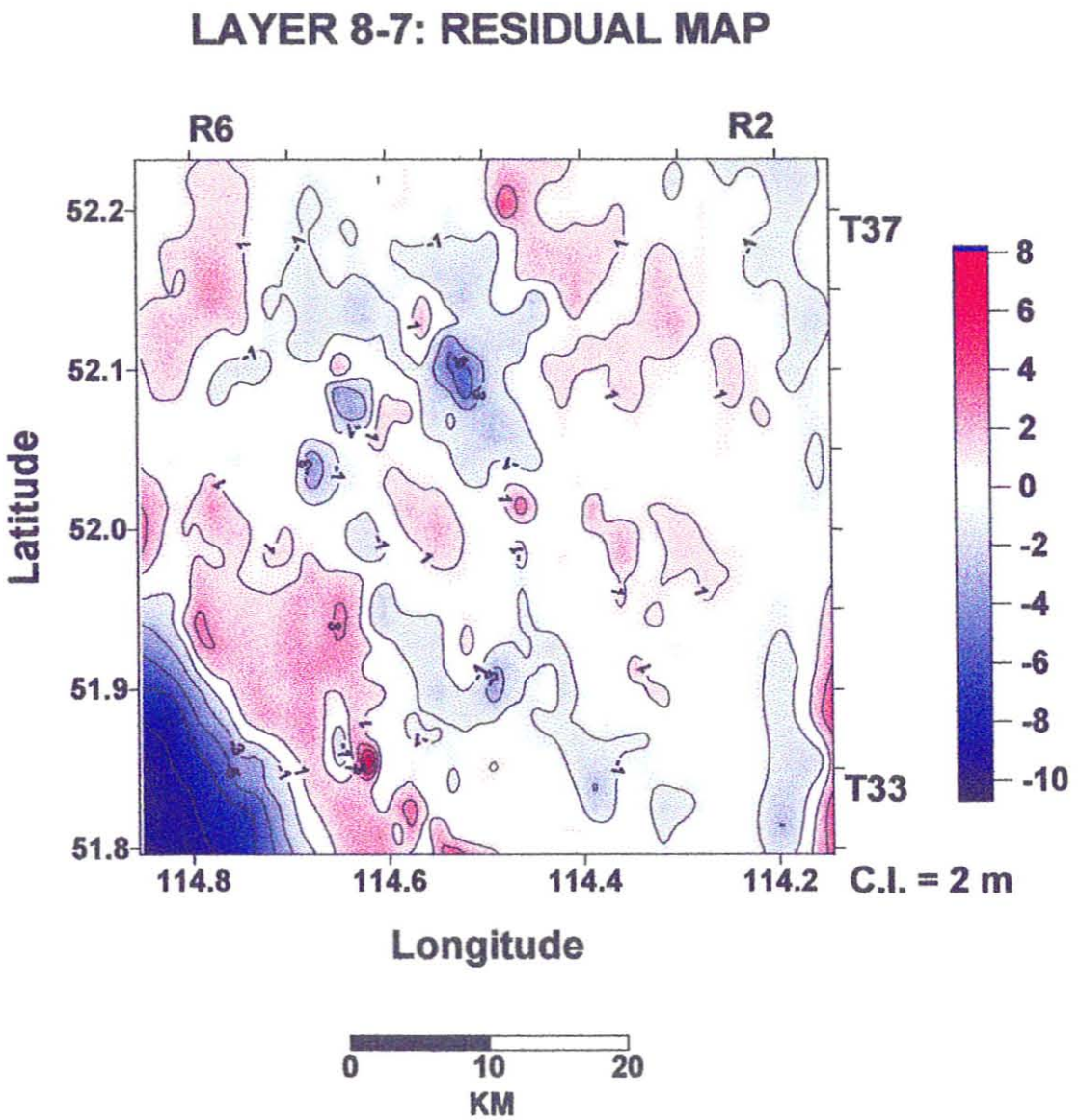
LAYER 8-7: RESIDUAL MAP
R6
R2
T37
T33
52.2
52.1
52.0
51.9
51.8
Latitude
114.8
114.6
114.4
114.2
Longitude
C.I. = 2 m
8
6
4
2
0
-2
-4
-6
-8
-10
0
10
20
KM

Figure 32.

5.1.6 Layer 9-8

Layer 9-8 extends from a flooding surface (pick 9) through a fining upward succession to the base of the Cardium.

The maps of Layer 9-8 are shown in Figures 33, 34, and 35. The isopach thicknesses of this unit range from 41 to 62.2 m. The average thickness is 50.3 m with a standard deviation of 3.7 m. On the isopach map (Figure 33), the layer is thickest in the south with approximately E - W oriented contours that veer to NE - SW as the layer becomes thinner to the northwest. The quadratic trend surface map (Figure 34) for this layer shows thinning from the southeast to the northwest with ENE - WSW contour trends in the southeast to NE - SW contour trends in the northwest. On the residual map (Figure 35), the thicknesses range from -5.9 to 6.3 m. The residual map shows no trends that resemble the isopach or quadratic trend surface maps.

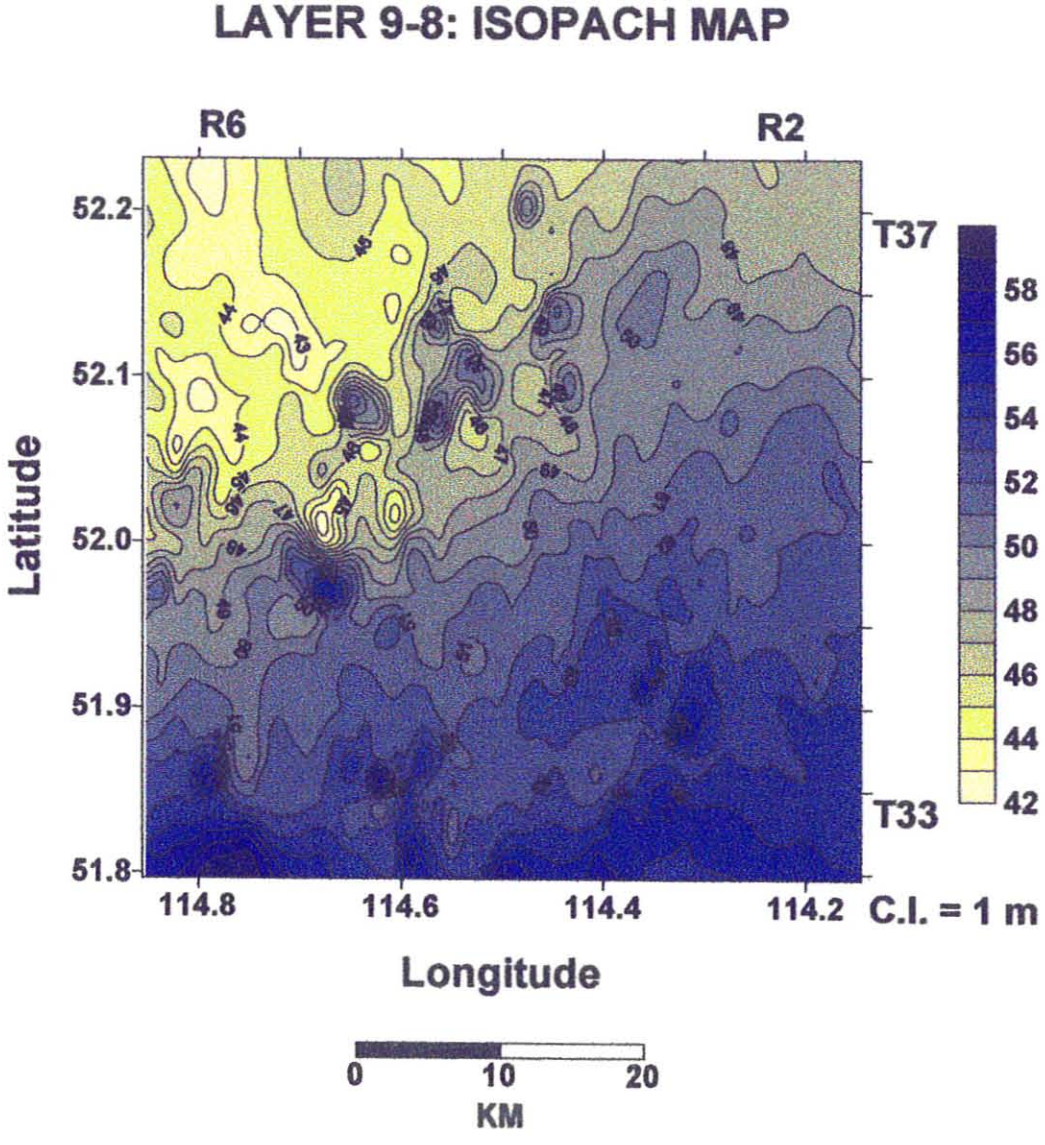
LAYER 9-8: ISOPACH MAP
R6
R2
T37
T33
52.2
52.1
52.0
51.9
51.8
Latitude
114.8
114.6
114.4
114.2
Longitude
C.I. = 1 m
58
56
54
52
50
48
46
44
42
0
10
20
KM

Figure 33.

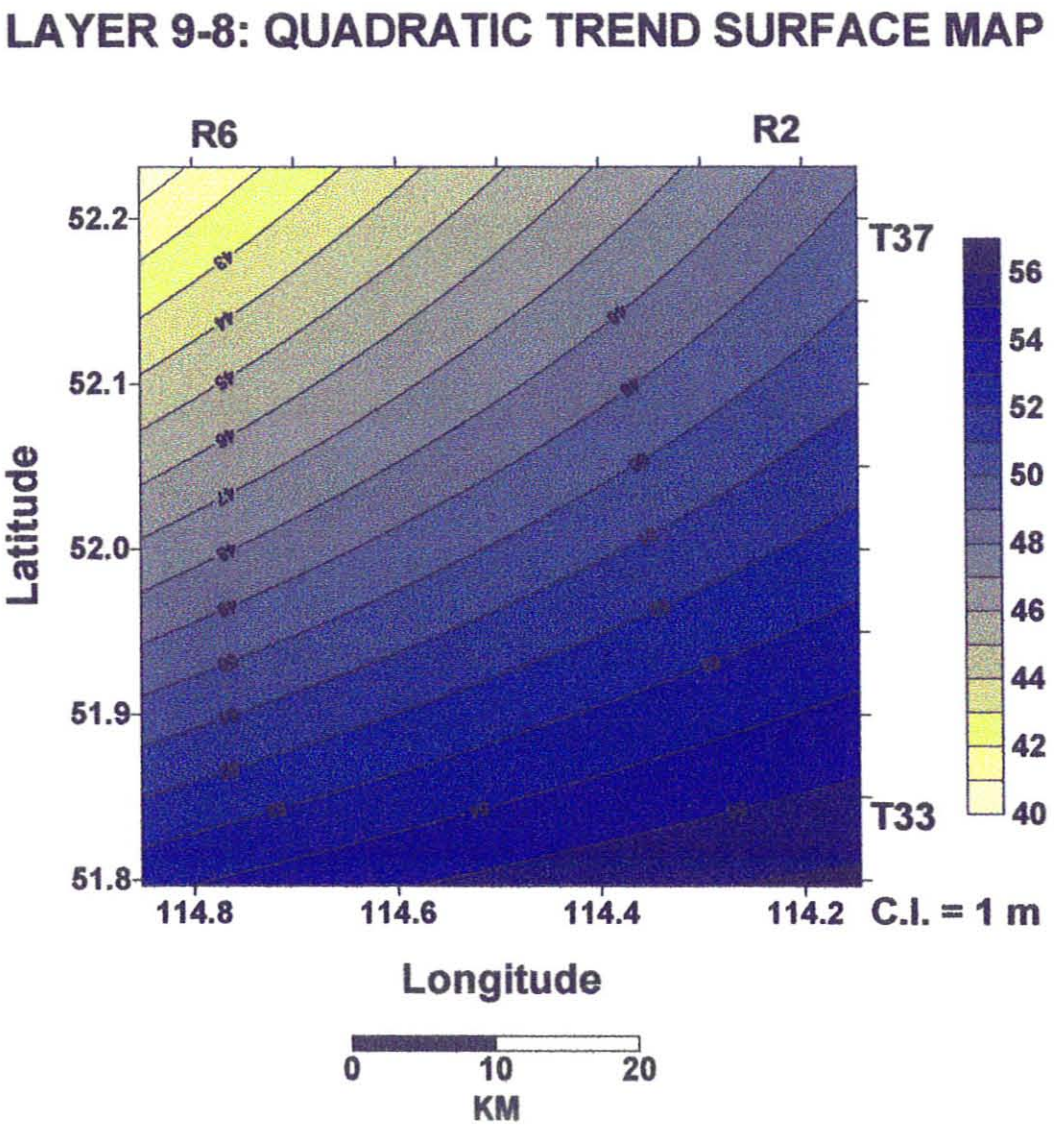
LAYER 9-8: QUADRATIC TREND SURFACE MAP
R6
R2
T37
T33
52.2
52.1
52.0
51.9
51.8
Latitude
114.8
114.6
114.4
114.2
Longitude
C.I. = 1 m
56
54
52
50
48
46
44
42
40
0
10
20
KM

Figure 34.

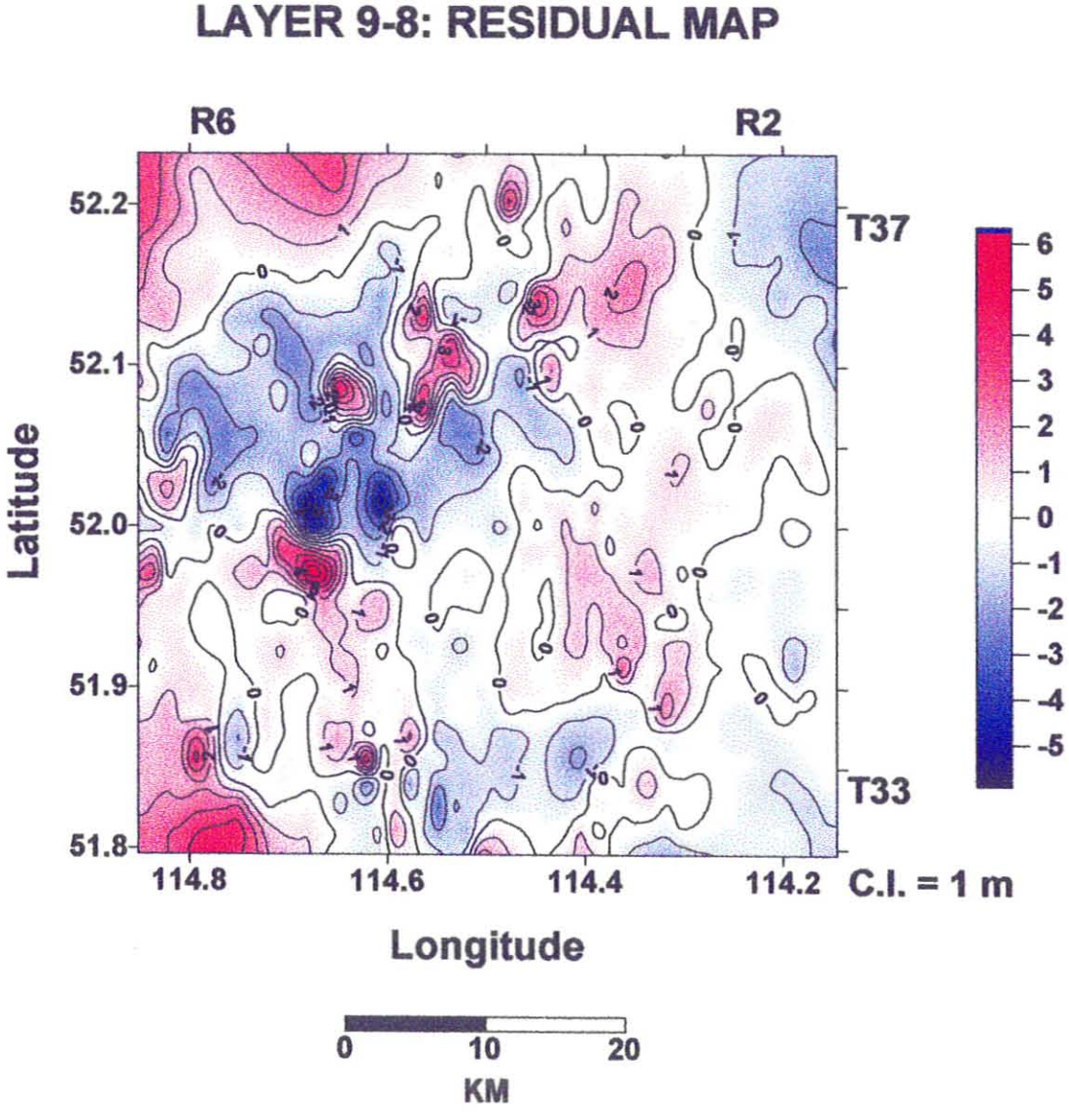
LAYER 9-8: RESIDUAL MAP
R6
R2
T37
T33
52.2
52.1
52.0
51.9
51.8
Latitude
114.8
114.6
114.4
114.2
Longitude
C.I. = 1 m
6
5
4
3
2
1
0
-1
-2
-3
-4
-5
0
10
20
KM

Figure 35.

5.1.7 Layer 10-9

Layer 10-9 is coarsening upwards succession bounded at its base and top by a flooding surface (picks 10 and 9 respectively).

The maps of Layer 10-9 are shown in Figures 36, 37, and 38. The isopach thicknesses range from 6.7 to 32 m. The average thickness is 17.1 m with a standard deviation of 4.3 m. On the isopach map (Figure 36), the layer is thickest in the northwest and thins to the southeast. The isopach trends have a NE - SW orientation. The quadratic trend surface map (Figure 37) shows this thinning from the northwest to the southeast with a general NE - SW orientation of the contour lines. On the residual map (Figure 38), the thickness range from -6.5 to 5.7 m. The only distinct trends illustrated on the residual map are in the southeast and have NE - SW contour trends.

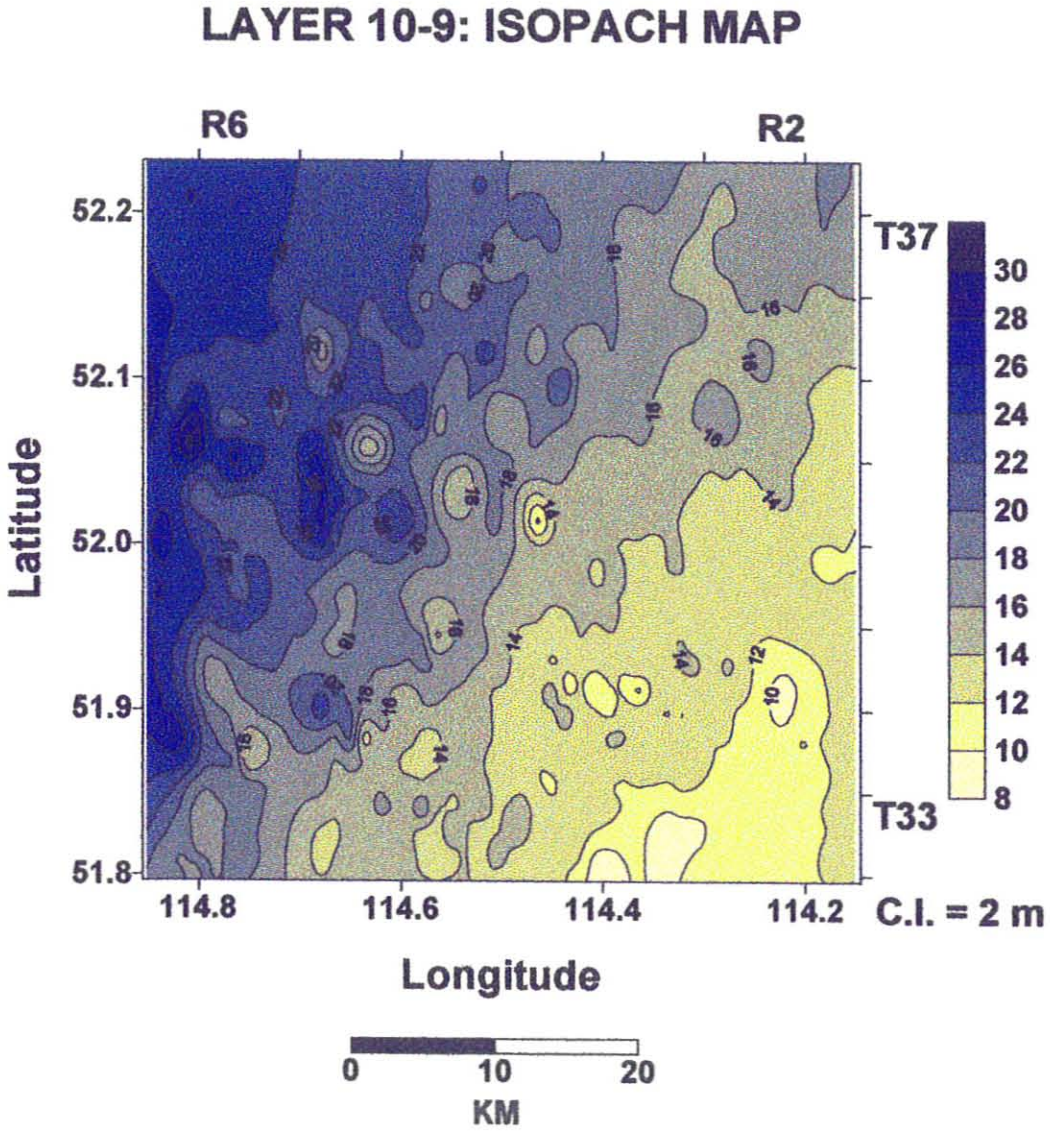
LAYER 10-9: ISOPACH MAP
R6
R2
T37
T33
52.2
52.1
52.0
51.9
51.8
Latitude
114.8
114.6
114.4
114.2
Longitude
30
28
26
24
22
20
18
16
14
12
10
8
C.I. = 2 m
0
10
20
KM

Figure 36.

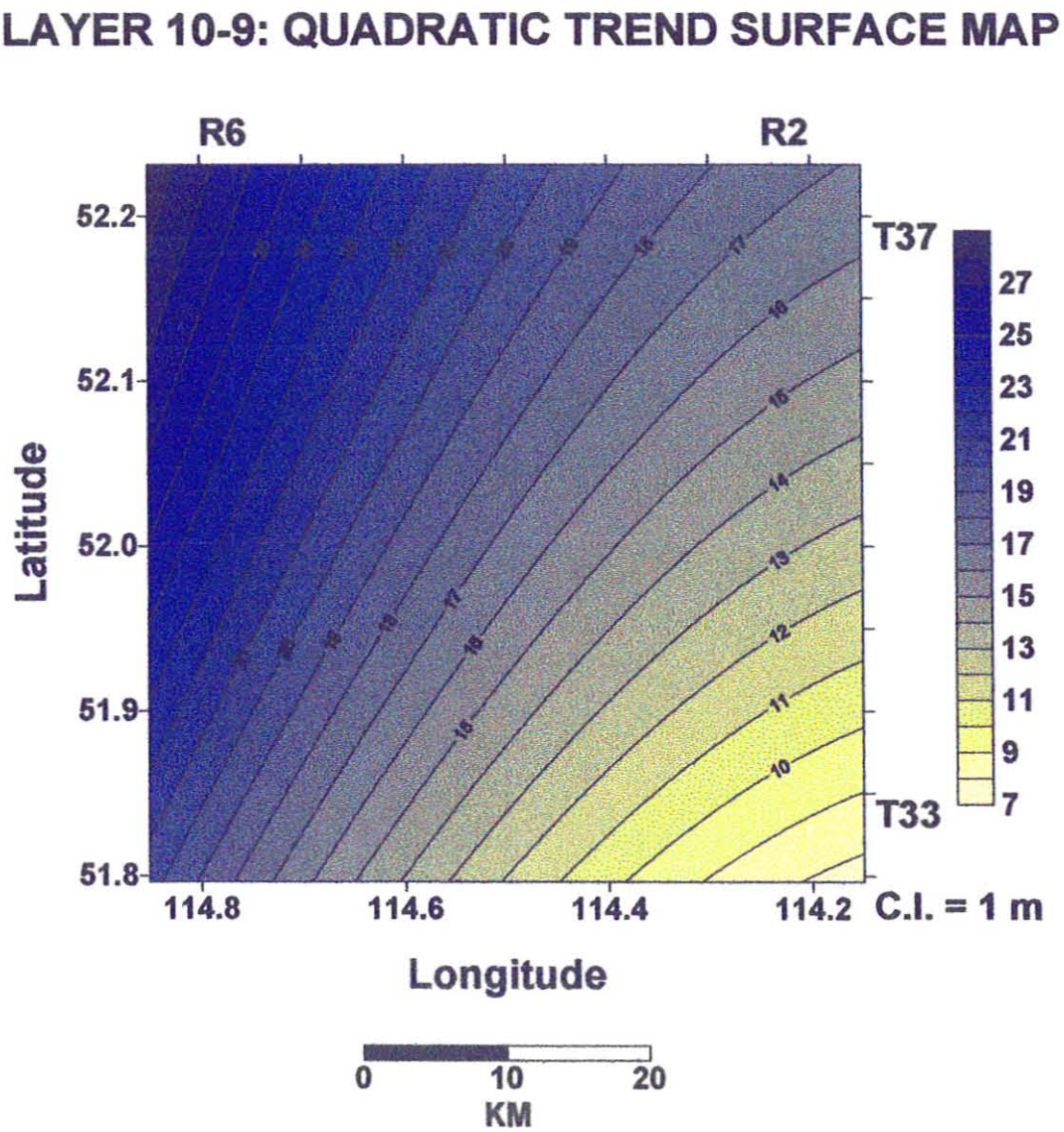
LAYER 10-9: QUADRATIC TREND SURFACE MAP
R6
R2
T37
T33
52.2
52.1
52.0
51.9
51.8
Latitude
114.8
114.6
114.4
114.2
Longitude
C.I. = 1 m
27
25
23
21
19
17
15
13
11
9
7
0
10
20
KM

Figure 37.

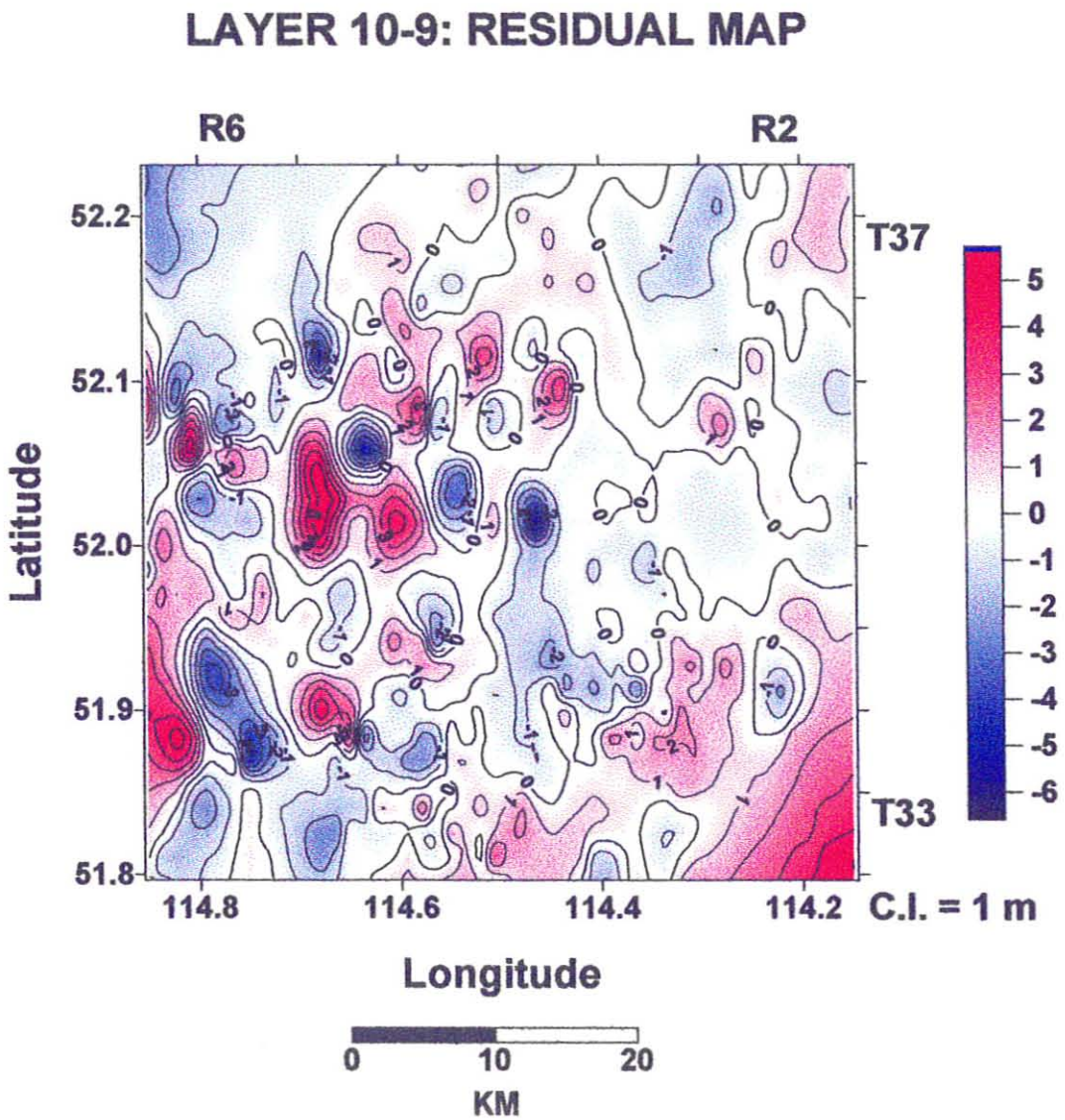
LAYER 10-9: RESIDUAL MAP
R6
R2
T37
T33
52.2
52.1
52.0
51.9
51.8
Latitude
114.8
114.6
114.4
114.2
Longitude
C.I. = 1 m
5
4
3
2
1
0
-1
-2
-3
-4
-5
-6
0
10
20
KM

Figure 38.

5.1.8 Layer 11-10

Layer 11-10 is a coarsening upward succession bounded by flooding surfaces. The lower flooding surface is sharp in the NE, and becomes more gradual to the SW, and thus the inflection point was used to determine pick 11.

The maps of Layer 11-10 are shown in Figures 39, 40, and 41. The thicknesses of this layer range from 12.2 m to 39 m. The average thickness is 23.3 m with a standard deviation of 4.0 m. On the isopach map (Figure 39), the contour lines extend generally N - S. The layer is thickest in the west and thins to the east. The quadratic trend surface map (Figure 40) shows NW - SE contour trends in the east. The contour trends in west of this map trend in a trough shape that thickens from the southeast to the northwest. On the residual map (Figure 41), the thicknesses range from -6.5 to 11.6 m. The only distinct trends on the residual map are in the southwest and southeast. The southeast NE - SW oriented contours correspond to a low, whereas the NW - SE trends in the southwest are a high.

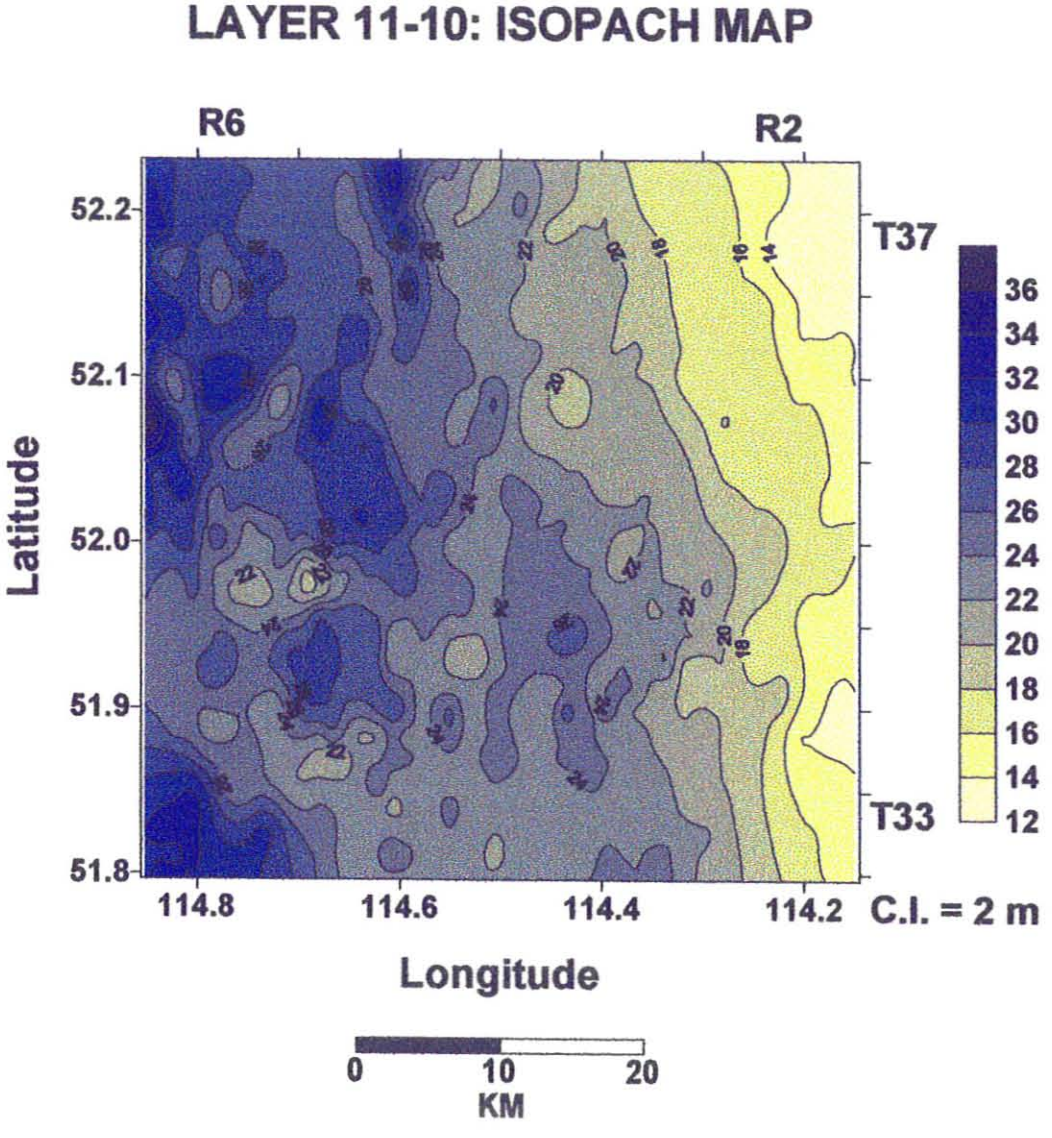
LAYER 11-10: ISOPACH MAP
R6
R2
T37
T33
52.2
52.1
52.0
51.9
51.8
Latitude
114.8
114.6
114.4
114.2
Longitude
C.I. = 2 m
36
34
32
30
28
26
24
22
20
18
16
14
12
0
10
20
KM

Figure 39.

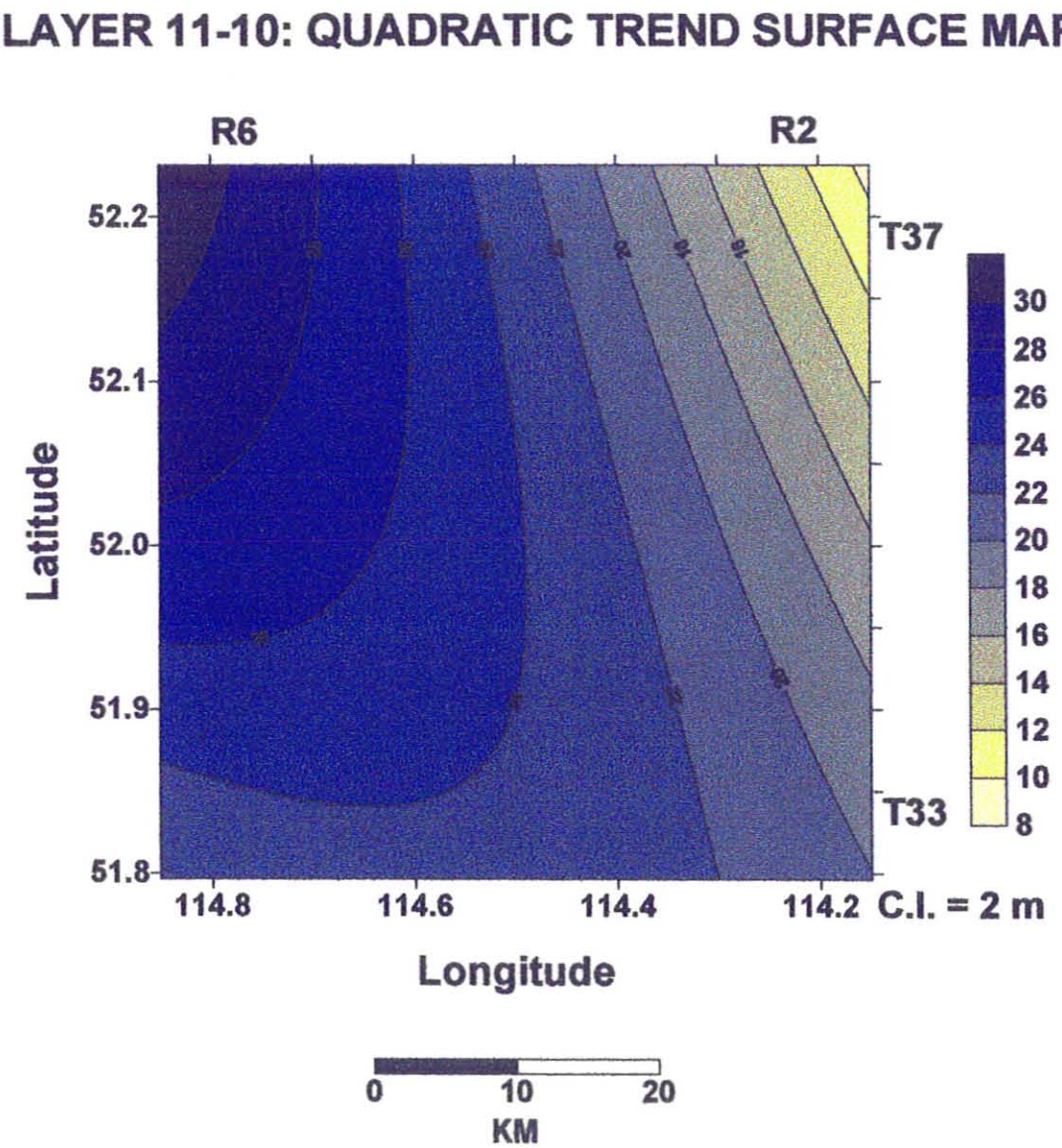
LAYER 11-10: QUADRATIC TREND SURFACE MAP
R6
R2
T37
T33
52.2
52.1
52.0
51.9
51.8
Latitude
114.8
114.6
114.4
114.2
Longitude
C.I. = 2 m
30
28
26
24
22
20
18
16
14
12
10
8
0
10
20
KM

Figure 40.

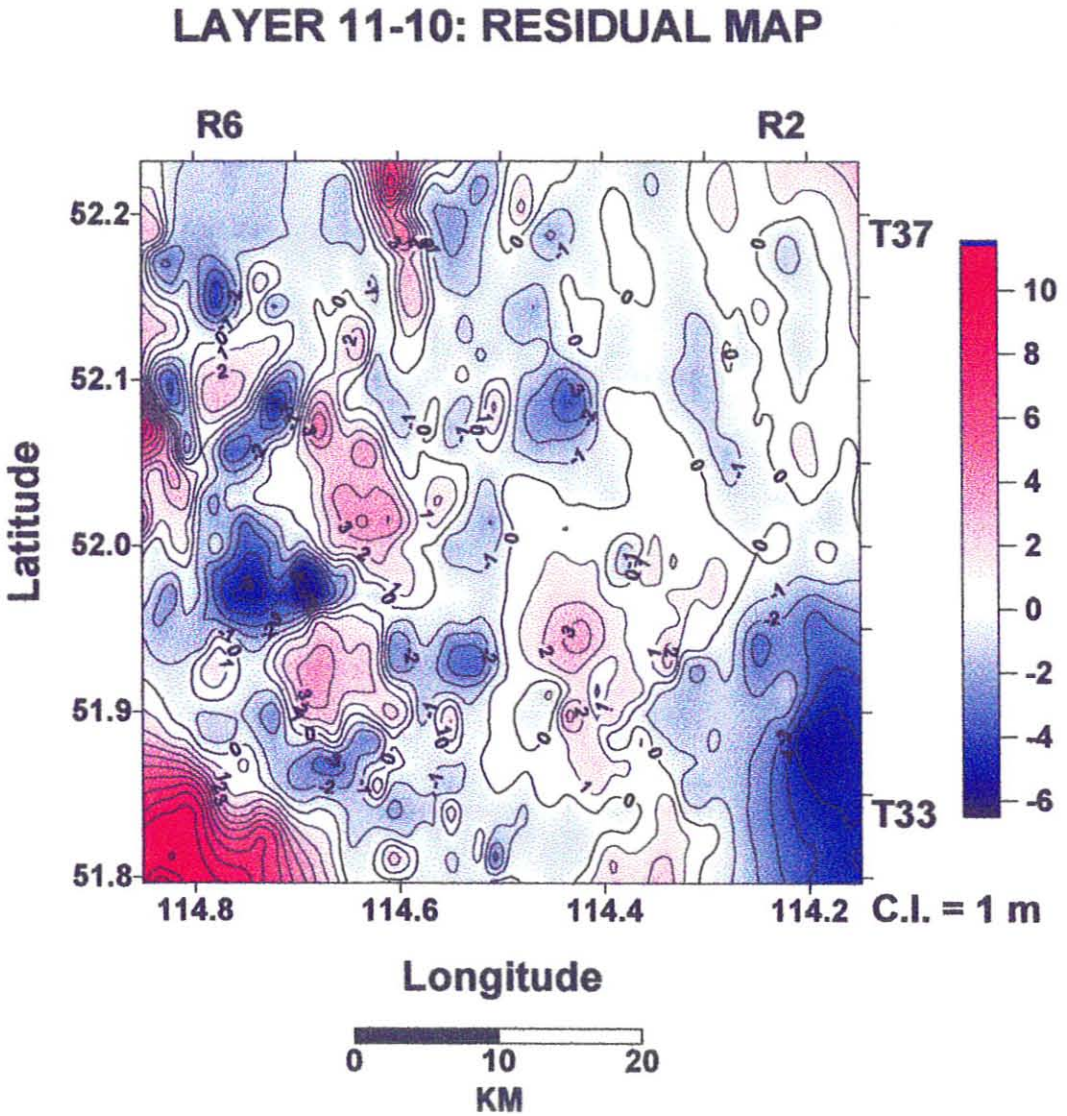
LAYER 11-10: RESIDUAL MAP
R6
R2
T37
T33
52.2
52.1
52.0
51.9
51.8
Latitude
114.8
114.6
114.4
114.2
Longitude
C.I. = 1 m
10
8
6
4
2
0
-2
-4
-6
0
10
20
KM

Figure 41.

5.1.9 Layer 12-11

Layer 12-11 is a coarsening upward succession that contains the Second White Speckled Shale. Pick 12 is an inflection point, and pick 11 is a flooding surface.

The maps of Layer 12-11 are shown in Figures 42, 43, and 44. The isopach thicknesses range from 24 to 38 m. The average thickness is 32.1 m with a standard deviation of 2.0 m. On the isopach map (Figure 42), there is a general thinning from the east to the west. On the quadratic trend surface map (Figure 43), the thinnest area occurs in the west. There is an overall thinning from south to west in the east. On the residual map (Figure 44), the thicknesses range from -7.4 to 4.6 m. The are several discrete N - S trends in the residual map. The trends highlighted in the residual map also appear in the isopach map.

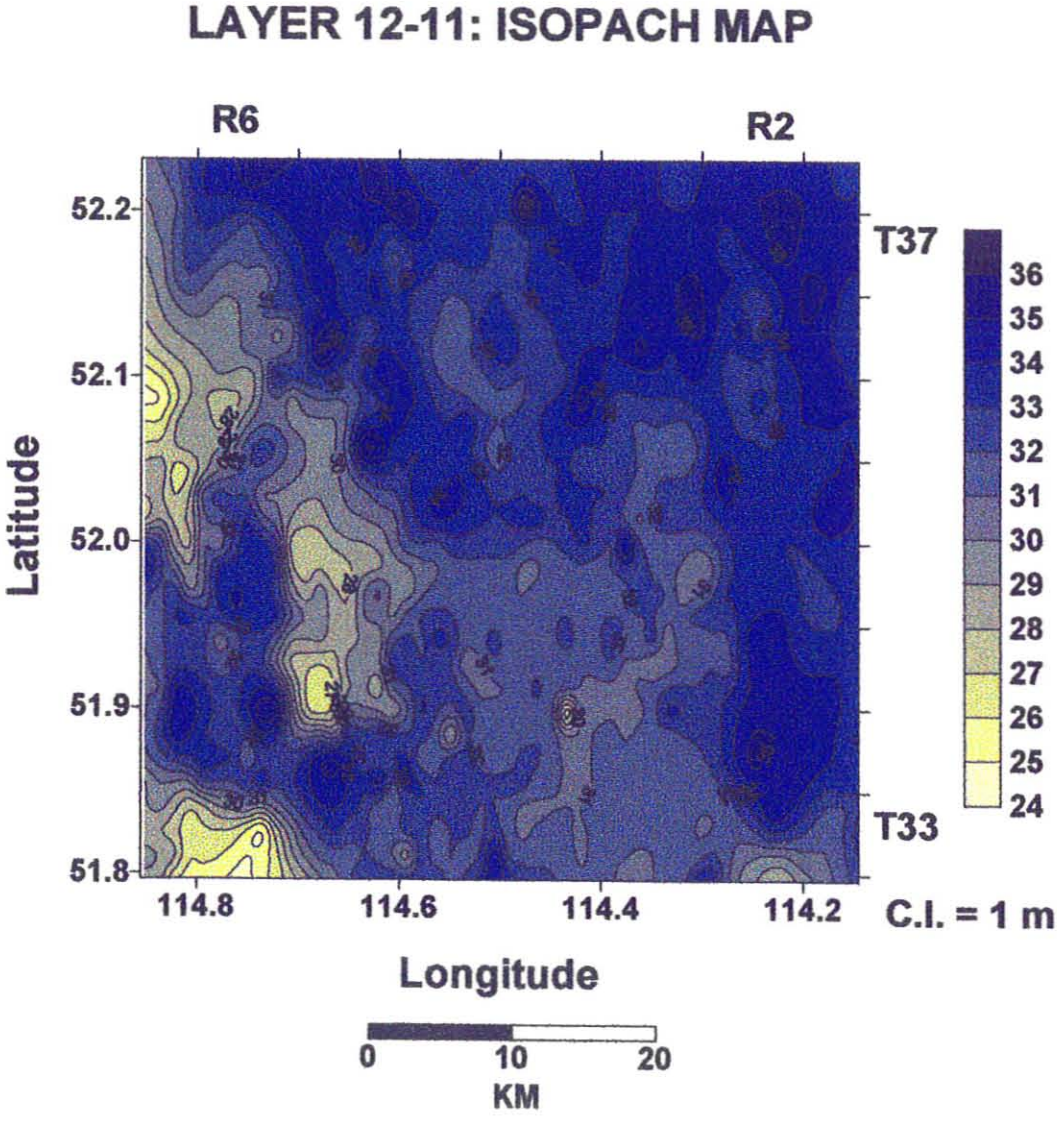
LAYER 12-11: ISOPACH MAP
R6
R2
T37
T33
52.2
52.1
52.0
51.9
51.8
Latitude
114.8
114.6
114.4
114.2
Longitude
36
35
34
33
32
31
30
29
28
27
26
25
24
C.I. = 1 m
0
10
20
KM

Figure 42.

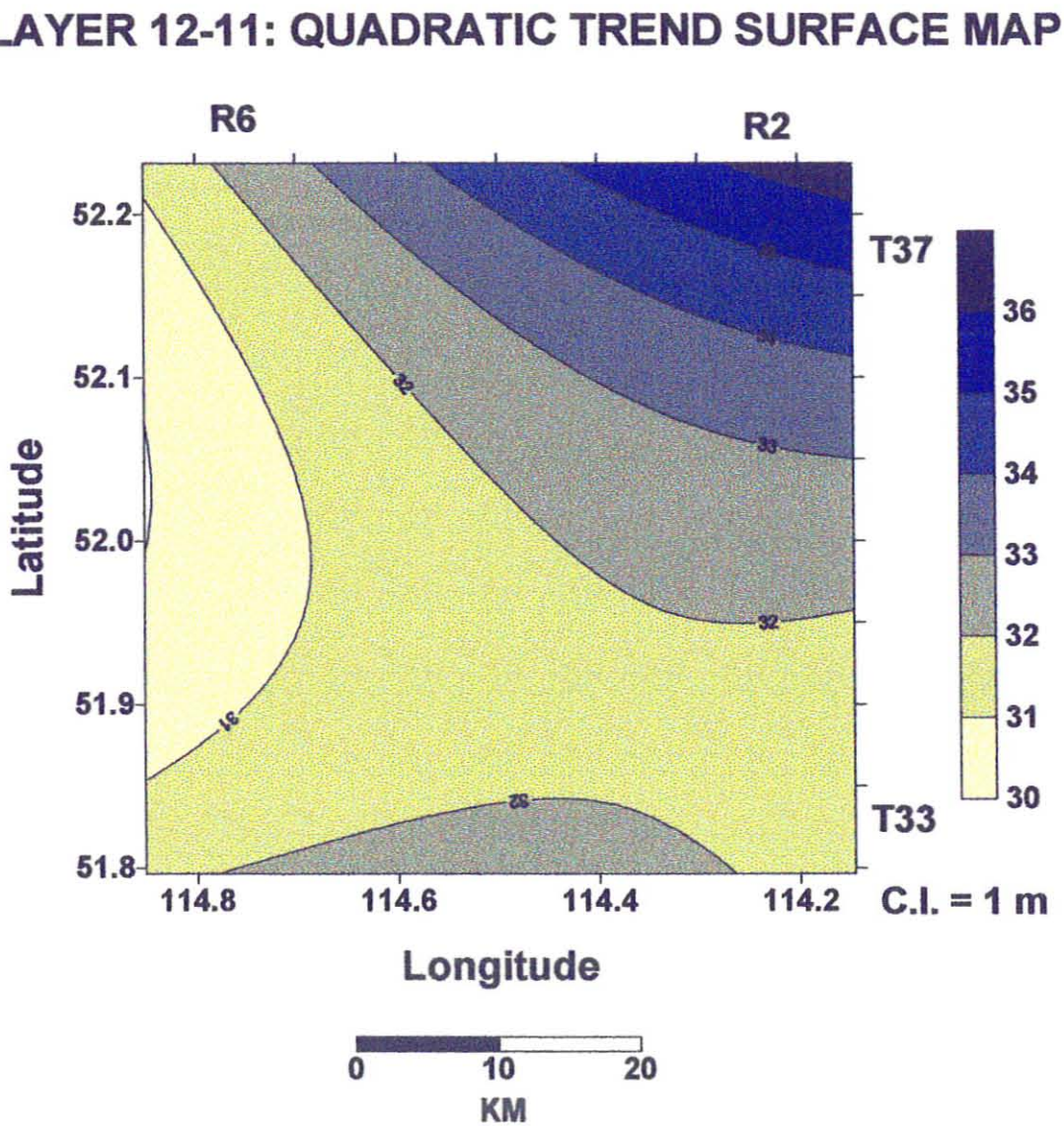
LAYER 12-11: QUADRATIC TREND SURFACE MAP
R6
R2
52.2
52.1
52.0
51.9
51.8
Latitude
T37
T33
36
35
34
33
32
31
30
C.I. = 1 m
114.8
114.6
114.4
114.2
Longitude
0
10
20
KM

Figure 43.

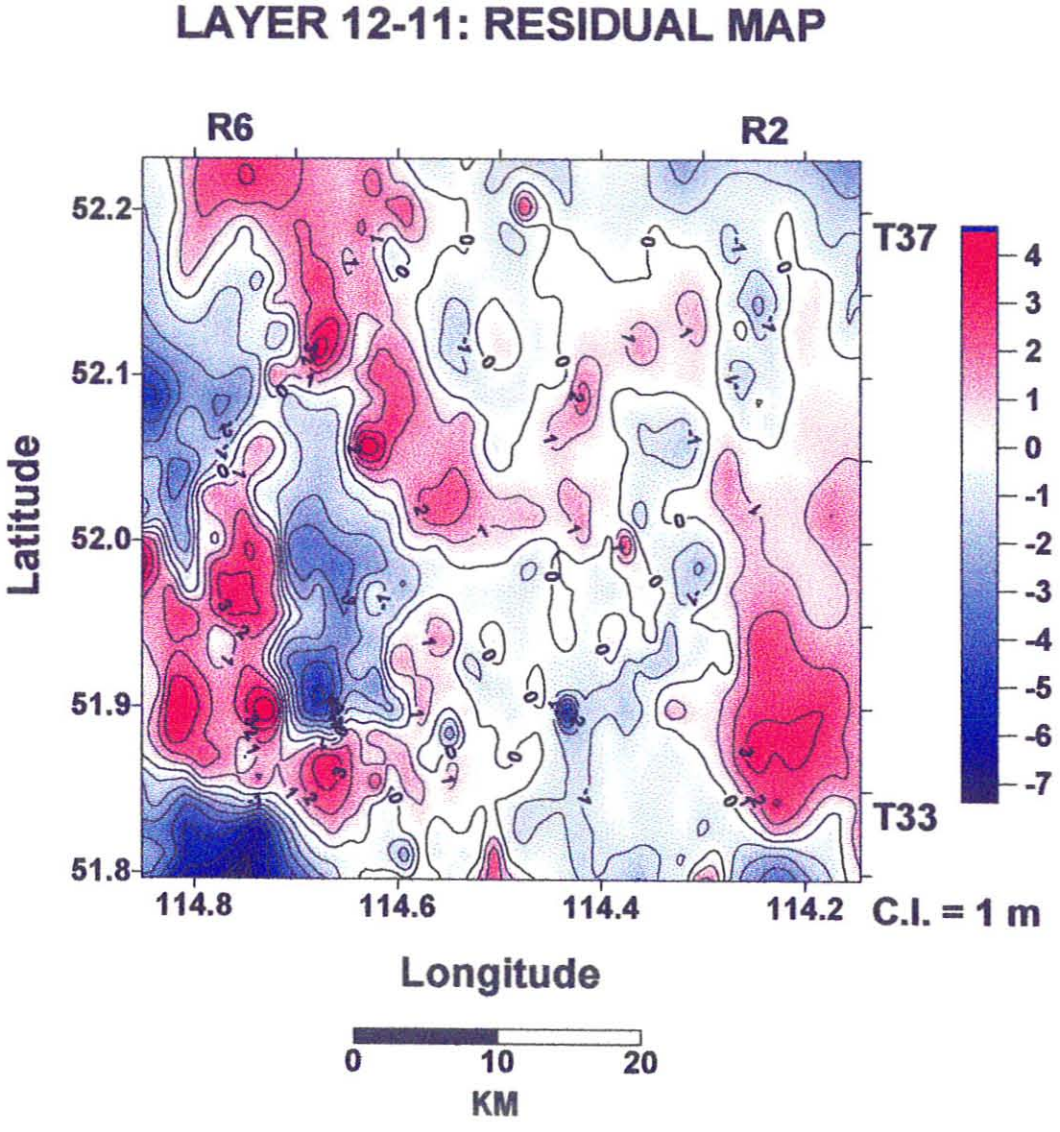
LAYER 12-11: RESIDUAL MAP
R6
R2
T37
T33
52.2
52.1
52.0
51.9
51.8
Latitude
114.8
114.6
114.4
114.2
Longitude
C.I. = 1 m
4
3
2
1
0
-1
-2
-3
-4
-5
-6
-7
0
10
20
KM

Figure 44.

5.1.10 Layer 13-12

Layer 13-12 is a sandy interval that fines upwards. Pick 13 is determined at the inflection point, and pick 12 at the flooding surface that terminates this sandy interval.

The maps of Layer 13-12 are shown in Figures 45, 46, and 47. The isopach thicknesses of this unit range from 19.8 to 35 m. The average thickness is 24.5 m with a standard deviation of 2.8 m. On the isopach map (Figure 45), the layer is thickest in the southwest and thins to the northeast. The isopach trends have a NW - SE orientation. The quadratic trend surface map (Figure 46) also shows NW - SE trends with thinning occurring from the southwest to the northeast. On the residual map (Figure 47), the thicknesses range from -2.4 to 4.3 m. There is an overall positive trend that is oriented NW - SE parallel to the regional trends. There are several positive trends that extend N - S such as in the east at approximately 114.2° longitude and in the west at about 114.75°.

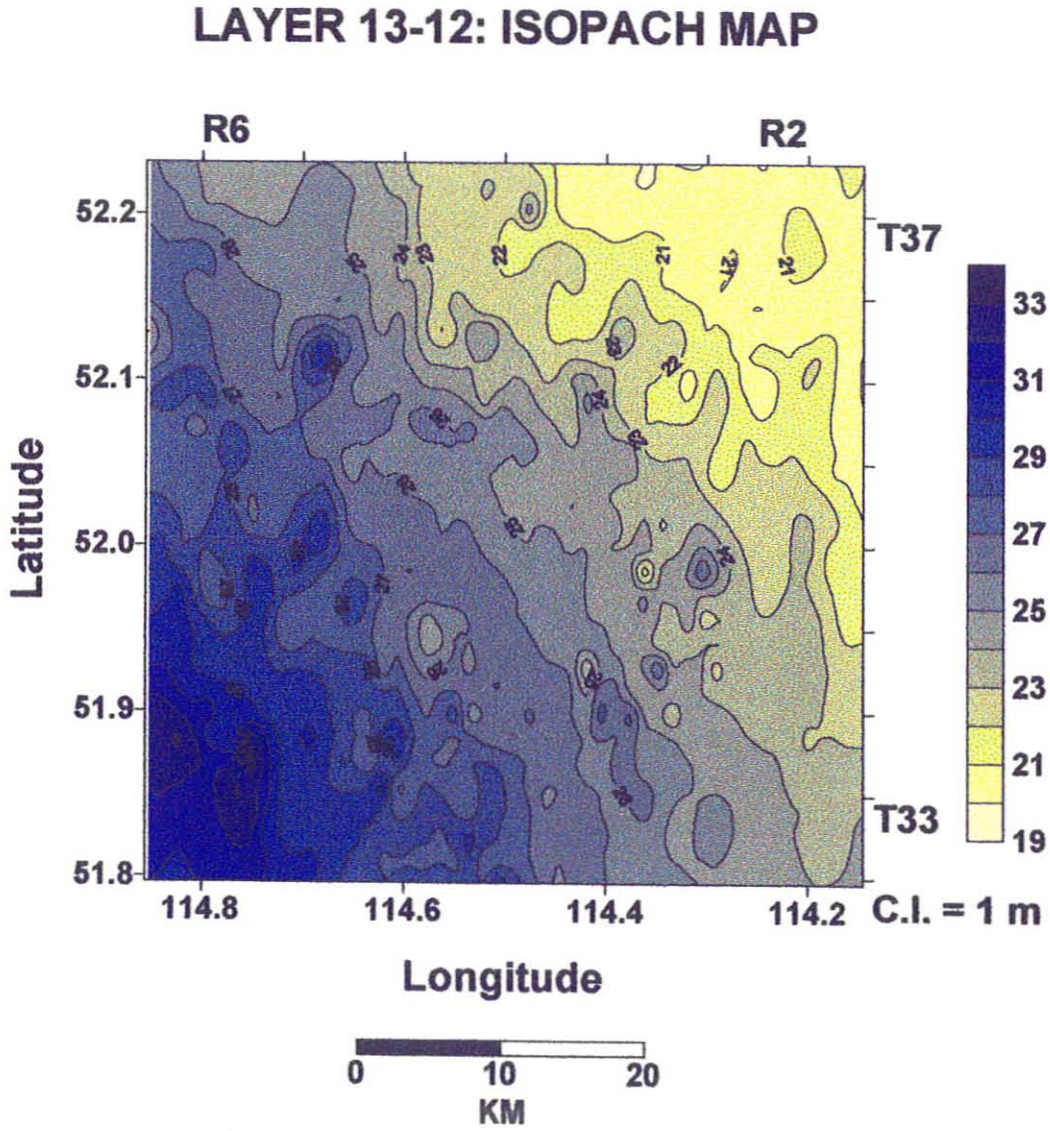
LAYER 13-12: ISOPACH MAP
R6
R2
T37
T33
52.2
52.1
52.0
51.9
51.8
Latitude
114.8
114.6
114.4
114.2
Longitude
C.I. = 1 m
33
31
29
27
25
23
21
19
0
10
20
KM

Figure 45.

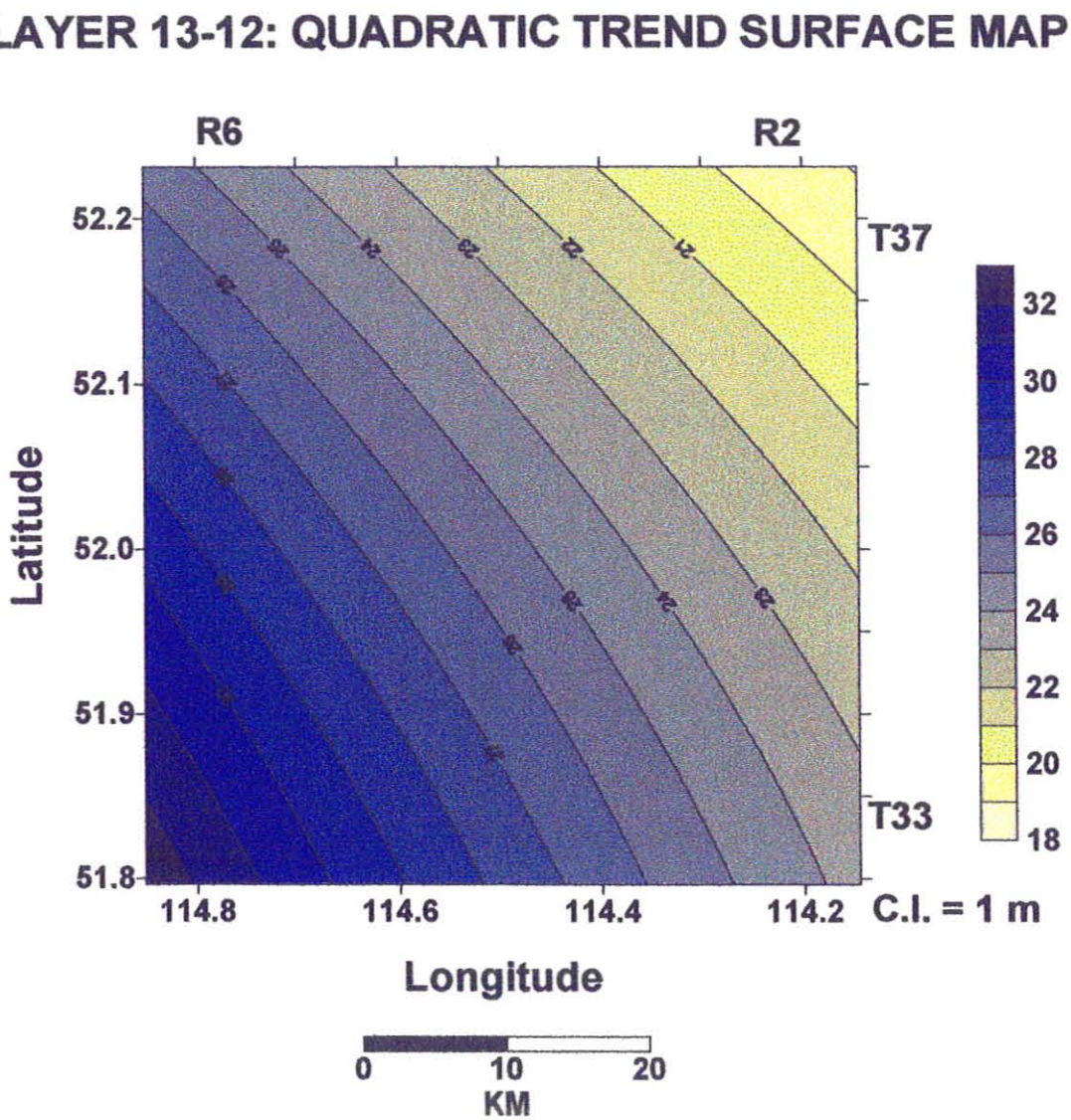
LAYER 13-12: QUADRATIC TREND SURFACE MAP
R6
R2
T37
T33
52.2
52.1
52.0
51.9
51.8
Latitude
114.8
114.6
114.4
114.2
Longitude
C.I. = 1 m
32
30
28
26
24
22
20
18
0
10
20
KM

Figure 46.

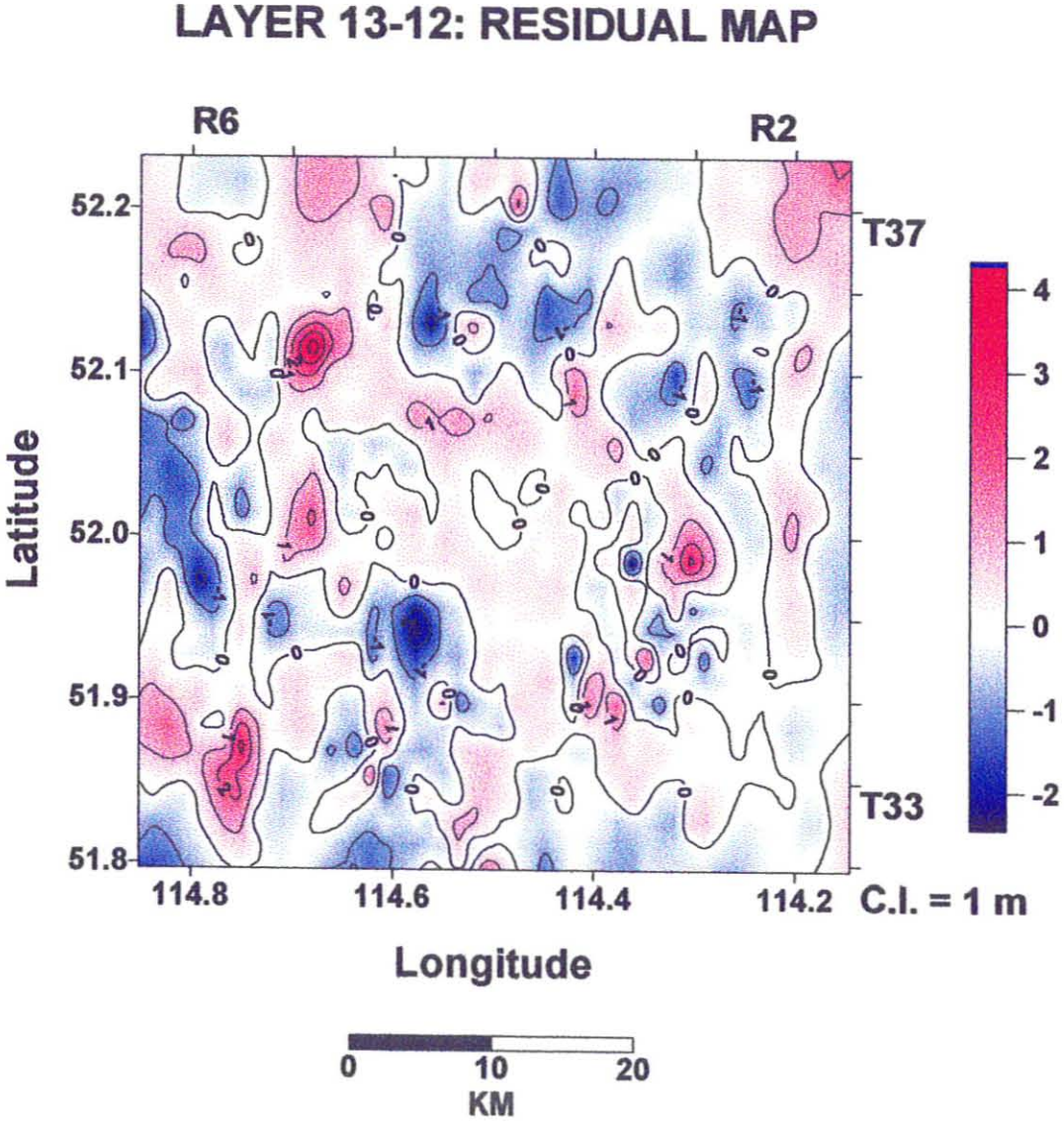
LAYER 13-12: RESIDUAL MAP
R6
R2
T37
T33
52.2
52.1
52.0
51.9
51.8
Latitude
114.8
114.6
114.4
114.2
Longitude
C.I. = 1 m
4
3
2
1
0
-1
-2
0
10
20
KM

Figure 47.

5.1.11 Layer 14-13

Layer 14-13 is a coarsening upward facies succession bounded below by the top of the Fish Scales Sand (pick 14), and at the top by a sharp contact of coarser material (pick 13).

The maps of Layer 14-13 are shown in Figures 48, 49, and 50. The isopach thicknesses range from 19.2 to 34 m. The average thickness is 25.1 m with a standard deviation of 2.1 m. The isopach map (Figure 48) shows overall thinning from the west to the east. The quadratic trend surface map (Figure 49) shows this thinning from the west to the east with general N - S contour lines that have a slight bend in center. On the residual map (Figure 50), the thicknesses range from -4.1 to 5.4 m. The overall trends on the residual map extend oblique to those shown on the quadratic trend surface map. Approximate E - W trends are observed around 51.9° and 52.1° latitude.

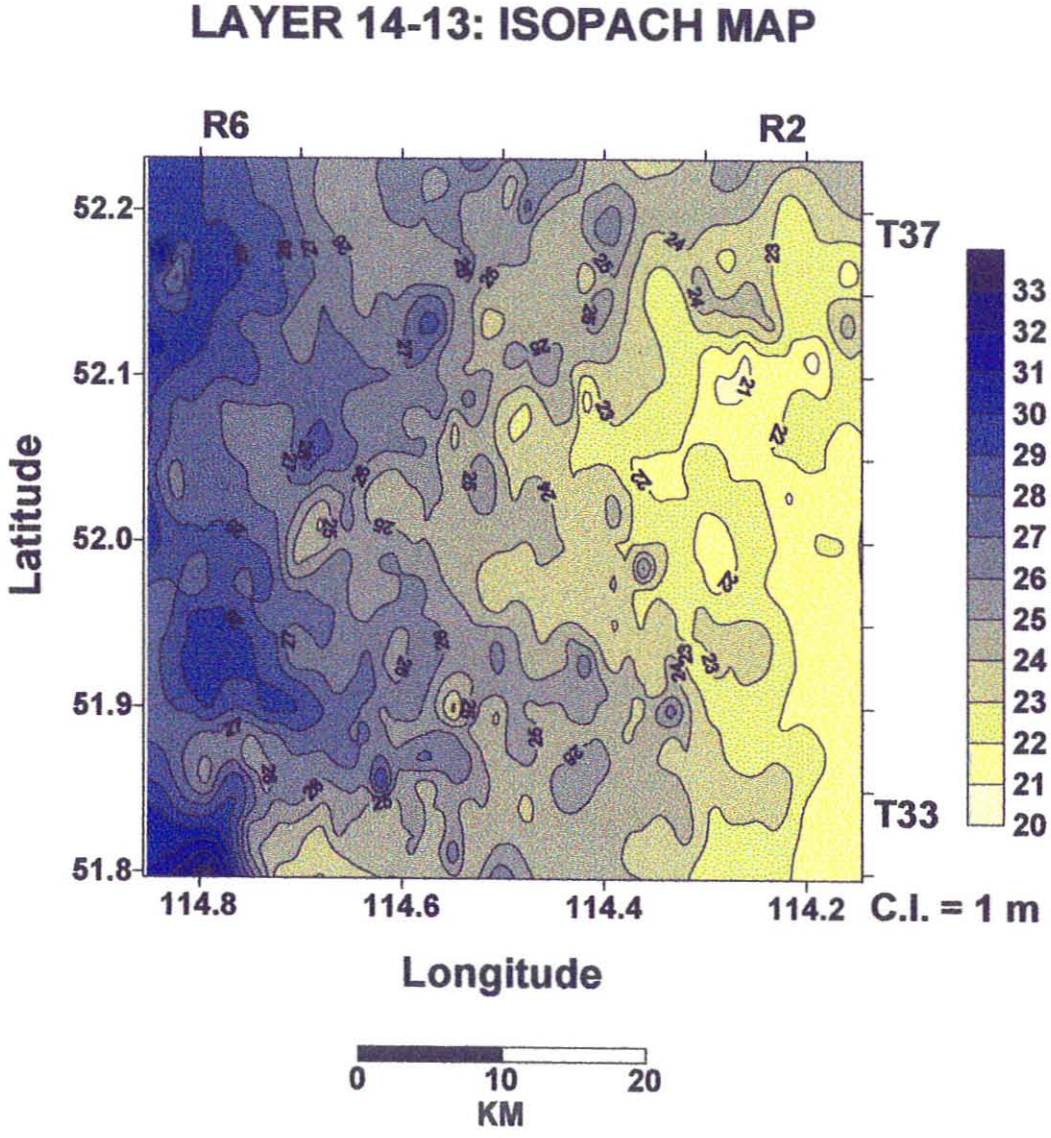
LAYER 14-13: ISOPACH MAP
R6
R2
T37
T33
52.2
52.1
52.0
51.9
51.8
Latitude
114.8
114.6
114.4
114.2
Longitude
C.I. = 1 m
33
32
31
30
29
28
27
26
25
24
23
22
21
20
0
10
20
KM

Figure 48.

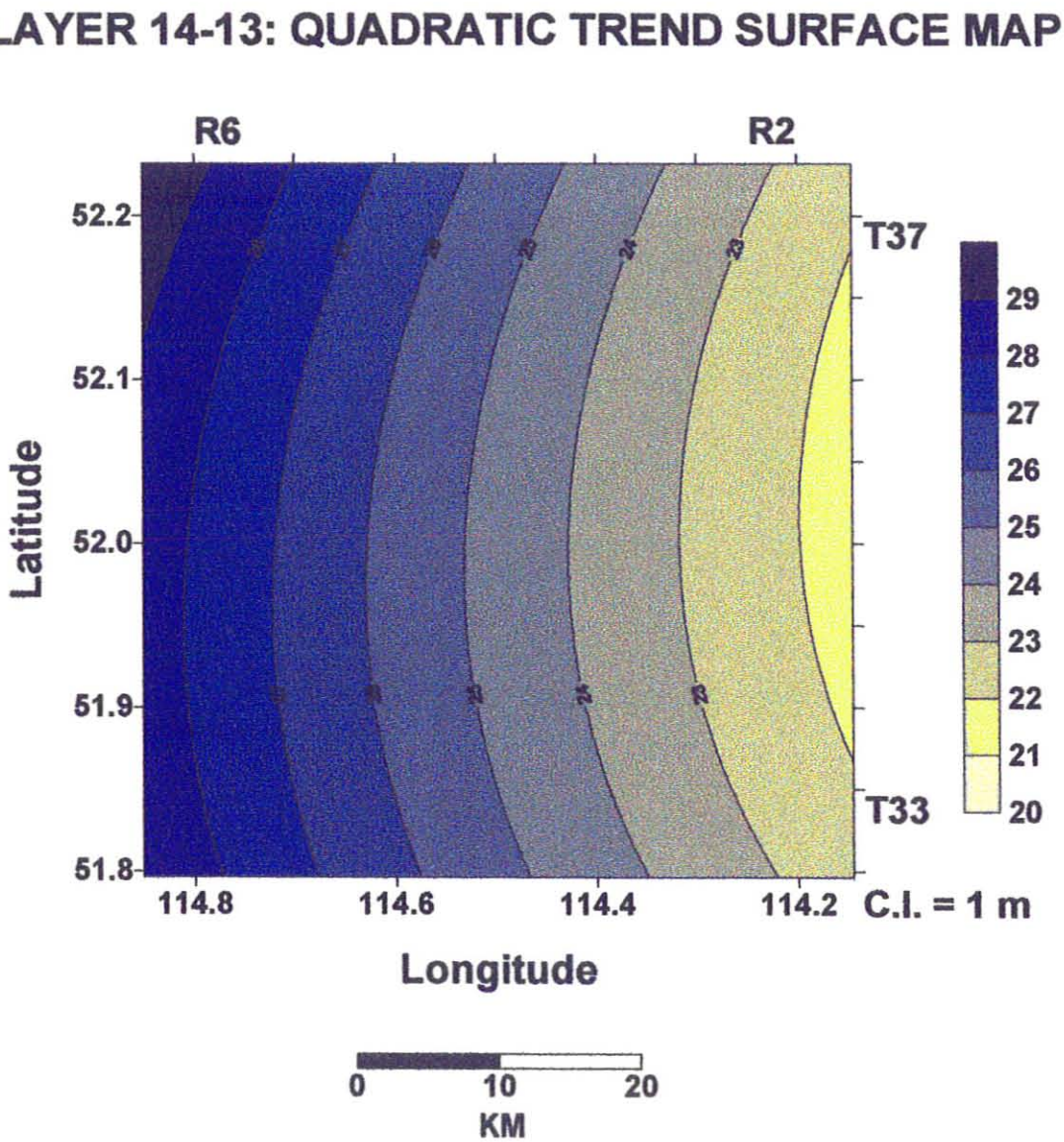
LAYER 14-13: QUADRATIC TREND SURFACE MAP
R6
R2
T37
T33
52.2
52.1
52.0
51.9
51.8
Latitude
114.8
114.6
114.4
114.2
Longitude
C.I. = 1 m
29
28
27
26
25
24
23
22
21
20
0
10
20
KM

Figure 49.

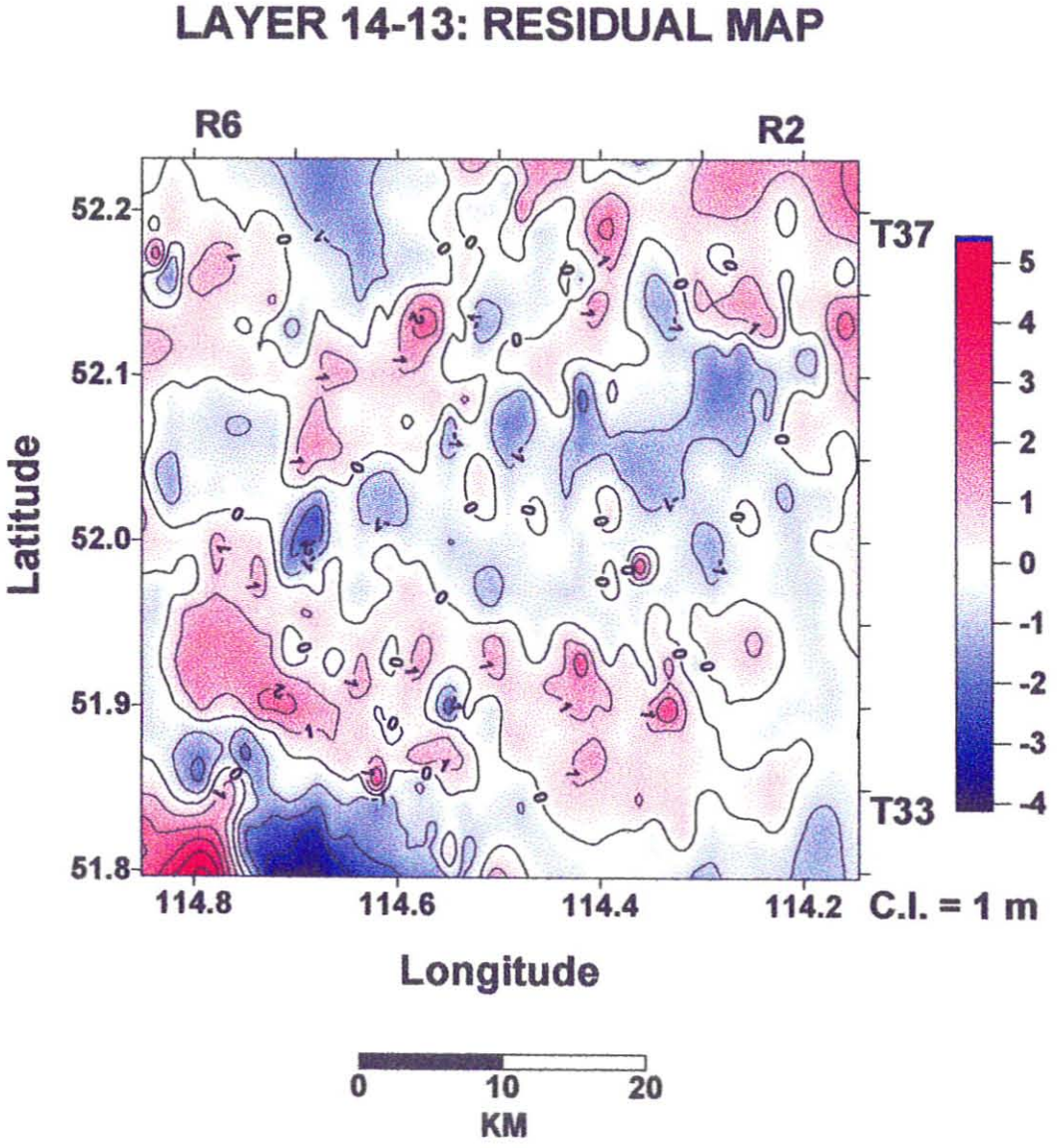
LAYER 14-13: RESIDUAL MAP
R6
R2
T37
T33
52.2
52.1
52.0
51.9
51.8
Latitude
114.8
114.6
114.4
114.2
Longitude
C.I. = 1 m
5
4
3
2
1
0
-1
-2
-3
-4
0
10
20
KM

Figure 50.

5.1.12 Layer 15-14

Layer 15-14 is the Fish Scales Sand. Pick 15, the base of the Fish Scales Sand, is a condensed horizon that shows an abrupt change in lithology used as the datum in the cross-sections. Pick 14 is the inflection point defining the top of this sand.

The maps of Layer 15-14 are shown in Figures 51, 52, and 53. The isopach thicknesses of this unit range from 6 to 15 m. The average thickness is 9.9 m with a standard deviation of 1.4 m. On the isopach map (Figure 51), there is a general thinning from the south to the north. The quadratic trend surface map (Figure 52) highlights regional trends thinning from the southwest to the northwest that are rather obscure on the isopach map. On the residual map (Figure 53), the thicknesses range from -3.2 to 2.3 m. Most of the contour lines on the residual map extend at oblique angles to the trends observed in the quadratic trend surface map. There are several N - S and E - W trends.

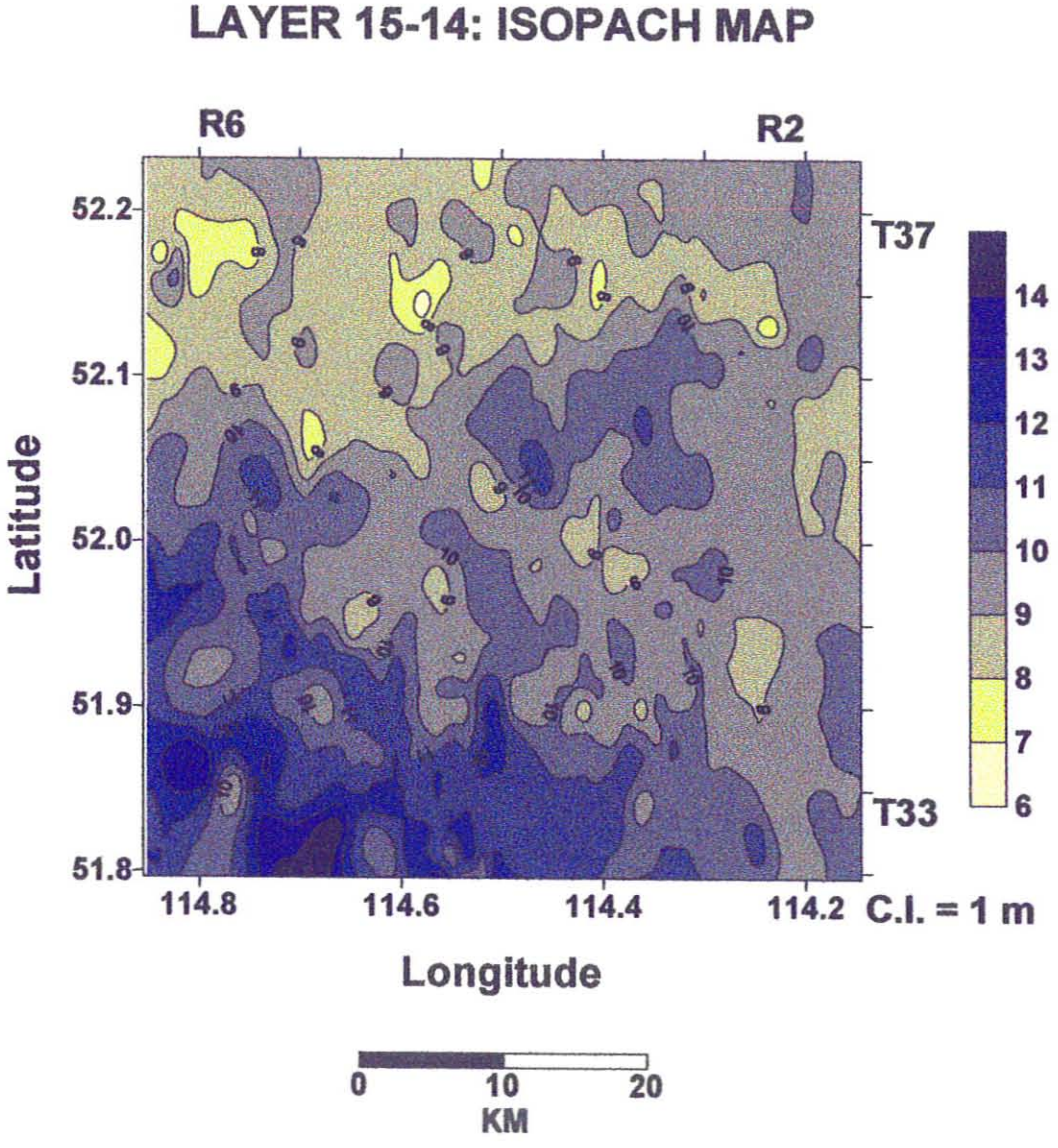
LAYER 15-14: ISOPACH MAP
R6
R2
T37
T33
52.2
52.1
52.0
51.9
51.8
Latitude
114.8
114.6
114.4
114.2
Longitude
C.I. = 1 m
14
13
12
11
10
9
8
7
6
0
10
20
KM

Figure 51.

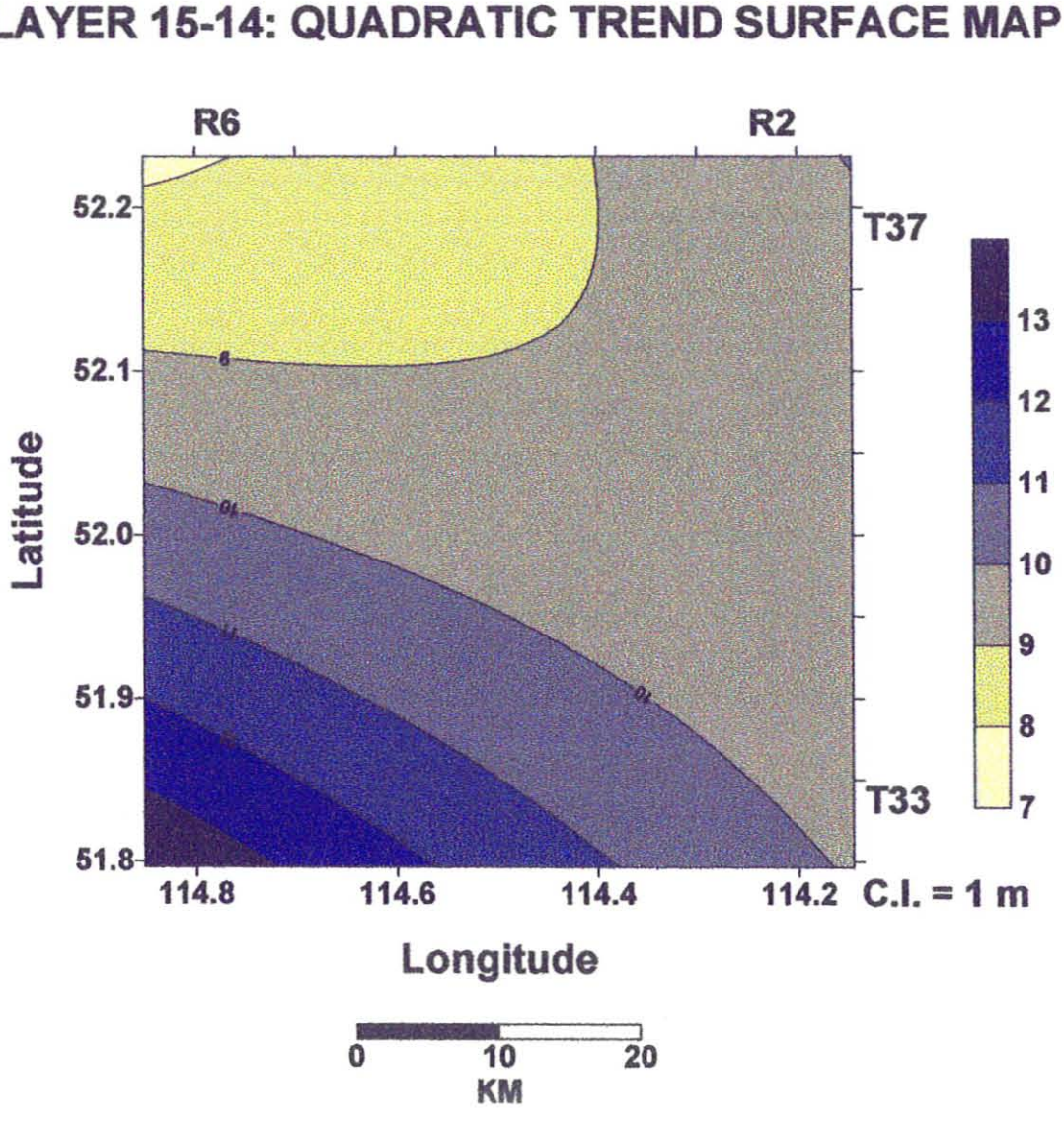
LAYER 15-14: QUADRATIC TREND SURFACE MAP
R6
R2
T37
T33
52.2
52.1
52.0
51.9
51.8
Latitude
114.8
114.6
114.4
114.2
Longitude
C.I. = 1 m
13
12
11
10
9
8
7
0
10
20
KM

Figure 52.

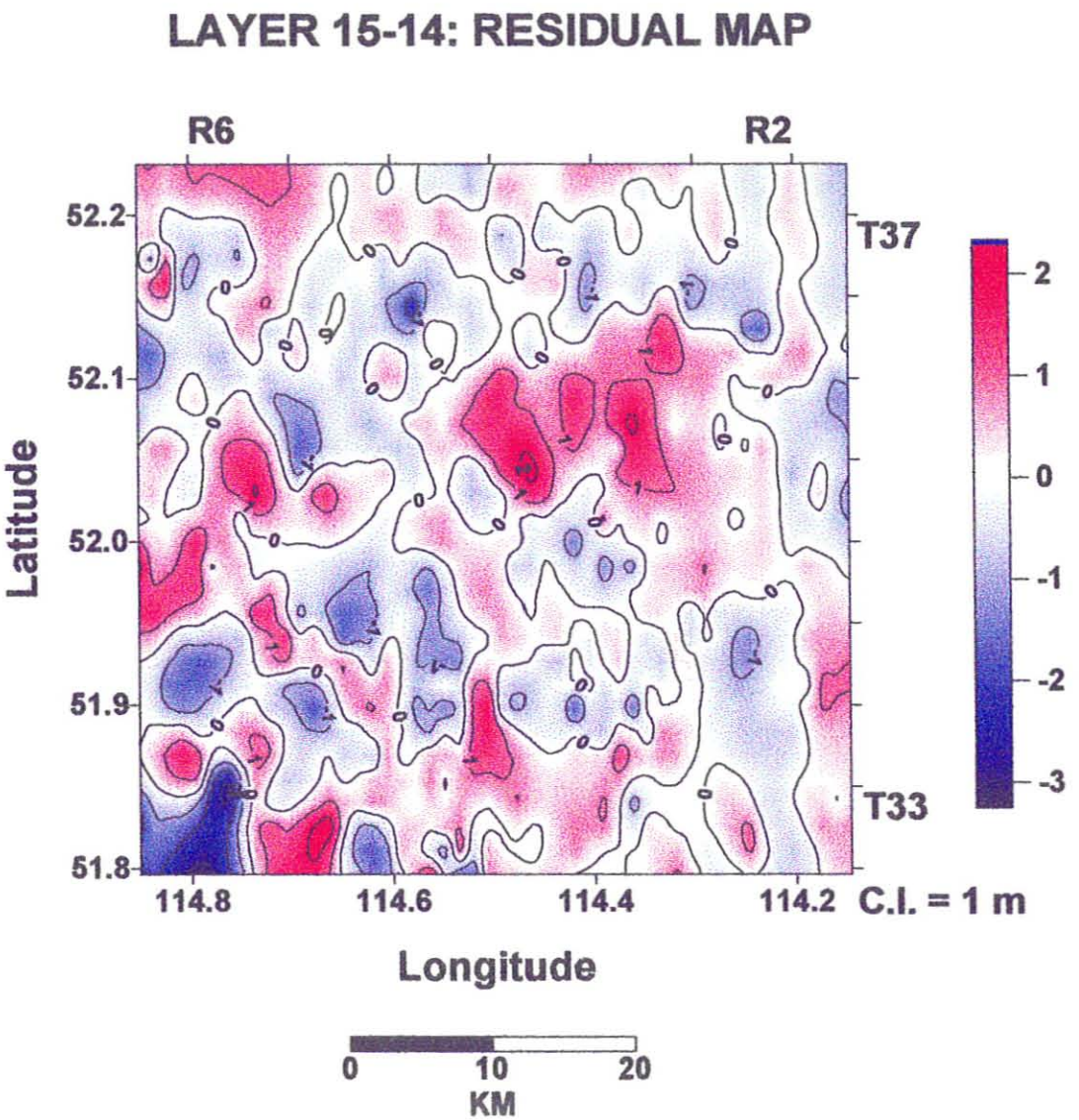
LAYER 15-14: RESIDUAL MAP
R6
R2
T37
T33
52.2
52.1
52.0
51.9
51.8
Latitude
114.8
114.6
114.4
114.2
Longitude
C.I. = 1 m
2
1
0
-1
-2
-3
0
10
20
KM

Figure 53.

5.1.13 Layer 16-15

Layer 16-15 is the Westgate Formation; bounded abruptly at the base by the flooding surface (pick 16) that terminated the Viking sand, and at the top by the condensed horizon of the base of the Fish Scales Sand (pick 15).

The maps of Layer 16-15 are shown in Figures 54, 55, and 56. The isopach thicknesses of this unit range from 8 to 38 m. The average thickness is 20.5 m with a standard deviation of 5.1 m. On isopach map (Figure 54), the isopach contours trend NW - SE. This layer shows an overall thinning from the northeast to the southwest. The quadratic trend surface map (Figure 55) shows similar NW - SE contours that thin from the northeast to the southwest. On the residual map (Figure 56), the thicknesses range from -5.8 to 8.3 m. The trends of the contour lines observed in the residual map are very similar to those observed in the isopach map. On the residual map there are NW - SE oriented highs in the southwest and northeast corners as well as a high that trends from the northwest to southeast of the map. Between these highs are corresponding lows that are also bounded by NW - SE oriented contours.

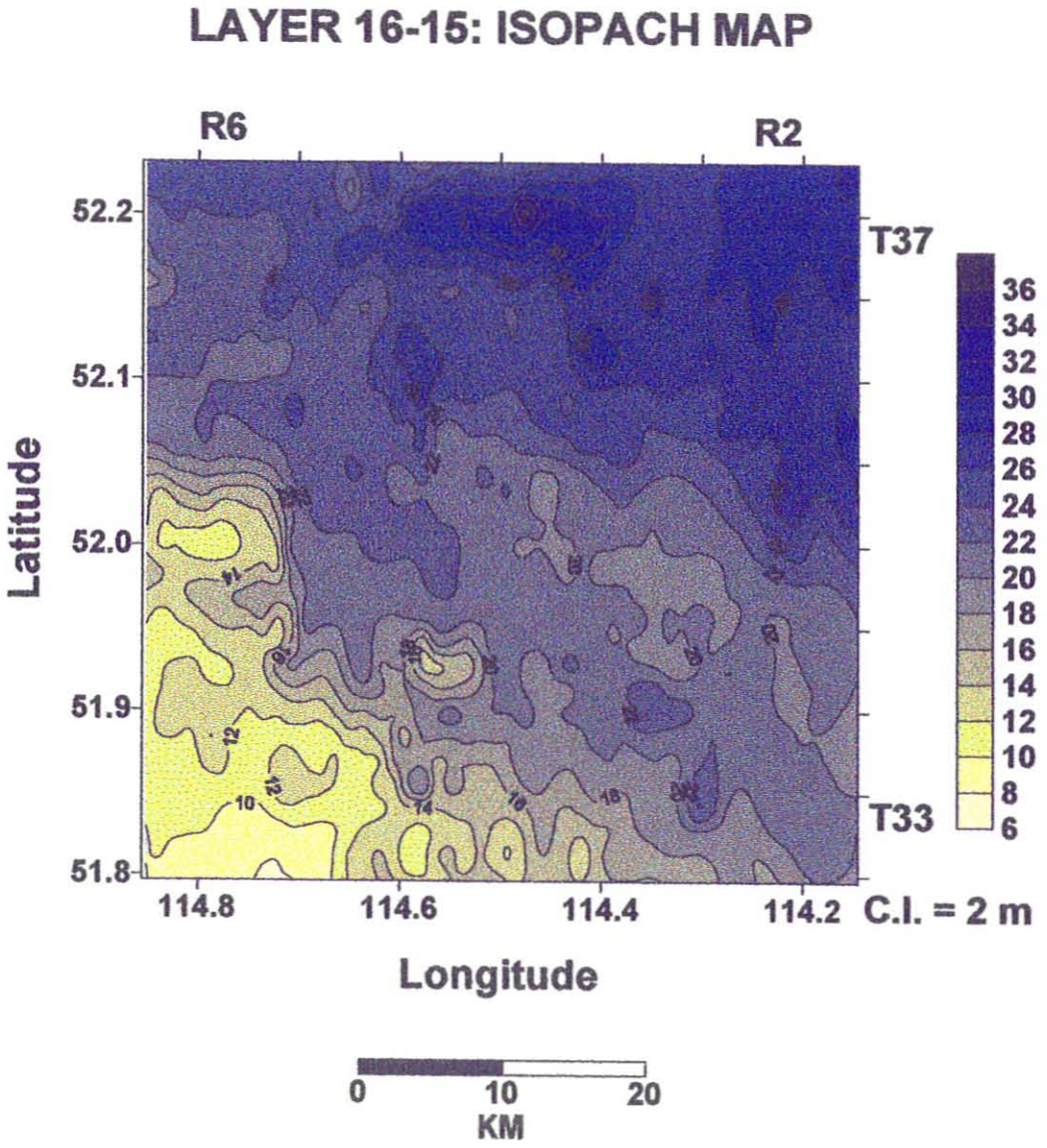
LAYER 16-15: ISOPACH MAP
R6
R2
T37
T33
52.2
52.1
52.0
51.9
51.8
Latitude
114.8
114.6
114.4
114.2
Longitude
C.I. = 2 m
36
34
32
30
28
26
24
22
20
18
16
14
12
10
8
6
0
10
20
KM

Figure 54.

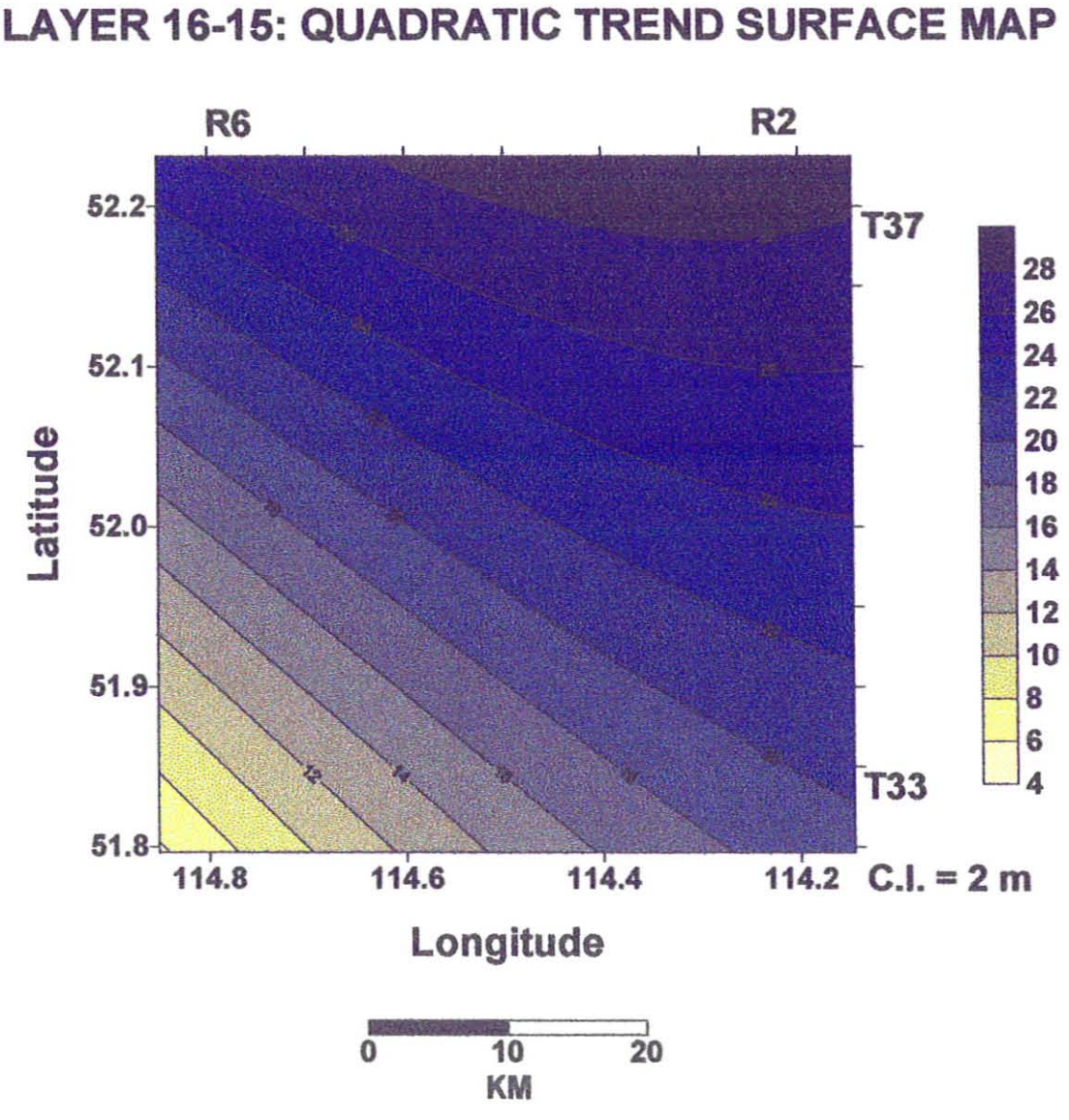
LAYER 16-15: QUADRATIC TREND SURFACE MAP
R6
R2
T37
T33
52.2
52.1
52.0
51.9
51.8
Latitude
114.8
114.6
114.4
114.2
Longitude
C.I. = 2 m
28
26
24
22
20
18
16
14
12
10
8
6
4
0
10
20
KM

Figure 55.

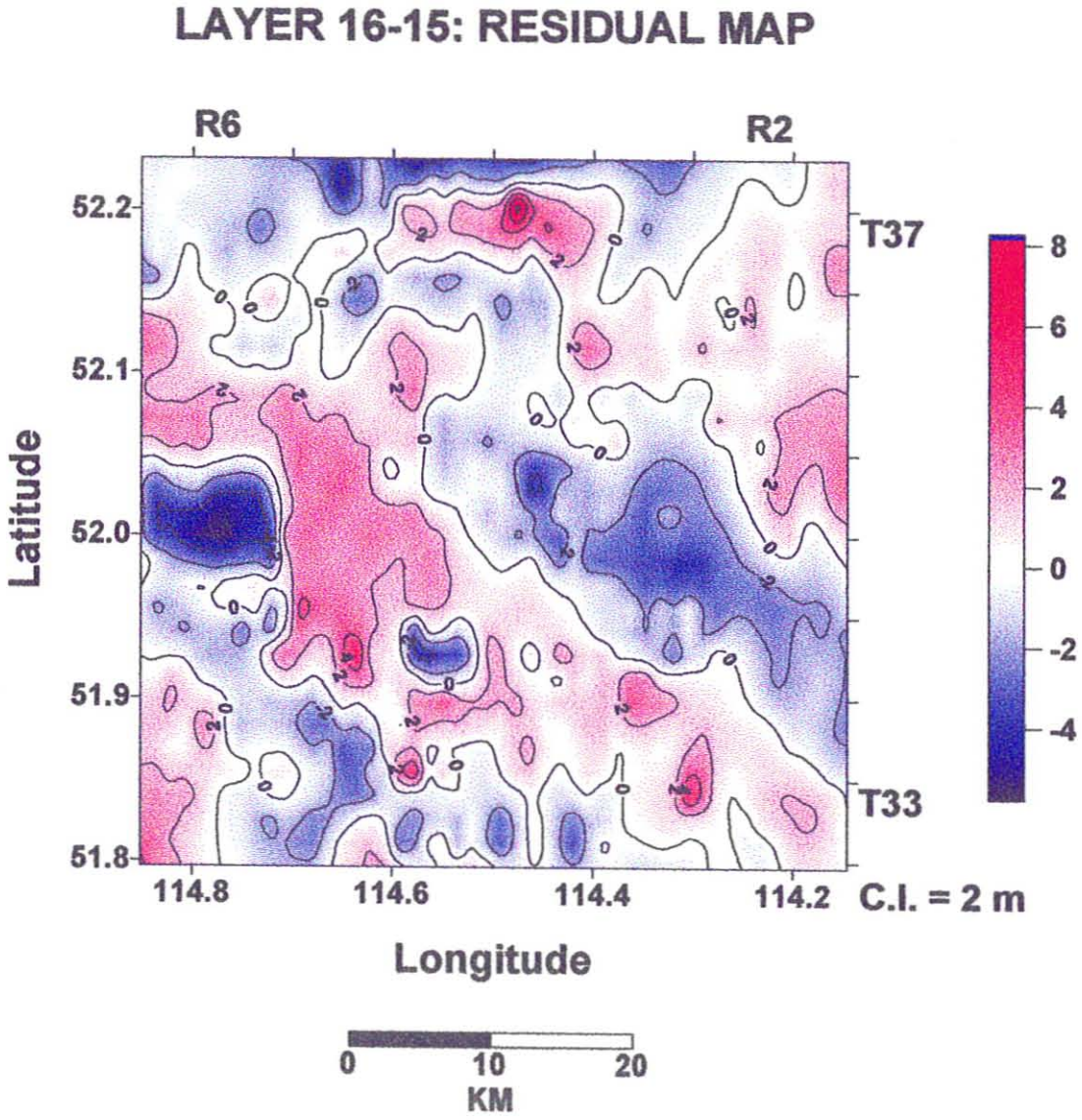
LAYER 16-15: RESIDUAL MAP
R6
R2
T37
T33
52.2
52.1
52.0
51.9
51.8
Latitude
114.8
114.6
114.4
114.2
Longitude
C.I. = 2 m
8
6
4
2
0
-2
-4
0
10
20
KM

Figure 56.

CHAPTER 6: INTERPRETATIONS

A summary of the thinning directions and residual trends for each layer are shown in Table 1. Layers 4-2, 6-4, 12-11, 13-12, and 15-14 have thinning trends from the southwest to northeast. Layers 7-6 and 9-8 show thinning trends from the southeast to the northwest. Layers 8-7, 11-10, and 14-13 have regional thinning trends from the west to the east. Layer 10-9 shows a general thinning trend from the northwest to the southeast. Layer 16-15 shows a general thinning trend from the northeast to the southwest. Layer 2-1 is thinnest in a NW-SE trending trough that thickens to the NE and SW. Therefore, the thinning directions change from layer to layer. No persistent trends propagate through the intervals studied.

The variations of thinning directions are likely due to tectonic movements of the foreland basin floor. There is no indication of these trends being influenced by basement control. The tectonics of the dip directions could be due to various factors such as; tilting of the sea floor, sediment supply, differing area of sediment input, accommodation space, subsidence, uplift, isostatic movements, and sediment circulation in the basin.

Strong residual trends occur at oblique angles to regional trends in Layers 4-2, 7-6, 14-13, and 15-14. This implies variations in the controls influencing the deposition on a regional scale versus a more localized scale, which could be due to direction of sediment input and circulation in the basin.

TABLE 1: Regional thinning trends and residual trends observed in each layer. NAT - no apparent trends. Weak trends are indicated in brackets.

LAYER	THINNING DIRECTION	RESIDUAL TRENDS
2-1	Thinnest area trends NW-SE as a 'trough'; thickens to NE and SW	NW to SE
4-2	SW to NE	(N to S and E to W)
6-4	SW to NE	(N to S and E to W)
7-6	SE to NW	NW to SE
8-7	W to E	NW to SE
9-8	SE to NW	NAT
10-9	NW to SE	NAT
11-10	W to E	NAT
12-11	SW to NE	NW to SE
13-12	SW to NE	NW to SE
14-13	W to E	NW to SE
15-14	SW to NE	NAT
16-15	NE to SW	NW to SE

CHAPTER 7: CONCLUSIONS

7.1 Conclusions

Trends in the residual maps occur at oblique angles to the regional trends illustrated in the isopach and quadratic trend surface maps indicating separate controls influencing the depositional thicknesses.

The regional trends indicated by the isopach and quadratic trend surface maps vary from layer to layer. Thus, the factors controlling sedimentation and depositional centers change significantly between layers.

No trends propagate throughout the section studied, indicating that there is no controlling factor from the basement affecting all of the layers.

7.2 Implications of Conclusions

There is no indication that tectonic controls from the basement dictated the orientation of the linear Cardium sandbodies studied in this area. Thus the present sedimentological interpretation that these sandbodies were deposited during a lowstand and then abandoned on the shelf during the subsequent transgression is adequate for this area.

7.3 Future Research

Since there is no indication of basement influence on the orientation of the sandbodies studied in this thesis, it is suggested that the database area be expanded in order to determine the controls influencing the geometry and

orientation of similar sandbodies outside of this area.

More technical mapping programs could be used to manipulate the data in different methods, and thus possibly assist in interpretation of the data.

Structural maps corrected from kelly bushing or the Base of the Fish Scales Sand would assist in highlighting the structural aspects of this data. Seismic lines would also assist in delineating the large scale features of the area.

No attempt was made to compensate for the effects of differential compaction (due to lithological variations) or differential subsidence. By correcting for these factors, the original properties and structure of the rocks could be considered.

REFERENCES

Bergman, K.M., and R.G. Walker, 1987, The importance of sea level fluctuations in the formation of linear conglomerate bodies: Carrot Creek Member, Cretaceous Western Interior Seaway, Alberta, Canada, Journal of Sedimentary Petrology, v. 57, p. 651-655.

Bergman, K.M., and R.G. Walker, 1988, Formation of Cardium erosion surface E5, and associated deposition of conglomerate; Carrot Creek field, Cretaceous Western Interior Seaway, Alberta, *in* James, D.P., and D.A. Leckie, Eds., Sequences, stratigraphy, sedimentology: surface and subsurface: Canadian Society of Petroleum Geologists, Memoir 15, p. 15-24.

Berven, R.J., 1966, Cardium sandstone bodies, Crossfield-Garrington area, Alberta, Bulletin of Canadian Petroleum Geology, v. 14, p. 208-240.

Cant, D.J., Zuni Sequence: The Foreland Basin / Lower Zuni Sequence: Middle Jurassic to Middle Cretaceous *in* Ricketts, B.D., Ed., Western Canada Sedimentary Basin - A Case History: Canadian Society of Petroleum Geologists, Calgary, 1989

Davies S.D., and R.G. Walker, 1993, Reservoir geometry influenced by high-frequency forced regressions within an overall transgression: Caroline and Garrington fields, Viking Formation (Lower Cretaceous), Alberta, Bulletin of Canadian Petroleum Geology, v. 41, no. 4, p. 407-421.

Downing, K.P., and R.G. Walker, 1988, Viking Formation, Joffre Field, Alberta: Shoreface origin of long, narrow sand body encased in marine mudstones, American Association of Petroleum Geologists Bulletin, v. 72, no. 10, p. 1212-1228.

Haq, B.U., J. Hardenbol, and P.R. Vail, 1987, Chronology of fluctuating sea levels since the Triassic. Science, v. 235, p. 1156-1167.

Hart, B.S., and A.G. Plint, 1993, Tectonic influence of deposition and erosion in a ramp setting: Upper Cretaceous Cardium Formation, Alberta Foreland Basin, The American Association of Petroleum Geologists, v. 22, no. 12, p. 2092-2106.

Hein, F.J., M.E. Dean, A.M. Delure, S.K. Grant, G.A. Robb, and F.J. Longstaffe, 1986, The Viking Formation in the Caroline, Garrington and Harmattan East Fields, Western South-Central Alberta: Sedimentology and Paleogeography, Bulletin of Canadian Petroleum Geology, v. 34, no. 1, p. 91-110.

Jones, R.M.P., 1980, Basinal isostatic adjustment faults and their petroleum significance, Bulletin of Canadian Petroleum Geology, v. 28, no. 2, p. 211-251.

Leckie, D., 1986, Tidally influenced, transgressive shelf sediments in the Viking Formation, Caroline, Alberta, Bulletin of Canadian Petroleum Geology, v. 34, no. 1, p. 111-125.

Pattison, A.J., and R.G. Walker, 1991, Deposition and interpretation of long, narrow sandbodies underlain by a basinwide erosion surface: Cardium formation, Cretaceous Western Interior Seaway, Alberta, Canada, Journal of Sedimentary Petrology, v. 62, p. 292-309.

Plint, A.G., R.G. Walker, and K.M. Bergman, 1986, Cardium Formation 6. Stratigraphic framework of the Cardium in subsurface, Bulletin of Canadian Petroleum Geology, v. 33, p. 213-225.

Ross, G.M., and R.A. Stephenson, Crystalline Basement: The Foundations of Western Canada Sedimentary Basin, *in* Ricketts, B.D., Ed., Western Canada Sedimentary Basin - A Case History: Canadian Society of Petroleum Geologists, Calgary, 1989

Ross, G.M., R.R. Parrish, M.E. Villeneuve, and S.A. Bowring, 1991, Geophysics and geochronology of the crystalline basement of the Alberta Basin, western Canada, Canadian Journal of Earth Sciences, v. 28, p. 512-522.

Ross, G.M., B. Milkereit, D. Eaton, D. White, E.R. Kanasewich, and M.J.A. Burianyk, 1995, Paleoproterozoic collision orogen beneath the western Canada sedimentary basin image by Lithoprobe crustal seismic-reflection data, Geology, v.23, no.3, p.195-199.

Wadsworth, J.A., and R.G. Walker, 1991, Morphology and origin of erosion surfaces in the Cardium Formation (Upper Cretaceous, Western Interior Seaway, Alberta) and their implications for rapid sea level fluctuations, Canadian Journal of Earth Sciences, v. 28, p. 1507-1520.

APPENDIX 1

ACETATE SHOWING LOCATION OF DATA POINTS AND THE POSITION OF CAROLINE AND GARRINGTON IN THE STUDY AREA